Study of Biodiesel Emission Characteristics in Internal Combustion Engines

Oddgeir Tveit

NTNU

Norwegian University
of Science and Technology

Department of Energy
and Process Engineering

EPT-M-2015-99

MASTER THESIS

for

Student Oddgeir Tveit

Spring 2015

Study of biodiesel emission characteristics in IC engines

Studie av utslippskarakteristikk fra biodiesel i forbrenningsmotorer

Background and objective

Due to environmental concerns posed by the use of conventional fossil fuels in the transport, increased use of biofuels in the transport sector are expected in the foreseeable future. The technical requirements are high performance fuel mixtures that can withstand a wide range of operational conditions and yet do not compromise safety or efficiency. Technology development has followed a general trend towards fuel flexibility to increase use of sustainable biofuels in these sectors. Fuel flexibility represents one of the most directly implementable actions proposed. The term fuel flexibility is often used to describe the trend for combustion devices to be operated on variable set of fuels depending on availability and requirements. Hence, biofuels must have the ability to directly substitute and mix with traditional fuels and have the same qualities and characteristics. Since biofuels change characteristics during storage (aging), different types of additives are common to ensure high quality over time. These are used to ensure that the fuel can withstand aging and comply with ASTM standards over reasonable time. However, little is known about the effect of such additives on the combustion and emission formation process. In this master project the available engine in the motor lab will be used to test selected blends of biofuels, and the exhaust gas emissions will be monitored using advanced gas analyzing equipment. The experimental tests will be compared with numerical data obtained from calculations using fuel surrogates.

The following tasks are to be considered:

1) Litterateur study
    i)   Combustion in IC engines
    ii) Biofuels and emissions
    iii) Experimental and numerical engine research
2) Experimental study of biodiesel in engine test rig
    i)   Combustion
    ii) Nitrogen oxides emissions using gas analyszer (Horiba)
    iii) Particle measurements using aerosol size spectrum measurements
3) Verification by means of stochastic reactor simulations using LogeSoft.

-- ” --

Within 14 days of receiving the written text on the master thesis, the candidate shall submit a research plan for his project to the department.

When the thesis is evaluated, emphasis is put on processing of the results, and that they are presented in tabular and/or graphic form in a clear manner, and that they are analyzed carefully.

The thesis should be formulated as a research report with summary both in English and Norwegian, conclusion, literature references, table of contents etc. During the preparation of the text, the candidate should make an effort to produce a well-structured and easily readable report. In order to ease the evaluation of the thesis, it is important that the cross-references are correct. In the making of the report, strong emphasis should be placed on both a thorough discussion of the results and an orderly presentation.

The candidate is requested to initiate and keep close contact with his/her academic supervisor(s) throughout the working period. The candidate must follow the rules and regulations of NTNU as well as passive directions given by the Department of Energy and Process Engineering.

Risk assessment of the candidate's work shall be carried out according to the department's procedures. The risk assessment must be documented and included as part of the final report. Events related to the candidate's work adversely affecting the health, safety or security, must be documented and included as part of the final report. If the documentation on risk assessment represents a large number of pages, the full version is to be submitted electronically to the supervisor and an excerpt is included in the report.

Pursuant to "Regulations concerning the supplementary provisions to the technology study program/Master of Science" at NTNU §20, the Department reserves the permission to utilize all the results and data for teaching and research purposes as well as in future publications.

The final report is to be submitted digitally in DAIM. An executive summary of the thesis including title, student's name, supervisor's name, year, department name, and NTNU's logo and name, shall be submitted to the department as a separate pdf file. Based on an agreement with the supervisor, the final report and other material and documents may be given to the supervisor in digital format.

☒ Work to be done in lab (Water power lab, Fluids engineering lab, Thermal engineering lab)
☐ Field work

Department of Energy and Process Engineering, 14. January 2015

Olav Bolland
Department Head

Terese Løvås
Academic Supervisor

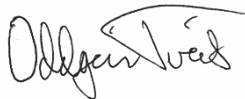Research Advisor: Azhar Malik and David Embersson

Preface

This report is the result of the Master thesis "Study of biodiesel emission characteristics in IC engines" at NTNU in spring 2015. The report is written for the Department of Energy and Process Engineering.

The objective of this report is to see the effect of biodiesel on the exhaust gas characteristics and engine performance of a diesel engine, when compared with a conventional diesel. Combustion in diesel engines has been studied using experiments and numerical simulations.

Firstly I like to thank my academic supervisors Terese Løvås and David Emberson for hours of help and guidance, and the help from Azar Malik for guidance with the particle sampler and help with the simulations. Their help has been extraordinary and much appreciated. I would also like to thank ECO1 for supplying the biodiesel used in the experiments.

The help from David Emberson has been particularly important, I am very grateful for his guidance and company in the lab.

Lastly I would also like to express my gratitude to my girlfriend Kristine Klungerbo, her help and support has been exceptional, and hugely appreciated.

_____

Oddgeir Tveit
Trondheim, June 2015

II

Abstract

Due to environmental concerns, biodiesel has become increasingly important as it shows significant environmental benefits. The aim of this project is to analyze the behavior of different types of biodiesels in a diesel engine, and compare this with the behavior of conventional diesel. Biodiesel changes the emission characteristics in a diesel engine in different ways, depending on the type of biodiesel. In this project two different types of biodiesels are used, a first generation biodiesel and a second generation biodiesel. These have different fuel properties such as cetane number, energy content, viscosity and density. To analyze how these fuels change the exhaust gas characteristics and engine performance, the focus has been on experiments using a modern turbocharged diesel engine. Simulations were also done to study the experimental findings in more detail.

The difference in emission characteristics when using biodiesel are most often seen as increased NOx emissions and decreased PM emissions, but this is not always the case. The experiments in this project yielded lower NOx emissions for both types of biodiesel, and higher PM emissions for the first generation biodiesel. The results from the experiments are thoroughly discussed in this report, with reference to the cylinder pressure curves, the heat release rate curves and the fuel properties.

The simulations were done using two different surrogate fuels for conventional diesel, n-heptane and a mixture of n-decane and 1–methylnaphthalene. But also methyldecanoate as a surrogate for biodiesel. The simulations showed that the two diesel surrogates simulated diesel with varying accuracy, both in engine performance and engine emissions. Proper biodiesel simulations in a diesel engine were not obtained and biodiesel was therefore simulated in an HCCI engine model instead.

Sammendrag

På grunn av miljøhensyn, blir biodiesel stadig viktigere, biodiesel har betydelige miljøgevinster sammenlignet med standard diesel. Målet med dette prosjektet er å analysere oppførselen til ulike typer biodiesel i dieselmotorer, og å sammenligne denne oppførselen med oppførselen til standard diesel. Biodiesel forandrer utslipps-karakteristikkene i dieselmotorer på forskjellige måter, avhengig av typen av biodiesel. I dette prosjektet er to forskjellige typer biodiesel brukt, en førstegenerasjons biodiesel og en andregenerasjon biodiesel. Disse to har ulike kjemiske egenskaper slik som cetantall, energiinnhold, viskositet og tetthet. For å analysere hvordan de ulike drivstoffene endrer utslipps-karakteristikkene og motorytelsen, har fokuset i denne rapporten primært vært på eksperimenter med en moderne turbo-diesel-motor, men også simuleringer har blitt gjort, for å studere de eksperimentelle resultatene i bedre detalj.

Forskjellen i utslipps-karakterstikk ved bruk av biodiesel er oftest sett på som økte NOx utslipp og reduserte PM utslipp, men dette er ikke alltid tilfelle. Forsøkene i dette prosjektet resulterte i lavere NOx utslipp for begge typer biodiesel, og høyere PM utslipp for første generasjons biodiesel. Resultatene fra forsøkene er grundig gjennomgått og tolket med henvisning til sylindertrykk-kurver, varmefrigivnings-kurver, og kjemiske egenskaper.

Simuleringene ble gjort ved hjelp av to forskjellige surrogat drivstoff for standard diesel, n-heptan og en n-dekan og 1-metylnaftalen blanding. Men også methyldecanoate som et surrogat for biodiesel. Simuleringene viste at de to diesel surrogatene simulerte standard diesel med varierende nøyaktighet, både i motorytelse og utslipp. Det ble ingen vellykkede biodiesel simuleringer i en dieselmotor modell, og biodiesel ble derfor simulert i en HCCI motormodell i stedet.

Nomenclature

Symbol: Unit:

TDC   Top dead centre

BDC   Bottom dead centre

V_d Displacement volume   liters

V_c Clearance volume mm^3

B   Bore   mm

L   Stroke   mm

a   Crank radius   mm

CAD   Crank angle degrees   °

N   Rotational speed   RPM

l   Connecting rod length   mm

A/F   Air to fuel ratio

ϕ Equivalence ratio

bmep   Brake mean effective pressure   Pa

sfc   Specific fuel consumption   mg/J

η_{fc} Fuel conversion efficiency

HRR   Heat release rate   J/°

CN   Cetane number

P   Power   W

T   Torque   J

NOx   Nitrogen oxides

PM   Particulate matter

CO   Carbon monoxide

IVC   Inlet Valve Closure

MD   Methyldecanoate

HCCI   Homogeneous charge compression ignition

Table of Contents

List of Figures:

List of Tables

1   Introduction

Our energy demands are continuously rising, and as a consequence, we are emitting many million metric tonnes carbon dioxide more every year from burning fossil fuels [1]. To avoid the worst effects of global warming the United Nations have set a goal to limit the change in global temperature to 2 degrees Celsius [2]. Reaching this means cutting the emissions of CO_2, while still meeting the increasing energy demands. Renewable energy such as biodiesel has grown increasingly popular because of this, and will become an important part of our future energy structure [3].

The transport sector was responsible for 28.7 % of the world's energy consumption in 2007, and the sector is still growing. The transport sector is highly dependent on an easily stored energy source and an infrastructure that supports it. Liquid fuels are still the most easily stored energy form, and gas stations are available all over the world. Implementing renewable alternatives in the transport sector is therefore not as straight forward [4]. The only viable renewable option yet is biofuels, which can come in liquid form and provides sufficient environmental advantages compared to petroleum based fuels. The term biofuel refers to any solid, liquid or gaseous fuel that consist of, or is derived from biomass. Biomass could be any known biological matter, and modern biofuels come from resources that require less than 100 years to regenerate, such as plants and trees. In this sense biofuels are renewable. [5]

There are many different types of biofuels, where ethanol and biodiesel are the most common. To be a viable substitute for fossil fuels, biofuels must have superior environmental benefits. Relative to fossil fuels, after the energy used in production is considered, greenhouse gas emissions are reduced by 12% when using ethanol and by 41% when using biodiesel [6]. From this, biodiesel could be considered as the most environmentally friendly biofuel. However, the use of biodiesel in the transport sector may be limited by the high levels of pollutants in diesel engines. [4]

The diesel engine experienced a big increase in sales in Europe with the introduction of the modern turbocharged diesel engine in the 1990's. The diesel engine is more fuel efficient than petrol engines, and was previously considered cleaner than petrol engines. Because of recent advances in petrol engines and stricter emission standards, diesel engines are now considered to have too high levels of harmful pollutants. Diesel engines have higher amounts of the exhaust gas pollutants nitrogen oxides (NOx) and particulate matter (PM) than petrol engines. According to the World Health Organization PM and NOx are some of the most dangerous air contaminants. As diesel engines increased its market share in the transport sector, this resulted in increased amounts of NOx and PM worldwide, and polluted air caused 3.7 million premature deaths in 2012 [4]. Today the problem with pollutants is so bad that cities are starting to ban diesel engine driven vehicles altogether. In May 2015, Oslo city council approved a law making it possible to ban diesel engines from the city on the most polluted days of the year [7].

The high level of pollutants from diesel engines can be explained by the lack of efficient exhaust gas catalysts available. Without an exhaust gas after-treatment system the pollutant level in petrol engines are just as bad, or even worse, than in diesel engines [8]. The typical values of engine exhaust gas components of petrol engines and diesel engines, without an exhaust gas after treatment, is shown in table 1.

Table 1: Typical values of exhaust gas components in diesel engines and petrol engines [9]

Exhasut gas component	Diesel engine	Petrol engine
NOx	350 -1000 ppm	100 - 4000 ppm
HC	50 - 330 ppm	500 - 5000 ppm
CO	300 -1200 ppm	1000 - 6000 ppm
PM	65 mg/m^3	0 mg/m^3
O$_2$	10-15 %	0.2 – 2 %

Table 1 shows that diesel engines produce considerably lower amounts of carbon monoxide (CO), unburnt hydro carbons (HC) and NOx than petrol engines. However, petrol engines have the advantage of having very efficient after treatment systems available, called three-way catalysts. A three-way catalyst can efficiently remove three of the worst exhaust gas pollutants CO, HC and NOx [8]. A three-way catalyst does unfortunately not work on diesel engines because of the high level of oxygen in the diesel exhaust. The oxygen content in the diesel exhaust is a consequence of the diesel engine combustion concept and is hard, if not impossible, to remove. Oxygen reacts with the same catalyst material as NOx, and there are currently no efficient NOx removal techniques which work in gasses with high oxygen content like in the diesel engine exhaust. Available diesel engine after-treatment systems can efficiently remove CO and HC, but not NOx. In addition to high NOx levels diesel engines have high PM emissions, which is hard to completely remove as well. Diesel particle filters reduce the levels, but some PM emissions will always go through the filter. [8]

Even though diesel engines are associated with poor pollutant levels, there are many possible solutions. Biodiesel does not behave exactly like a petroleum based diesel and changes the exhaust gas characteristic of the diesel engine in complex ways. Biodiesel exhaust gas is often considered to have lower levels of PM and higher level of NOx. However the changes in emissions between biodiesel and petroleum based diesel is complex, and dependent on the type of biodiesel. [10]

There are still many unanswered questions about the use of biodiesel and how it changes the diesel engine exhaust gas emissions [10]. This report aims to through laboratory experiments to investigate the exhaust emission of a diesel engine, running on two different types of biodiesel, a first generation biodiesel and a second generation biodiesel, and to compare these fuels with a conventional petroleum based diesel. Data gained from these experiments will be compared with theoretically expected behavior and simulated results. In this report it will be shown that the typical assumption of low PM and high NOx from biodiesel exhaust is not always correct.

The report begins with a thorough walkthrough of the relevant theory. First with the theory of the combustion engine in section 2.1, then the paper narrows down to diesel engine emissions and biofuel theory in section 2.2 and 2.4, respectively. Then the theory behind experimental and numerical engine research is discussed in section 2.5 and 2.6. Section 3 goes through the procedures and setup for the engine experiments, the numerical simulation and the processing of the resulting data. The experiments in this report are performed with a modern turbocharged diesel engine, the engine conditions are simulated using the software LOGEsoft, and all gathered data is processed using Matlab. The report finishes with a presentation of the results, together with a discussion of these. The experimental results are presented in section 4.1, before the simulated results in section 4.2. Lastly, the concluding remarks are given in section 5.

2 Theory

2.1 Internal Combustion Engine

2.1.1 General principle

In the most general form, an internal combustion engine is a device that converts chemical energy in fuels into useful mechanical energy, through a combustion process [11]. Combustion is the process of converting chemical energy into thermal energy, using fuel and an oxidizer [12]. Internal refers to the combustion process taking place inside the engine, in a combustion chamber. There are many internal combustion engine concepts, but the most common is the reciprocating engine. The reciprocating engine concept uses pistons that move up and down, driven by the thermal energy from the combustion process [13].

The combustion process is a set of reactions which release energy or heat through oxidization. A typical combustion reaction is the methane-oxygen reaction:

$$CH_4 + 2O_2 \rightarrow CO_2 + 2H_2O + energy \tag{1}$$
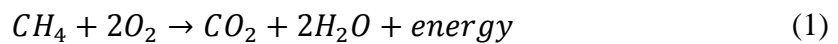
All combustion reaction are exothermic reactions, meaning that they release energy to the environment. This energy is what can be converted into useful mechanical energy in a reciprocating engine [12].

The modern reciprocating engine is a four stroke engine. It is called a four stroke engine because the engine does four piston movements before it completes the combustion process. The four strokes makes it possible to complete a thermodynamic cycle. The four stroke engine concept is shown in figure 1. One stroke refers to one piston movement from the top position to the bottom [11]. The four strokes are:

1. The intake stroke:
   Air is injected into the combustion chamber while the piston is moving down.

2. The compression stroke:
   The piston moves upwards and compresses the gas to a much lower volume. When the piston is close to the top, combustion is initiated and the pressure increases rapidly.

3. The power stroke:
   The increase in pressure caused by combustion forces the piston to move down.

4. The exhaust stroke:
   The piston moves upwards and pushes out the exhaust gas.
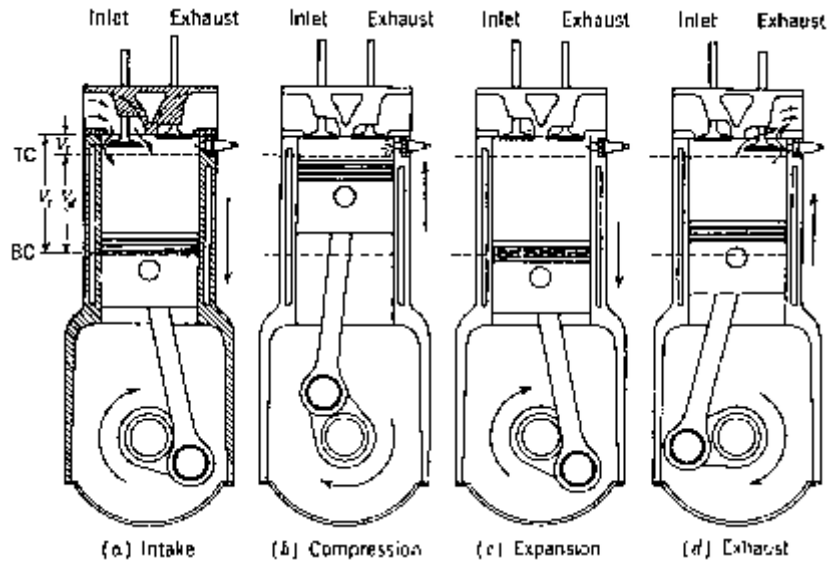
Figure 1: The four strokes in the four stroke engine concept [11]

During the four strokes the valves are responsible for injecting air and extracting exhaust gas. The valves can be seen at the top of the cylinder in figure 1. The inlet valve opens during the intake stroke and the exhaust valve opens during the exhaust stroke. The valves make it possible to remove the exhaust gas and to get new supply of combustion reactants, being fuel and oxidizer, into the combustion chamber. This allows the combustion reaction to take place repeatedly and form a thermodynamic cycle [11]. The actual thermodynamic cycle in a reciprocating engine can be seen in figure 2.
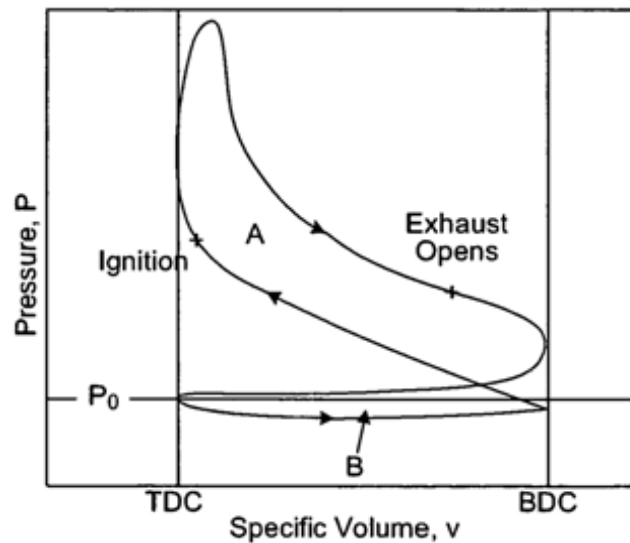
Figure 2: Actual thermodynamic cycle in a reciprocating engine [14]

An actual thermodynamic cycle means that it is not simplified in any way. In figure 2 top dead center (TDC) and bottom dead center (BDC) refers to the top and bottom piston positions respectively [11]. By following the cycle in figure 2 one can recognize how the four piston strokes form a thermodynamic cycle:

1. The intake stroke begins at TDC at pressure P_0, in the lower left corner of figure 2. During the intake stroke the volume increases and air is injected into the engine. At BDC, in the lower right corner of figure 2, the intake stroke is finished and the compression stroke begins.

2. The compression stroke begins at BDC at pressure P_0, in the lower right corner of figure 2. As the compression stroke unfolds the piston moves upwards. This lowers the volume in the cylinder and the pressure increases. During the compression stroke the fuel is injected and as the pressure increases, the fuel forms an ignitable mixture with air. A typical ignition point is seen right before TDC, and is indicated in figure 2. After ignition the pressure rises drastically as the fuel combust.

3. The power stroke begins at TDC at high pressure, in the top left corner in figure 2. The high pressure obtained from combustion pushes the cylinder all the way down to BDC, and pressure decreases accordingly. The combustion process endures through the power stroke, and the duration of the combustion depends on how much fuel that is injected. Figure 2 shows that the peak pressure occurs just after TDC, early in the power stroke. At this point the pressure-rise from the combustion is no longer higher than the pressure-decrease from the downward-moving piston.

4. The exhaust stroke begins at BDC, in the right end of figure 2. The engine exhaust valves will open just before BDC in the power stroke, and during the exhaust stroke the exhaust is pushed out of the cylinder. The pressure inside the combustion chamber is constant P_0 as the volume decreases and the exhaust gas is pushed out. Finally at TDC, all exhaust gas is pushed out and the engine cycle is complete.

The thermodynamic cycle makes it possible to calculate the produced work during the engine cycle. When the engine cycle is shown in a pressure-volume diagram (PV-diagram), as in figure 2, the area inside the cycle loop represent the work produced or consumed by the engine cycle. In a reciprocating engine the PV-diagram consist of two cycle loops, the power loop and the exhaust loop marked with letter A and B respectively in figure 2. Area A in the engine cycle represents the work produced by combustion and area B represents the work consumed by the exhaust stroke and intake stroke [11].

To convert the work created by the thermodynamic cycle into useful mechanical energy, the piston is connected to a crankshaft. The crankshaft converts the oscillating movements of the piston into rotating movement, which is what rotates the wheels in a car [13]. There are several ways of connecting the cylinders to a crankshaft, some engine concepts are shown in Figure 3.

1 In-line engine   3 Radial engine
2 V-engine   4 Flat engine
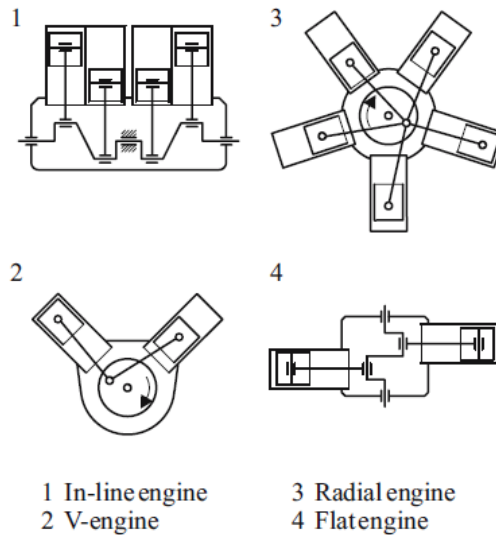
Figure 3: Reciprocating engine concepts connecting the cylinders to the crankshaft [13]

The V-engine and in-line engine are the most common engine concepts. The in-line engine has the cylinders placed in a row, in an upright position, and it has the advantage that it is easy to manufacture and service. However, the vertically placed cylinders make the in-line engine tall and long. The V-engine acts as compromise between the easy to produce and service in-line engine, and the very compact flat-engine. The V-engine has its cylinders placed in an angle, so the engine becomes lower and shorter, allowing a lower and shorter hood. This gives the car a more aerodynamic shape and lowers the center of mass [15].

2.1.2 Engine geometry

The crankshaft is essential to the internal combustion engine. The crankshaft position is used as a reference to where the piston is in the engine cycle. The position of the crankshaft is then given in crank angle degrees (CAD). To calculate the position of the piston in the cylinder from CADs, it is necessary to know the engine geometry, which is specific to all engine models. The engine geometry is commonly represented as shown in figure 4 [11]. Where the parameters used are.

V_d – Displacement volume (total cylinder volume)
V_c – Clearance volume (remaining volume when piston is at TDC)
B – Bore
L – Stroke
a – Crank radius
θ – Crank angle degrees (CAD)
l – Connecting rod length
s – Cylinder position/Distance traveled

6
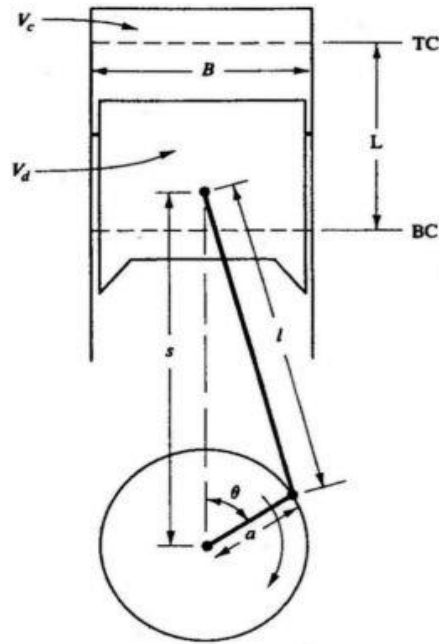
Figure 4: Engine geometry [11]

The ratio between the cylinder position and the CAD is:

$$s = a \cos \theta + \sqrt{l^2 - a^2 sin^2\theta} \tag{2}$$

The geometry parameters are what defines the geometry of an internal combustion engine, and equation 2 makes it possible to calculate the position of the piston if CAD is known. It is also possible to find the cylinder volume at any given CAD:

$$V = V_c + \frac{\pi B^2}{4}(l + a + s) \tag{3}$$

Another important parameter is the rotational speed, which is a measure of the piston speed and is normally measured in revolutions per minute (RPM) [11].

2.1.3 CI-engine and SI-engine

The reciprocating engines are commonly divided into two different categories, the spark ignition engines (SI-engine) and the compression ignition engines (CI-engine), depending on the way the fuel is ignited. The SI-engine ignites the fuel with a spark plug, while the CI-engine lets the air-fuel mixture inside the combustion chamber auto-ignite, due to the compression itself [11].

The PV-diagram shown in figure 2 is normally reduced to four simple steps. The shape of this simplified cycle depends on the engine type. The reason why a simplified presentation of the engine cycle is useful is because it is easier to apply in thermodynamic analysis, and makes it possible to calculate the theoretical work produced by the engine. The simplified thermodynamic cycle consists of several thermodynamic processes which are well known, and can be calculated analytically. The actual thermodynamic cycle, on the other hand, is too

7

complex to analyze analytically. The simplified thermodynamic cycles for the two engine concepts show the conceptual difference between them [13].

The SI-engine
The SI-engine was the first type of reciprocating engine. It has the advantage of good ignition control, as it uses a spark plug to ignite the fuel before the point where it will ignite by itself. The PV-diagram of the simplified thermodynamic cycle for an SI-engine, called the Otto cycle, is shown in figure 5. It consist of four steps [13]:

1-2   Adiabatic compression of the gas

2-3   **Combustion under constant volume represented as heat supplied**

3-4   Adiabatic expansion of the gas

4-1   Exhaust and intake stroke represented as heat out under constant volume
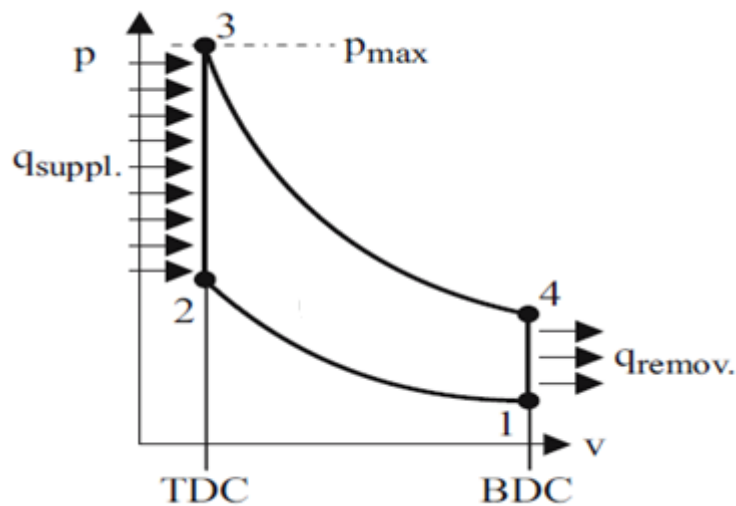
Figure 5: PV-diagram of the Otto cycle [13]

Diesel engines
The CI-engine is most commonly known as the diesel engine. The engine concept is named after Rudolf Diesel, who invented an engine in 1892 with the same basic functions as the modern diesel engine has today. The engine he invented had double the efficiency of the other engines at that time. This increased efficiency was achieved by managing to increase the compression ratio of the engine [16]. The simplified thermodynamic cycle is similar to an SI-engine apart from the combustion process, which happens under constant pressure. The PV-diagram of the simplified thermodynamic cycle for a CI-engine, called the Diesel cycle, is shown in figure 6. It consist of four steps [13]:

1-2   Adiabatic compression of the gas

2-3   **Combustion under constant pressure represented as heat supplied**

3-4   Adiabatic expansion of the gas

4-1   Exhaust and intake stroke represented as heat out under constant volume
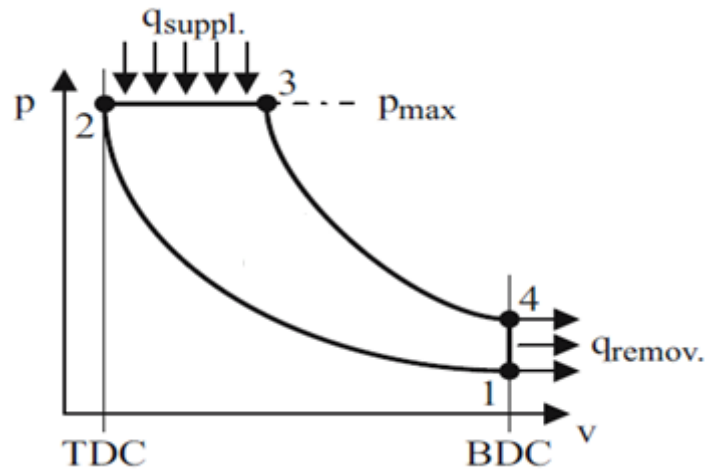
Figure 6: PV-diagram of the Diesel cycle [13]

The only difference between the Diesel cycle and the Otto cycle is that the combustion is assumed to be under constant volume in the Otto cycle, and constant pressure in the Diesel cycle. This difference is explained by the different ignition techniques. In the SI-engine the air-fuel mixture is ignited by ta spark plug at a certain cylinder volume, which increases the pressure. In the CI-engine the air-fuel mixture is auto-ignited when it reaches a certain pressure, and the volume increases. By allowing the diesel engine to auto-ignite, the cylinder pressure is able to reach a higher value than what is possible in an SI-engine. Higher pressure leads to a larger area inside the thermodynamic cycle, which means that more work is produced per engine cycle. This explains why the diesel engine has a better efficiency than the SI-engine [13].

2.1.4 Fuel injection

The evolution of the modern diesel engine has most importantly been impacted by the development of new fuel injection techniques. As diesel engines are ignited solely by compression, the only way to control the ignition process is by controlling the injection of fuel and air [16]. The fuel injection in diesel engines is characterized by three steps [17], as follows:

Step 1:   The injection process starts right before TDC

Step 2:   The air and fuel mixes, the fuel injection is continuous and the piston is moving upwards

Step 3:   When the pressure and fuel amount is high enough the mixture auto-ignites

The original fuel injection technique was indirect fuel injection, where valves was used to control the fuel injection. Modern diesel engines use direct fuel injection, which gives better control of the injection timing. Direct fuel injection can be controlled electronically with an Electronic Control Unit (ECU), while indirect injection was controlled mechanically through the camshaft directly opening and closing the valves. An ECU controlled injection system generally allows a more accurate and reliable injection process than a mechanical system. Another advantage is that it can be combined with a high pressure reservoir, called a common rail, that allows for higher injection pressure and therefore improves the mixing [16].

As the fuel injection systems have improved greatly, a higher level of control is achieved. This control leads to new potential injection techniques, such as multiple injections and changed injections timing. This improvement is beneficial as it may improve the performance of the engine in terms of power and emissions [13].

2.1.5 Engine parameters and definitions

Several parameters are often used when working with reciprocating engines. The most important will be explained subsequently.

Air to Fuel ratio

The air to fuel ratio is defined as the mass ratio of air and fuel. In other words, it is the amount of air injected divided by the amount of fuel injected. It is an important measure in order to understand the conditions inside the combustion chamber [11]. The air to fuel ratio is given by:

$$\left(\frac{A}{F}\right) = \frac{Air\ mass}{Fuel\ mass} \tag{4}$$

Equivalence ratio

When there is just enough oxygen present to convert all the fuel into completely oxidized products, the condition is called stoichiometric. This means that the only products of the combustion reactions are CO_2, H_2O and N_2. In internal combustion engines stoichiometric condition is rarely achieved, as it implies perfect mixing of fuel and air. The equivalence ratio is a measure of how far away from stoichiometric condition the engine is operating, and hence the difference between the stoichiometric air to fuel ratio and the actual air to fuel ratio [11]. The equation is given by:

$$\phi = \frac{(A/F)_{stoichiometric}}{(A/F)_{actual}} \tag{5}$$

This is a measure of the mixture composition. Mixtures that have $\varphi > 1$ are defined as rich mixtures, meaning that they are rich on fuel. Mixtures with $\varphi < 1$ are defined as lean mixtures, meaning that they are low on fuel [11]. Another common ratio is the relative air to fuel ratio λ, defined as:

$$\lambda = \phi^{-1} = \frac{(A/F)_{actual}}{(A/F)_{stoichiometric}} \tag{6}$$

Cylinder Pressure

The analysis of cylinder pressure is a technique that is very important in combustion engine technology. Pressure inside the combustion chamber can be measured, and cylinder pressure curves are plots of this pressure against CAD. Cylinder pressure curves give valuable information about the engine performance and is frequently used [16].

Brake mean effective pressure (bmep)

The brake mean effective pressure is a measure of an engine's ability to do work, relative to the engine size. The bmep makes it possible to compare engines of different sizes, and is defined as the work per cycle divided by the cylinder volume V_d [11]. The bmep for a four stroke engine can be calculated by:

$$bmep = \frac{P}{V_d N^*} \tag{7}$$

P is the engine power and N^* is the engine speed in cycles per second. For a four stroke engine N^* is the engine speed divided by 2, since there are two revolutions per cycle. By dividing the engine power by the engine speed, in cycles per second, the work per cycle is found.

Specific fuel consumption (sfc)

The specific fuel consumption is a measure of the engine's fuel consumption per power output. It indicates how efficiently an engine is using the injected fuel, and makes it possible to compare the fuel consumption of different engines. In other words, it measures the engine efficiency by the ratio between fuel injected and the power produced. SI-engines can typically never go below an sfc of 0.75 mg/J, while the best diesel engine can go below 0.55 mg/J [11]. The formula for specific fuel consumption is:

$$sfc = \frac{\dot{m}_f}{P} \qquad (8)$$

Fuel conversion efficiency
A more fundamental value of the engine performance is the engine fuel conversion efficiency. In contrast to the specific fuel consumption it takes the fuel heating value into account. The fuel conversion efficiency is a measure of an engine's ability to convert the energy in the fuel into engine power [11]. It can be calculated as follows:

$$\eta_{fc} = \frac{P}{\dot{m}_f \, Q_{HV}} = \frac{1}{sfc \, Q_{HV}} \qquad (9)$$

Q_{HV} is the fuel heating value, which is the heat that a fuel can release if it goes through complete combustion [12].

2.1.6 Combustion parameters and definitions
The combustion process is the driving force in the internal combustion engine, where the work produced and the resulting emissions are highly dependent on the combustion details. There are several important combustion parameters such as, mixing time, and evaporation. The most important combustion parameters are discussed subsequently.

Mixing
Combustion is, by definition, the process where a fuel reacts with an oxidizer and produces energy. For such a reaction to take place it is absolutely necessary for the fuel and oxidizer, normally air, to be properly mixed. A fuel can not react with the oxidizer if they are not in contact, and mixing of the fuel and oxidizer is therefore necessary. The time they are given to mix, called mixing time, is a very important parameter. In a reciprocating engine the mixing time is especially important since the piston is moving with a high velocity and time is limited [13].

Ignition delay
The ignition delay is the time between the start of injection (SOI) and the start of combustion (SOC), and it can be presented in microseconds or CAD. In a reciprocating engine the ignition delay is the same as mixing time [13].

Evaporation
Liquid fuels are normally used in internal combustion engines. In order for a liquid fuel to ignite inside the combustion chamber, it has to evaporate so that it mixes sufficiently with the air. An evaporated fuel mix well with air since they are both gasses, and a fuel will therefore normally not ignite before it has evaporated [13].

Flash point
The flash point of a fuel is the temperature and pressure at which the fuel begins to evaporate and form an ignitable mixture [18].

Premixed combustion
In reciprocating engines the fuel must be injected before the combustion can start. During the ignition delay the fuel mixes with air and forms an ignitable mixture. This mixture burns very quickly and is called premixed combustion since it mixes with an oxidizer before it ignites [13] [12].

Non-premixed combustion
If a fuel is not mixed properly, but still has sufficient pressure and temperature, and if there is an oxidizer present, the fuel may still ignite. In this case the fuel and air will mix during combustion. This is what is called non-premixed combustion [12] and in a diesel engine non-premixed combustion causes a diffusion flame [13].

Diffusion flame
A diffusion flame is created when the mixing time is too low to mix all the fuel and air. A diffusion flame is a result of non-premixed burning and is limited by the rate of mixing. It is often also called a mixing controlled flame. A diffusion flame has regions of high oxygen density and regions of high fuel density. The diffusion flame creates a plume that has the high air density regions in the outer layers and the high fuel density regions in the inner layers [14]. Figure 7 shows a detailed conceptual diffusion flame. The different zones in the diffusion flame is important for emission formation and will be explained further in section 2.2.
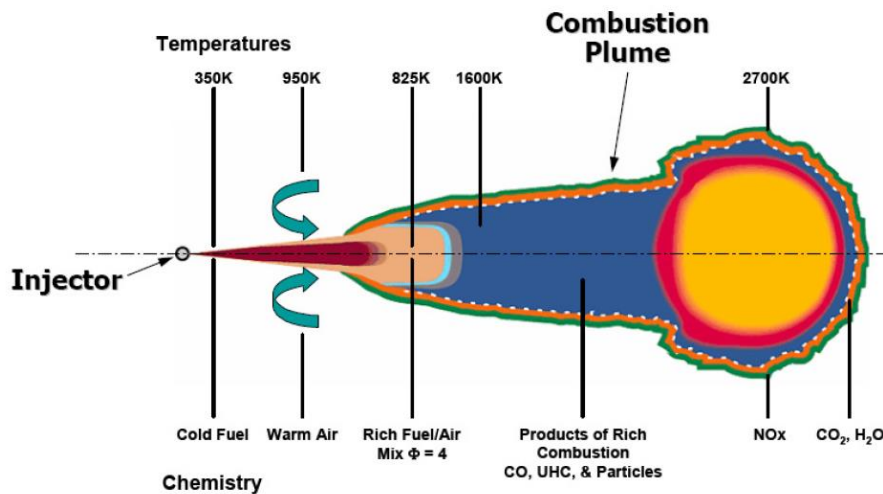
Figure 7: Diffusion flame [14]

Heat Release Rate (HRR)
The heat release rate is a measure that is used to evaluate how the fuel burns in the combustion chamber. The HRR is defined as the difference between the heat released from combustion and the heat transferred from the system [11]. The equation is:

$$\frac{dQ_{app}}{d\theta} = \frac{dQ_{comb}}{d\theta} - \frac{dQ_{ht}}{d\theta} \tag{10}$$

12

In equation (10) θ represents the CAD and the term apparent is used because the calculations are approximations of the real values as the real values cannot be measured. Equation (10) can be rewritten as:

$$\frac{dQ_{app}}{d\theta} = \frac{\gamma}{\gamma - 1} p \frac{dV}{dt} + \frac{1}{\gamma - 1} V \frac{dp}{d\theta} \tag{11}$$

In equation (11) γ is the specific heat capacity.

2.1.7 Heat release rate analysis

HRR is a very useful parameter when analyzing the combustion in a diesel engine. Figure 8 shows the typical heat release rate curve for a diesel engine.
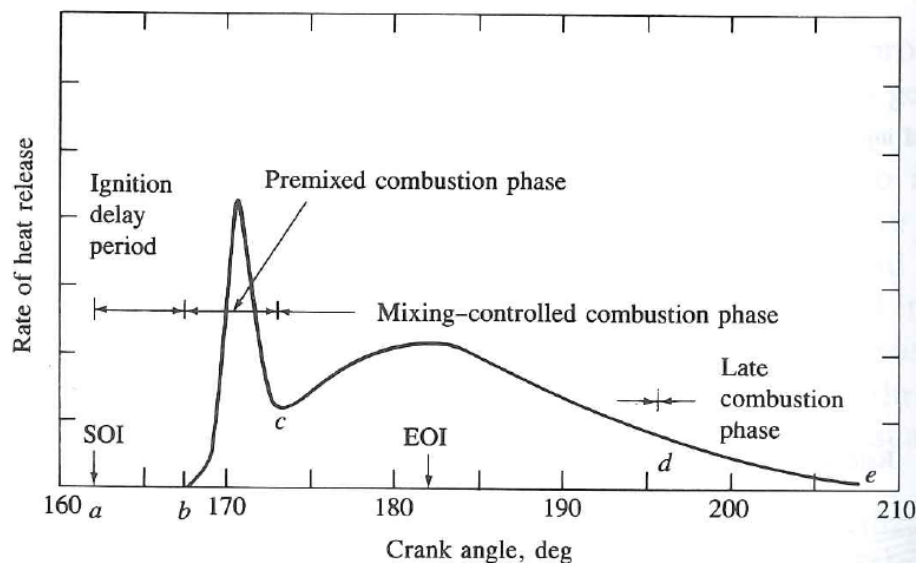
Figure 8: Typical HRR curve for diesel engines [11]

Figure 8 shows that the diesel engine combustion can be divided into four phases:

1. Ignition delay period
   The ignition delay period is the period from SOI until the HRR curve starts to rapidly increase. The rapid increase in HRR represents the SOC.
2. Premixed combustion phase
   The premixed combustion phase is caused by the ignition delay, leading to some premixed fuel combustion. The premixed fuel is the first to be ignited, causing an initial rapid increase in HRR.
3. Mixing controlled combustion phase (diffusion flame combustion)
   The mixing controlled combustion phase is the non-premixed diffusion flame period. It causes a stable heat release, but not as intense as the premixed combustion. The mixing controlled combustion starts after the premixed combustion since it is harder to ignite than the premixed fuel.
4. Late combustion
   The late combustion phase is caused by a small amount of remnant fuel which has not combusted during the other phases. This causes the HRR to last into the expansion stroke. The late combustion also includes the energy present in soot emissions, which has formed in the diffusion flame and oxidizes during the late combustion phase.

It is often challenging to find the ignition delay in diesel engines. The problem is that it is hard to measure SOC, but it can be measured with an optical transducer which measures the radiation

13

from the flame. However, if the engine is not fitted with an optical sensor it is common to define SOC through the cylinder pressure or the HRR. SOC can be defined as the minimum pressure rate that occurs after SOI on the cylinder pressure curve. Or it can be defined as when the HRR goes from negative to positive just after SOI [19].

Time until 50% heat release
A useful way to see how much fuel that combusts as a premixed flame and how much that combust as a diffusion flame, is by studying the time until 50% heat release. This is a measure of the time it takes before half the heat is released from the fuel. If the time until 50% heat release is high, it implies that the engine uses a long time to burn half of the fuel. If the engine uses a long time to burn the fuel, it coincides with a short initial premixed combustion phase and a predominant diffusion flame combustion phase. On the other hand, if the engine burns the fuel quickly, it coincides with a predominant premixed combustion phase. The time until 50% heat release is therefore a very useful parameter in order to analyze the effect of the different fuel properties [19].

2.2   Emissions in Diesel engines

2.2.1 Pollutants
There are substantial unwanted emissions in the diesel engine exhaust. Unwanted emissions are often referred to as pollutants. The most commonly known component of the exhaust gas is CO_2. But CO_2 is not considered a pollutant. The reason being that it does not pose a direct health hazard, and also because it is the main product of the stoichiometric combustion along with H_2O. In other words, there will be CO_2 emissions as long as there is a combustion process [13].

In addition to the stoichiometric pollutants, being CO_2, N_2 and H_2O, other emissions are also found in the diesel engine exhaust. These are considered pollutants as they are harmful for both health and the environment [13]. The different emissions that will be discussed are:

- Nitrogen oxides (NOx)
- Carbon monoxide (CO)
- Particulate matter (PM)

These emissions and their origin are explained in table 2.

Table 2: Pollutants in diesel engines and their origins [13]

Emission	Origin	In the engine
NOx	NOx is mainly formed when oxygen and nitrogen reacts at high temperatures in the combustion products. NOx can also be formed during the combustion and as a result of nitrogen in the fuel.	It forms in the products after combustion. Especially in the premixed combustion and in the outer layers of the diffusion flame, where the temperature is high and there is a lot of oxygen present.
CO	CO is a result of incomplete combustion. This happens if there is not enough oxygen in the mixture to react with all the fuel.	CO forms if there is too much fuel in the combustion chamber. It also forms in the inner layers of the diffusion flame, where there is more fuel than air.
PM	PM is unburnt particles that are larger than normal molecules. They consist of small liquid nucleation mode particles as well as larger solid accumulation mode particles.	Particulate matter normally forms in fuel rich areas of the diffusion flame. The exact formation of particles is complex, since there are several types and sources of PM [16].

2.2.2 Nitrogen Oxides (NOx)

NOx is the classification of all nitrogen oxides. In terms of diesel engine pollutants, it normally refers to NO and NO_2. NOx emissions can be formed in three different ways, these are thermal NOx, prompt NOx, and fuel NOx. In diesel engines thermal NOx the most common.

Thermal NOx
Thermal NOx represents the NOx created in the combustion products under high temperature, and is the biggest contributor to the NOx emissions. Most of these NOx emissions are NO molecules which will further oxidize to NO_2. The thermal NO is controlled by the extended Zeldovich mechanism, consisting of three fundamental reactions (12), (13) and (14) [16].

$$N_2 + O \leftrightarrow NO + N \qquad (12)$$

$$N + O_2 \leftrightarrow NO + O \qquad (13)$$

$$N + OH \leftrightarrow NO + H \qquad (14)$$
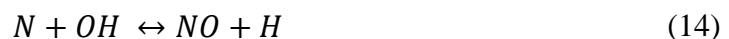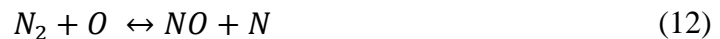
The reaction rate k of these reactions are (15), (16) and (17) respectively.

$$k_{12} = 7.6 \times 10^{13} e^{-38000/T} \tag{15}$$

$$k_{13} = 6.4 \times 10^{9} e^{-3150/T} \tag{16}$$

$$k_{14} = 4.1 \times 10^{13} \tag{17}$$

Reaction (12) and (13) are exponentially dependent on temperature and thus a little increase in temperature can cause a large increase in NO_x emissions. A doubling in temperature will increase the reaction rate k_{12} by a factor of 10^3. The first reaction, given by equation (12), is known to have a very high activation temperature due to the nitrogen triple bond that has to be broken. At 1800K, reaction (12) progresses 7-8 times slower than reaction (13) and (14), but reaction (12) has a very fast progression from 1800K and upwards [13].

Prompt NOx.
Prompt NOx formation is the formation of NOx in the flame front or in the outer layers of the diffusion flame. Prompt NO_x formation is separated from thermal NOx formation by the fact that prompt NOx happens when elements of the fuel reacts with the N_2 molecules in the air. Prompt NOx also differs from thermal NOx in that it can be formed already at 1000K [20].

Fuel NOx
Fuel NOx means the NOx produced by a possible fuel that contains natural nitrogen. Fuel nitrogen reacts as the first Zeldovich reaction (11). This NOx formation can happen at the same time as other NOx formation mechanisms and fuel NOx is common, but the amount of fuel NOx is often negligible compared to the total NOx emissions.

There are very high temperatures inside the combustion chamber of a diesel engine, hence thermal NOx is the most important NOx formation. Thermal NOx is, in contrast to PM and CO, most significant at close-to stoichiometric conditions. If the combustion process is stoichiometric, higher temperatures are produced. However, the formation of NOx is dependent on available oxygen. A stoichiometric reaction burns away all the fuel, and the formation of NOx in combustion engines is therefore highest at slightly lean conditions [13].

There is a trade-off between the pollutants. A rich fuel mixture in the combustion chamber will result in low NOx emissions, but in return there will be high amounts of CO. A representation of the correlation between CO and NOx is shown in figure 9. The NOx peak happens when λ is just above 1, meaning almost stoichiometric conditions [13].
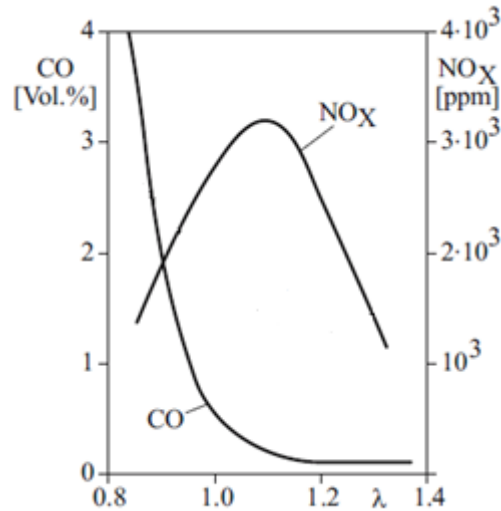
Figure 9: Relation between NOx and CO [13]

2.2.3 Particulate matter (PM)

Definition and classification

Particulate matter (PM) is the general term for any solid particles or liquid droplets that are dispersed in the exhaust gas or in the air. PM can consist of many different materials. Examples of PM include dust, dirt, soil and soot [21]. The normal way to define particles in the diesel engine exhaust gas, is as any material collected by an exhaust filter [22].

The structure and nature of PM is highly dependent on the conditions of the exhaust gas, as well as the fuel used. Since PM can consist of both dispersed liquid droplets and solid particles, it is normal that the different particles combine after combustion. This is called accumulation. Soot is one type of accumulated particles. Soot is formed in the locally fuel-rich areas during combustion, and is a result of incomplete combustion. Most of the soot is oxidized after formation, but some soot is brought out with the exhaust [23].

It is normal to separate particulate matter into two groups, nucleation mode particles and accumulation mode particles. Nucleation mode particles are very small particles, which normally are assumed to be mostly volatile sulfur and/or droplets of hydrocarbon compounds. Accumulation mode particles are the clusters of solid particles which has formed from the incomplete combustion and then accumulated together, such as soot. The nucleation particles and the accumulation particles will have different size distributions, and hence when one measures particulate emissions it is possible to distinguish between the two. A typical size distribution of particulate emissions is shown in figure 10 [22].

17
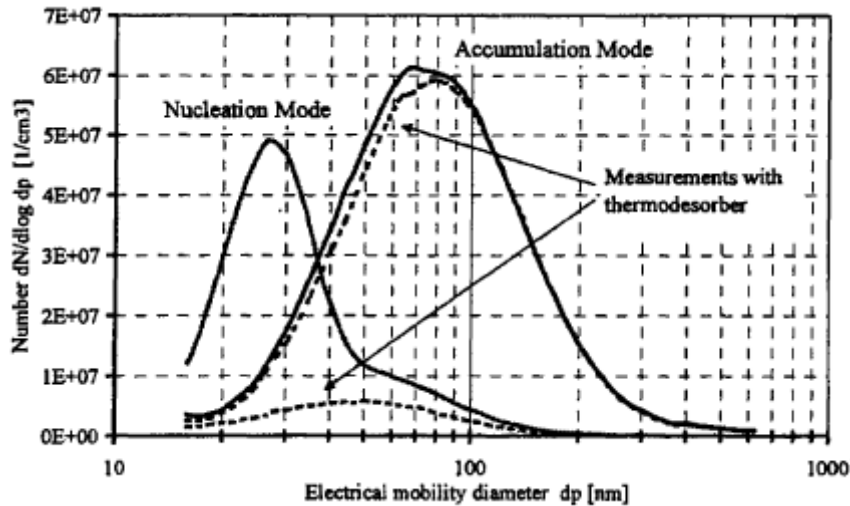
Figure 10: Size distribution of particulate emission [22]

Nucleation mode particulates have diameters ranging from 10 to around 60 nm, while the accumulation mode particles have a size ranging from 20 nm to 500 nm [22]. These diameter ranges can be seen in figure 10. Particles of a size less than 100 nm are often defined as ultrafine particles. The ultrafine particles are of particular interest as they oppose an extra health hazard, because they are able to penetrate deeper into human lungs than coarser PMs. This small particle size also makes it possible for harmful metals, adsorbed on the particle surface, to enter into the human circulatory system [24].

Formation of PM emission
Figure 7 showed the diffusion flame that is typical for the diesel engine combustion. Soot is most commonly formed in the fuel rich regions in the diffusion flame. Soot forms under such conditions because hydrocarbon fragments have a greater chance of colliding with other hydrocarbon fragments, and initiate growth rather than being oxidized [16].

A critical step in the soot formation process is when the hydrocarbon fragments form the first aromatic ring. After this step the first aromatic ring will grow and eventually form polycyclic aromatic hydrocarbons (PAHs). PAHs are aromatic rings linked together in one plane. Soot is formed when PAHs start to combine in a three dimensional scale [16].

Soot concentration is very high during combustion, but most of the soot is burnt off before the combustion is complete, and barely any initially formed soot will survive the oxidation in the flame. There is still some soot that does not oxidize and is brought through with the exhaust. Since the soot does not consist solely of carbon and the surrounding gas does not consist of pure oxygen, the oxidation rate depends on very complex reaction schemes [16].

2.2.4 Carbon monoxide (CO)
Carbon monoxide is produced from partial oxidation of a fuel during combustion. CO forms if there is not enough oxygen to produce CO_2. CO emissions are highly dependent on the equivalence ratio, and the concentration of CO increases with increasing equivalence ratio. In contrast to Soot, CO formation is one of the fundamental reaction-steps in the hydrocarbon combustion process [11]. CO formation during combustion can be summarized by the following reaction:

$$RH \rightarrow R \rightarrow RO_2 \rightarrow RCHO \rightarrow RCO \rightarrow CO \qquad (18)$$

18

R represents a CH radical and reaction (18) shows that the complete hydrocarbon RH eventually form CO through several intermediate species. CO is also an intermediate specie, and after reaction (18) CO reacts further to CO_2 if there is oxygen available. When CO_2 is formed, the combustion process is complete. The oxidation of CO to CO_2 happens at a slower rate than reaction (18), and therefore CO emissions are more common than emissions from other intermediate combustion species [11]. The oxidation of CO to CO_2 can be seen in reaction 19:

$$CO + OH \rightarrow CO_2 + H \tag{19}$$

The reaction rate of equation (19) is given by:

$$k_{19} = 6.76 \times 10^{10} e^{T/1102} \tag{20}$$

Equation 20 shows that the oxidation of CO to CO_2 is dependent on temperature. This is important since the temperature drops in the combustion chamber during the engine power stroke, and CO can develop [13]. Hence there are two main ways for CO emission to form. Firstly, CO form if there is not enough oxygen available to complete the combustion process, and secondly CO forms if the temperature is too low for CO to oxidize to CO_2 [13].

2.3 Fuel properties and emissions

2.3.1 Cetane number
The cetane number (CN) is a measure of the ignition quality of the fuel. The cetane number is based on two reference fuels: n-hexadecane and heptamethylnonane (HMN) [11]. The relation is given in equation 21:

$$CN = (percent \ n - hexadecane) + 0.15 \times (percent \ HMN) \tag{21}$$

N-hexadecane has high ignition quality and pure n-hexadecane has a cetane number of 100. HMN has very low ignition quality and pure HMN has the bottom cetane number of 15 [11].

The cetane number of a fuel is found by running the fuel through a standardized test engine, where ignition delay can be measured. Then a mixture of n-hexadecane and HMN with the same ignition delay is found, and used to find the fuel cetane number through equation 25 [11].

A fuel with high cetane number will ignite easier than a fuel with a low cetane number. Therefore high cetane number fuels have a short ignition delay, while low cetane number fuels have a long ignition delay [11].

2.3.2 Cetane number and emissions

NOx Emissions

As the cetane number increases, the NO_x level generally decreases. This is because a high cetane number represents a short ignition delay, meaning that the fuel ignites earlier than other fuels and leaves little mixing time. This will cause a lower temperature inside the combustion chamber because of a low amount of premixed combustion and a high amount of diffusion flame combustion. Diffusion flame combustion produces lower temperatures than premixed combustion. This is why a high cetane number fuel will get lower amounts of thermal NOx emissions [25]. However, this is not always the case. Some studies show that as the combustion advances in the engine, this leads to higher temperatures for longer, and therefore higher NOx emissions [10].

CO emissions

The cetane number also effects the CO emissions. Higher cetane number results in a lower possibility for formation of rich fuel zones, which are suitable for CO formation. This is best explained by the diffusion flame, as seen in figure 7. Higher cetane number results in a larger amount of diffusion flame combustion. The diffusion flame consists of large areas that are either too lean for CO formation or too rich for CO formation. A premixed flame however is more homogeneously mixed, and CO emissions easily form. In other words, an increased cetane number leads to reduced CO emissions [10].

Particulate matter

The effect of cetane number on PM emissions is hard to define. PM emission are mostly dependent on the chemical structure of the fuel [10]. However, a fuel with a high cetane number will have a larger diffusion flame period, which is associated with larger amounts of soot formation [16].

2.3.3 Fuel oxygen content, heating value and viscosity

Fuel oxygen content

Some fuels have oxygen in the chemical structure of the fuel. This is often seen in biofuels. Large fuel oxygen content is normally associated with lower CO emissions because of a more complete combustion, but also higher NOx emissions due to higher temperatures during combustion [10].

Heating value

The heating value is the energy content in the fuel. If the fuel has a low heating value, it means that it produces less energy when combusted than a fuel with high heating value. A lower energy content in the fuel can cause a lower adiabatic flame temperature, which leads to lower thermal NOx [26].

Viscosity

The fuel viscosity will change the emission characteristics as it may change the vaporization of the fuel. If a fuel has high viscosity and density, it has been shown to have decreased rates of vaporization of the fuel, and therefore reduced ignitability. A lower vaporization rate would lead to lower NOx emissions and higher CO emissions because the fuel becomes harder to combust [10].

2.4 Different Fuels

Fuel for diesel engines comes in different variants. A petroleum diesel fuel is composed of several petroleum fractions with a boiling range of 180 – 380 °C and a density of around 0.85 kg/m^3 [27]. Petroleum diesel fuel is a middle distillate because it utilizes the part of the crude oil that is heavier than gasoline, but without the heaviest crude oil components. Petroleum based diesel has a carbon number in the range of C_9-C_{20} and historically it was a residual from gasoline production [28]. Biodiesel is a liquid fuel with similar properties as a petroleum diesel fuel, but has a biomass origin [29].

The fuels that are used today are under control of local authorities. They have established standard requirements for different fuels, to control that all the fuel sold is safe to use. They also control that the fuel has sufficiently low levels of lead and sulphur which causes harmful pollutants. In Europe, automotive diesel fuels are regulated by the EN590 standard which specifies requirements including, maximum amount of sulphur, minimum cetane number to mention a few. The main requirements in EN590 are shown in table 3 [30].

Table 3: Main requirements in EN590 for petroleum diesel fuels [30]

Property	Unit	Lower limit	Upper limit
Cetane number	-	51	-
Density at 15 °C	kg/m³	820	845
Viscosity at 40 °C	mm^2/s	2.00	4.50
Flash point	°C	55	-
Sulphur content	mg/kg	-	350
Water content	mg/kg	-	200
FAME content	vol%	-	7

2.4.1 First generation biodiesel

Biodiesel can be produced from several sources. The first generation biodiesel is a long chained fatty acid methyl ester (FAME) produced from vegetable oil or animal fat. FAME can be produced from almost any vegetable oil or animal fat, though the most common feedstocks today are rapeseed and soybeans [29].

First generation biodiesel most often shows lower energy content than conventional diesel and often a small decrease in cetane number. First generation biodiesel normally has a higher density and viscosity as well. However, these properties depend heavily on the type of biodiesel and how the biodiesel is produced [31]. In Europe the first generation biodiesel is regulated by the EN 14214 standard. The main requirements in EN14214 are shown in table 4 [32].

Table 4: Main requirements in EN14214 for first generation biodiesel [32]

Property	Unit	Lower limit	Upper limit
Cetane number	-	51	-
Density at 15 °C	kg/m³	860	900
Viscosity at 40 °C	mm^2/s	3.5	5.0
Flash point	°C	101	-
Sulphur content	mg/kg	-	10
Water content	mg/kg	-	500
FAME content	vol%	-	100

Table 4 shows that the first generation biodiesel has higher density, viscosity and flash point requirements than the conventional petroleum diesel.

2.4.2 Second generation biodiesel

Fatty acid fuels put an additional pressure on food supplies during a time of rapidly increasing demand for food [11]. This is why second generation biodiesel has been developed. Second generation biodiesels are based on biomass of cellulosic mass. Second generation biodiesels can be produced from biomass in a variety of ways using processes as fast pyrolysis, hydrothermal liquefaction and gasification with Fisher-Tropsch. The fuel produced from these processes can be utilized in a diesel engine, either right after the conversion or by converting the fuel into biodiesel using after treatments. This is just like how petroleum crude oil is refined into diesel and gasoline. We often refer to these fuels as biomass to liquid (BTL) fuels [11]. Second generation biodiesel is most often associated with high cetane numbers, and low densities and viscosities. The energy content of the second generation biodiesel is normally close to conventional diesel [16].

2.4.3 Emissions in engines using Biodiesel

NOx emissions from biodiesel

The use of biodiesel in diesel engines has varying effects on the NOx emissions. Research has shown that biodiesel NOx emissions can not simply be explained by the change in a single fuel property. The change NOx emissions is rather a result of a number of different changes in fuel properties. These interact and can reinforce or cancel each other, depending on the engine conditions [58]. The most important changes in fuel properties are:

1. *Changed cetane number*
   Biodiesels can have different cetane numbers than conventional diesels. This leads to changes in premixed combustion and diffusion flame combustion fractions, and these factors is known to change the NOx emissions. The cetane number for different types of biodiesels vary and is dependent on the type of biodiesel [58] [59].
2. *Changed chemical structure*
   The chemical structure of biodiesels change the way that the fuel combust. There are many changes in chemical structure from conventional diesel to biodiesel, but the most important ones are density, viscosity, and the fuel oxygen content. A higher fuel oxygen content is often seen in biodiesels, and this may lead to higher flame temperature and therefore higher NOx emissions. The density and viscosity can cause the biodiesel to vaporize earlier, and therefore ignite easier, which will increase the NOx emissions [10] [59].

The different chemical structure and the changed cetane number will interact, and sometimes it will cause an increase in NOx emissions and sometimes it will cause a decrease in NOx emissions. This is not only dependent on the type of biodiesel, but also on the engine type and engine conditions. The most common result when using biodiesel is increased NOx emissions [10] [58] [59].

CO emissions from biodiesel

It is a common trend that CO emissions reduce, if conventional diesel is replaced by biodiesel. Allot of research has focused on this, and reductions as high as 84.4% has been found [10]. In general CO emissions are very dependent on:

1. *Cetane number*
   A change in cetane number changes the CO emissions directly by changing the amounts of premixed combustion and diffusion flame combustion.
2. *Fuel oxygen content.*
   An increased fuel oxygen content leads to more complete combustion, and therefore it most often reduce the CO emissions.

Both of the cetane number and the fuel oxygen content different in biodiesel, and most usually there is an increase in both parameters, which explains the CO reduction [10].

PM emissions from biodiesel.
PM emissions is of particularly interest when working with biodiesel. This is because one of the concerns with biodiesel is that the exhaust has a higher amount of ultrafine particles. Which causes a larger health concern than courser particles [24], as mentioned in section 2.2.3.

Much research has focused on testing for PM emissions from biodiesel, as well as blends of conventional diesel and biodiesel. Generally, results show decreased PM emissions [10] [58]. However, PM can be measured in different ways and small particulates are difficult to measure. The most common PM measurement technique is gravimetric, which only measures the total mass of PM. If the number of PM is measured instead it may show very different results, since larger sized particles weigh more [37].

The most important properties of biodiesel that affects the PM emissions are:

1. *Fuel aromatic content*
   High amounts of aromatic hydrocarbons in the fuel are known to increase the soot formation since, aromatic hydrocarbons form PAHs more easily than other hydrocarbons. Biodiesel normally have higher aromatic content than other fuels.
2. *Cetane number*
   The change in cetane number can cause a larger amount of diffusion flame combustion, which can lead to higher PM emissions.
3. *Fuel oxygen content*
   The fuel oxygen content is important since it can oxidize soot after the combustion, hence reducing the PM emissions [10].

2.5   Experimental engine research

To find out how different types of fuels affect the emissions in diesel engines, experimental engine research is essential. Experimental engine research refers to any experiment done with any type of engine. In this section it will be explained how emission measurements, cylinder pressure measurements and engine torque measurements are done during experiments. While running engine experiments, emissions can be collected from the exhaust, cylinder pressure can be measured inside the combustion chamber and the engine torque can be measured from the crank shaft. There are several techniques and different equipment to use, and with stricter emissions standards more is required from the measurement equipment [33].

2.5.1 NO$_x$ and CO measurements
There are several ways to measure NO$_x$ and CO. Two of the most common, are chemiluminescence measuring and infrared spectroscopy and are also the methods used for the engine experiments in this report.

Chemiluminescence NOx measurements
Chemiluminescence is the most common type of NO_x analyzer. It is based on supplying ozone (O_3) into a fraction of the exhaust gas. The O_3 then reacts with NO inside the analyzer and forms NO_2. The reaction is:

$$O_3 + NO \rightarrow NO_2 + O_3 \qquad\qquad (22)$$

This reaction is used because the NO_2 molecule that is formed is in a so-called excited state. When a molecule is in an excited state it has an elevated energy level, and NO_2 will relieve this extra energy, right after the reaction, as light. Light emitted from chemical reactions, is called chemiluminescence light, and this is what a chemiluminescence NO_x analyzer measures. It is possible to show that if the supply of O_3 into the analyzer is constant, the intensity of the chemiluminescence light is a function of the NO concentration. By measuring the light that is emitted inside the analyzer, one can predict the NO_x concentration in the exhaust gas [34].

Infrared spectroscopy.
An infrared (IR) spectrometer is a measurement technique based on the ability molecules have to absorb infrared light of different wave-lengths. An IR spectrometer will send an infrared light beam at the sample molecules in the exhaust gas and measure how much of the radiation that is absorbed. Gases ability to absorb radiation is a thoroughly researched phenomenon, and the wave-lengths that the different gases are able to absorb are well known. By measuring which wave-lengths the gas absorbs it is possible to calculate which substances it contains and the amounts of these substances. There are several ways to process the absorption data, one of these techniques is non-dispersive infrared (NDIR) [35]. NDIR sensors use a wavelength filter and an infrared detector. The purpose of the wavelength filter is to separate each wavelength, so that they can be measured individually. With a span of infrared light sent through a gas, one can see which wave-lengths that are missing, since all the radiation that passes though the gas is measured by the infrared detector [36].

2.5.2 PM measurements
There are several ways to measure PM emissions. The regulatory method is based on the gravimetric method, a simple filter which collects the particles, and then afterwards weighs them [22]. However, other methods will give a better understanding of the different elements of PM emissions. The particle sampler used in this project is a type of mass spectrometer, called a difference mobility spectrometer (DMS). The DMS has the advantage that it can measure the size distribution of the particles, and not just the total mass of particles as a gravimetric filter.

Mass spectrometry.
A mass spectrometer works by producing charged particles of the substance it wants to measure, and then it calculates the mass of each substance by measuring how much the substances are deflected by an electromagnetic field [37]. The mass spectrometer applies a constant charge rate to each particle that it measures. Depending on the mass of each substance they will contain different amounts of static electricity afterwards. When charged, the different compounds go through the electromagnetic field. Since they contain different amounts of static electricity, the compounds will be deflected differently, depending on their mass. It is then possible to calculate the mass of each compound, depending on the amount of deflection they show. There are several types of mass spectrometers, but they all work by this basic principle [37] [38].

In a mass spectrometer that measures PM emissions, it is particularly important to dilute the gas to separate the particles from each other, and to vaporize any liquid droplets. Too high amounts of particles will clog the spectrometer, and liquid droplets will disturb the

measurements. After the dilution process in the PM mass spectrometer, the particles go through the actual spectrometer. Since all PM consist of more or less the same material, the calculated weight is directly linked to the particles size. PM mass spectrometers can with good accuracy measure particles in the range of 100–200 nm. The lowest measurable size of commercial instruments is about 30 nm aerodynamic diameter [22].

A difference mobility spectrometer (DMS) is a mass spectrometer with a higher resolution than the standard mass spectrometer. Some DMSs can measure particles as low as 5nm aerodynamic diameter. DMS uses a corona charger, a classification column and a series of sensors to measure the size and the amount of particles [22].

2.5.3 Pressure measurements

Piezoelectric transducers are the most common pressure sensors for measuring cylinder pressure in combustion engines. Piezoelectric transducers generate an electric signal that is dependent on the pressure variation in the combustion chamber. The piezoelectric transducers are based the phenomenon that an electric charge accumulates in a crystal, when the crystal is subjected to a mechanical stress, such as pressure. The piezoelectric transducer measures the electric charge in the crystal it contains, and in reality it measures the pressure acting on the sensor [39].

Any sensor inside the combustion chamber of an engine is subject to very high temperature variations. This causes a thermal drift on the sensor. For the piezoelectric pressure sensor, this means that during measurements the measured pressure will gradually drift away from the actual value. This leads to a gradually increasing offset in the pressure measurements. Piezoelectric pressure sensors are actually the most commonly chosen pressure sensor for use inside combustion chambers, because of the resilience against high temperature effects. However, there are still some thermal drift in all pressure sensors and this drift has to be corrected when analyzing the results [39].

2.5.4 Torque and power measurements

To understand the engine performance, the power produced in the engine is a very important parameter. Experimentally, the engine power is calculated from the engine torque:

$$P = 2\pi NT \tag{23}$$

Engine torque is normally measured using a dynamometer. A dynamometer works by connecting the crank shaft from the engine to a dynamometer rotor [11]. A principle drawing of a dynamometer is show in figure 11.
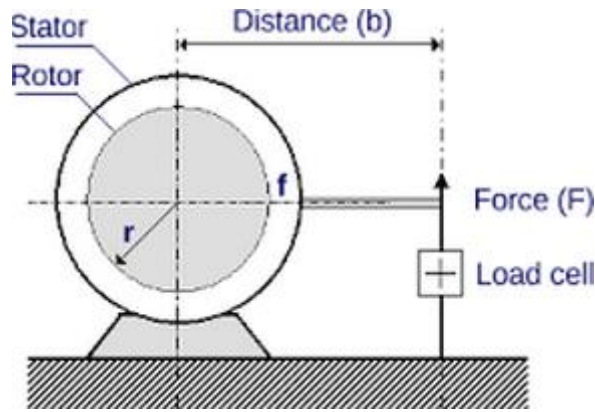
Figure 11: Principle of a dynamometer [11]

The dynamometer rotor is connected with some sort of resistance through the stator. The resistance can be electromagnetic, hydraulic or mechanical. The stator is held stationary and the force it takes to hold it stationary can be measure using a load cell [11]. This force multiplied by the distance between the crank and the load cell, is the engine torque:

$$T = Fb \qquad (24)$$

2.6 Numerical engine research

The model used when simulating engines numerically is normally divided into two parts; the physical model and the chemical model. Generally, the physical model can be solved using equations from thermodynamics and fluid mechanics in computational fluid dynamics (CFD). However, in a combustion engine the chemical reactions must be taken into account as well and a chemical model is necessary. Chemical models are solved numerically using mechanism files. These files describe the reactions that take place during combustion, and their reaction rates. The mechanism files in the chemical models are created separately and have to be solved in parallel with the physical model [40].

One of the difficulties with numerical engine research is the parallel solving of a physical model and a chemical model. The reason why this is difficult is because many combustion reactions happen very fast, and the reaction rates change with the flow characteristics. To get a hold of all the information from these reactions, the time step of the numerical analysis has to be very short and much lower than what is necessary for a physical model [40]. The difference in time scales between the two models is illustrated in figure 12.
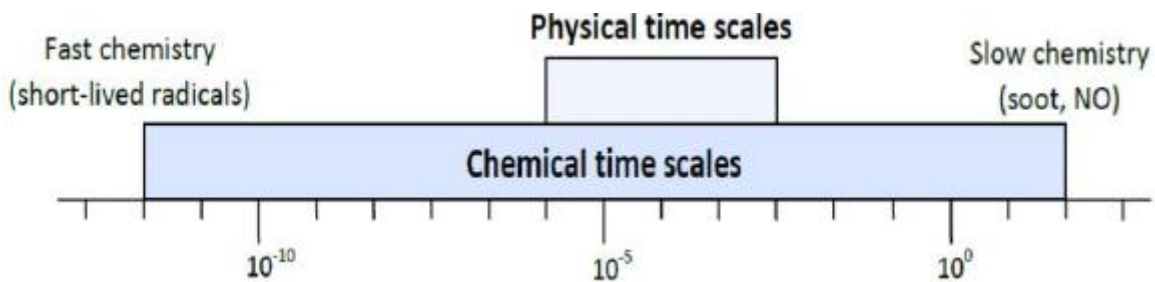
Figure 12: Differences in chemical time scales and physical time scales [40]

In the time scales fast chemistry changes are happening much faster than the physical modelling time scales. By using timescales as low as 10^{-10}, the physical problem would take very long to

26

solve. By choosing timescales in the range of 10^{-4} to 10^{-8} one would lose important information about the short lived radicals. Therefore, to achieve a fast computing speed, one has to do assumptions. This leads to two possible ways to simplify the model. One can disregard the short lived radicals in the chemical model or one can do simplifications of the physical model. In engine applications both simplifications are used [41].

2.6.1 Physical modelling

The physical modelling is here referred to as the solving of physical properties such as temperature, pressure and flowrate. The physical model can be solved using CFD with great results and details. However, a CFD model has a very high computational power demand, and it is quite complex to set up. A way to simplify is by creating one or more zones in the control volume and to consider each of these zones to have uniform physical properties. In other words, the control volume is replaced by one or more homogeneous zones [41].

The physical models used in numerical engine research can be classified in four categories; single-zone models, multi-zone models, probability density function-based stochastic rector models (PDF-based SRM) and full-CFD models. These models will be discussed subsequently.

Single-zone models
Single-zone models are the simplest form of numerical engine research, it involves having just one single zone in the entire control volume. This means that the physical properties are the same everywhere in the control volume. Simulations using single zone models become a pure a chemical analysis of the reaction mechanisms in the engine. The advantage with this model is that is it fast to simulate, however the disadvantage is that it often wrongly predicts the conditions after the reactions. Single-zone models normally result in over-predicted cylinder pressure, under-predicted combustion duration and inaccurate emission estimates. One of the main reasons for the inaccuracy predictions is that it does not take the cooler temperatures and the imperfections at the walls into account. [42]

Multi-zone models
Multi-zone models were created to overcome the errors in the single-zone models. With the multi-zone models separate zones at the walls are used, taking the effect of the walls into account. This approach leads to a fast model which includes the important geometrical and thermodynamic effects of the walls into account, while avoiding the significant computational time required by a full CFD analysis. In total, the multi-zone models give better predictions than the single-zone models. However, the multi-zone model is still a very simplified approach and has large inaccuracies, especially in emission calculations [42].

PDF-based SRM
To improve the multi-zone models further, the SRM model was introduced. The SRM model is so called PDF-based, which means that it uses statistical analysis to describe the physical properties. The multi-zone and single-zone models are based on the assumption that the fluctuations in the physical properties are negligible within each zone. However, to get accurate emission predictions, this is not a good enough assumption. PDF-based SRM models replace the assumption of homogeneous volume based zones with mass based zones, called particles. The SRM model assumes that there is a global equivalence ratio within the combustion chamber, but that each particle can have different equivalence ratios and are able to mix with other particles [41] [42].

Each particle in the SRM model represents a point in the PDF distribution. However the particles are set to follow the thermodynamic and fluid mechanic laws over time. So, for each time step, the PDF distribution will change. The PDF distributions follow a function, which is

derived from the conservation of mass and energy. An example of a PDF-based temperature distribution is shown in figure 13.
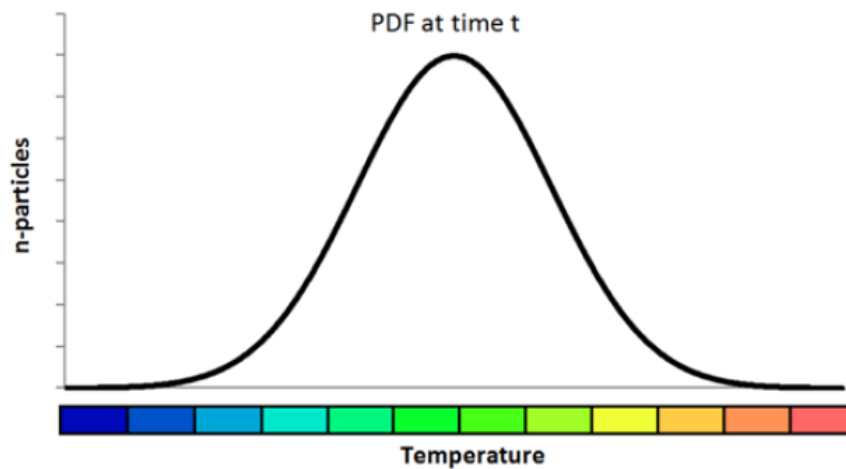
Figure 13: PDF distributed temperature [40]

In figure13 one can see the theoretical bell-shaped PDF for temperature, where the majority of particles have mid-range temperatures and no particles have very low or very high temperatures. The benefit with the SRM is that it provides a way to capture the effects of in-homogeneities and turbulence in the combustion chamber, while not being as computationally demanding as full CFD [40].

Full CFD
If the governing equations are solved directly the physical properties become most accurate. The three zones based models (single-zone, multi-zone and PDF-based SRM) assume that parts of the combustion process is homogeneous. However, with a full CFD model, the physical properties are calculated directly and are never assumed homogeneous. [40] [41]

The advantage of a full CFD is that it handles geometry related turbulent flow inside the engine. CFD models provide flow, energy, concentration and turbulence fields by solving all the governing equations. [40] [42].

2.6.2 Chemical modeling
Chemical modelling involves simulating the chemical kinetics of a system and defining which reactions that take place. Chemical kinetics is the study of reaction rates, and when combined with the thermodynamics from the physical modeling, the reaction rates can be used to determine how fast reactions occur. The modelling is based on a mechanism file which defines the chemical model of the system. The results are heavily dependent on the mechanism that is chosen. The result show how the initial conditions evolve into changes in physical properties and exhaust gas products [41] [42].

The chemical model starts with a mixture of a fuel and an oxidizer. The model solves chemical reactions and calculates the emissions and heat. Typically, the model and the mechanism file become more complex with more complex fuels. For example, a simple fuel like hydrogen has a mechanism file of less than 10 chemical components. These chemical components are most commonly referred to as species. More complex fuels may have several hundred species. Since the mechanism files can be very complex, it is often necessary to simplify them and this is called mechanism reduction [41] [42].

Sometimes the simulation requires as accurate mechanism files as possible, called detailed mechanisms. The detailed mechanisms are raw data files, and include all known reactions for a given fuel. Even though using a detailed mechanism increases the model complexity and simulation time drastically, they can be essential for simulating some combustion processes when a very accurate prediction of emissions is needed. Often when choosing the mechanism size it is a matter of choosing the accuracy of the simulation. Generally if one increase the size of the mechanism, it leads to an exponential increase in simulation time [41].

It is from the detailed mechanism files that the reduced mechanisms are created. These are typically common when dealing with complex and high carbon number fuels. The challenge with this reduction is to reduce the size of the mechanism file while still being able to correctly calculate the chemical process. Mechanism reduction is very important in chemical modelling, but it is considered out of the scope of this project, even though reduced chemical models are used. It is important to know that reduced chemical models may contain errors due to mechanism reduction [42].

2.6.3 Surrogate fuels

Even though chemical mechanisms can be reduced drastically using reduced mechanisms, full diesel mechanisms are not realistic. All liquid fuels, whether they are produced from a fossil source or from a renewable source, consist of several different chemical species. Developing chemical mechanisms for such complex fuels are simply too difficult. Diesel fuels are composed of hundreds of species, and fundamental data for all of these species are not available [54]. The complexity of the diesel fuel is demonstrated in figure 14.
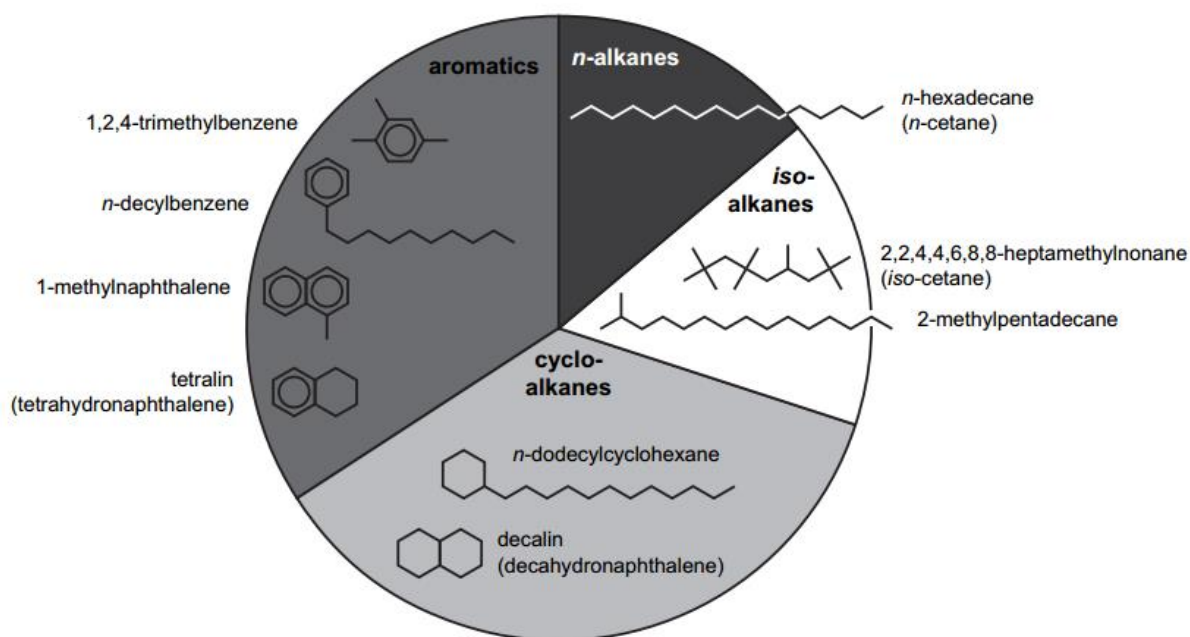
Figure 14: Different chemical classes in a diesel fuel and examples of chemicals in these classes

Figure 14 shows that diesel consist of n-alkanes, iso-alkanes, cyclo-alkanes and aromatics, and each one these groups consist of many chemical species. Even if the fundamental data for all of these species were available, models that represents all of these components would be too large to simulate [53].

The solution is to use one or more simple species as a replacement for the liquid fuel. These replacements are called surrogate fuels. Surrogate fuels are used to emulate the chemical properties of the real fuels, and it simplifies the model greatly. A surrogate fuel needs to represent both the chemical and physical characteristics of the target fuel. This is so that the surrogate properly emulates both the combustion characteristics, and the injection, vaporization, and mixing processes [53]. Finding one single specie that can emulate all these different chemicals is very hard, and choosing the wrong surrogate is often easily visible in the ignition qualities and emission changes in the surrogate fuel. Therefore, it often common to use several species, however for each specie added, the mechanism file increases in size [54].

Most diesel surrogate fuels are n-alkanes. This is because it is then to emulate the actual chain-length of the original diesel fuel. Some common species used as diesel surrogates are n-heptane or heavier alkanes such as n-decane, n-dodecane and n-hexadecane in combination with an aromatic specie [54].

3 Methodology

3.1 Experiment Equipment

The test-rig at the EPT Varmeteknisk engine lab consist of a modern diesel engine. It is mounted on a Stuska hydraulic-dynamometer test bench, which measures and takes away the torque created by the engine. The engine also has several sensors mounted, that allow the user to monitor the working conditions of the engine. In this section the most important equipment used in the experiments will be introduced.

3.1.1 Engine

The engine is a Mercedes Benz in-line 6 cylinder diesel engine, with model name OM 613. The engine is seen in figure 15. The engine is a year 2000 model and it has a direct injection, common-rail injection system and a variable geometry turbocharger. The engine geometry and specifications are shown in table 5.
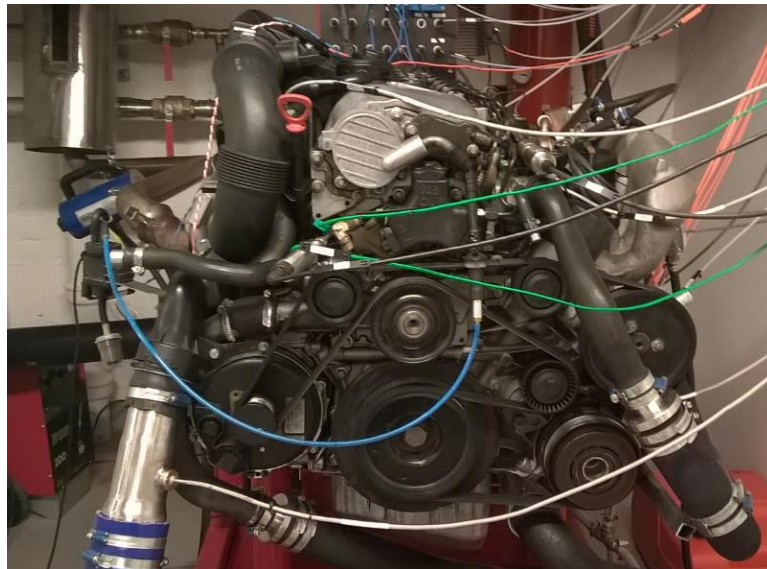
Figure 15: Engine seen from front.

Table 5: Engine specifications [43]

Engine manufacturer	Mercedes Benz
Engine code	OM 613
Engine type	Turbocharged diesel
Cylinders	6
Capacity (cylinder volume) [liters]	3.2
Bore [mm]	88.0
Stroke [mm]	88.3
Connecting rod length [mm]	145.0 [44]

3.1.2 Water-Brake

The dynamometer mounted to the engine is a hydraulic dynamometer, also called a water-brake. It uses water the stator to expose of the forces created in the engine. The water-brake works by having a propeller that spins around on different water levels, the higher the water level, the higher torque can be stopped by the brake. The water runs through the water-brake

continuously, and the water flow never stops. This allows the water level to be easily changed, and the temperature increase from the mechanical work of the propeller will not be a problem [45].

The water brake mounted on the engine test rig is a double propeller water-brake, where two propellers are mounted in series. This makes it possible to have a higher maximum load.

Figure 16: Hydraulic dynamometer (Water Brake) mounted to the engine.

Figure 16 shows the case containing the two propellers in grey. The propellers are connected to the drive shaft behind the red cover, in the right corner in the picture. On the top of the two propellers one can see where the water comes in. The water goes through the red horizontal tube on top of the grey containers, and there are two vertical tubes going in to the propellers. Just outside the picture at the bottom of the grey containers is where the water leaves to the deposit tank.

3.1.3 Water-brake system setup
The whole system with the water-brake is a quite complex system. Since the brake is directly dependent on the water level, it is also dependent on a steady water supply. Therefore it is built a system of tanks and pumps to handle the inlet and outlet water usage. This system can be seen in figure 17.

Process flow diagram - Brake system in engine lab

Pump to tank:
l = 270 cm
Δh=145 cm

Pump 2

Tank 2
Wall
• Volume: 467 liter

Brake to tank:
l = 140 cm
Δh = -25 cm

h = 82cm

Tank to pump:
l = 65 cm
Δh = 0 cm

Wall
Pump to engine:
l = 605 cm
Δh= 50cm

Water brake

Tank 1:
• Total volume: 1329 liter
• Real volume: 545 liter

Pump 1:
• Unknown characteristics
• 53/54 HP
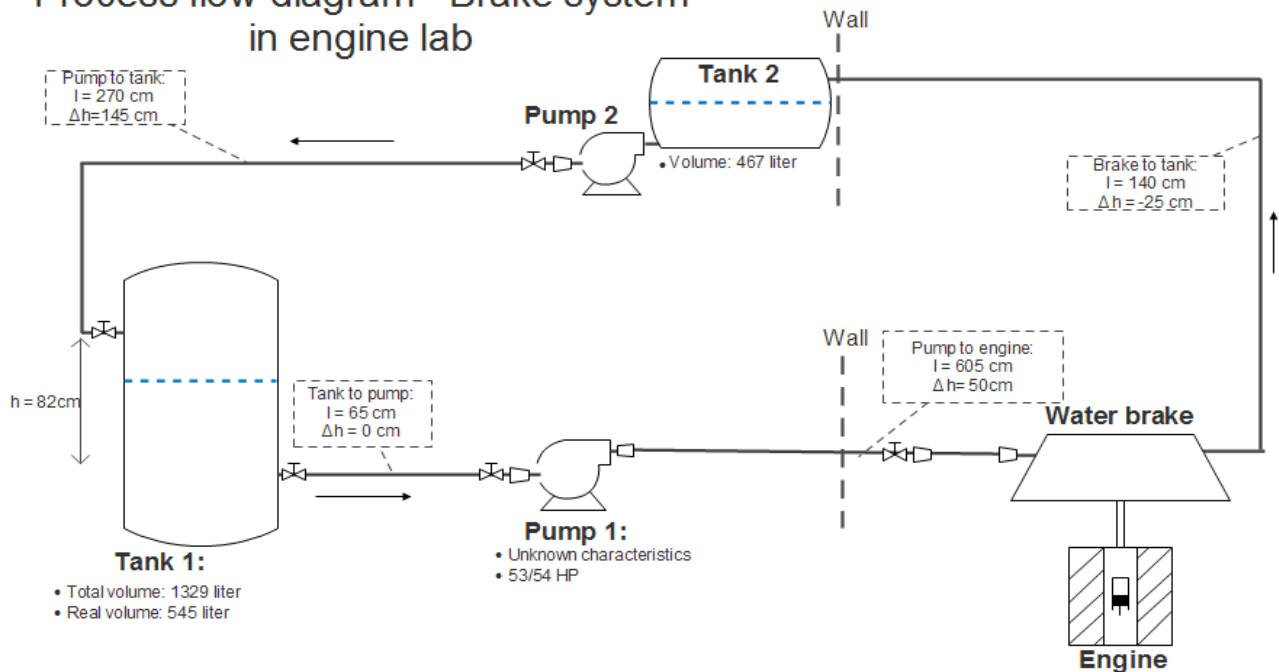
Engine

Figure 17: Process flow diagram of the water-brake system

As seen in figure 17 the system involves two tanks, two pumps and 13m of piping in addition to the water brake and diesel engine. The two tanks and pumps have different functions.

- Pump 1 is responsible for the direct water flow into the water-brake. It delivers the required amount of water into to brake and is therefore the controlling factor of the engine load.
- Tank1 is the delivery tank to pump 1. It is responsible to deliver enough water so that the water-brake never runs out.
- Pump 2 is responsible to hold the water level in tank 1 at a high enough level. It measures the level of the tank and if the level is too low, the pump will start working. Pump 2 therefore works in cycles dependent on the water consumption of the water-brake.
- Tank 2 is the deposit tank for the water-brake. It stores the water that comes out of the brake and keeps it until pump 2 starts to pump it back into tank 1. The water in the water-brake system therefore goes in a loop, which makes it independent on any water supply.

3.1.4 Sensors

To measure the required data to analyze the performance of the engine, the test engine is mounted with many sensors. The sensors measure the most import engine working parameters and emissions. There are two sets of data gathering systems on the engine. They are based on whether the measurements are done at high speed or low speed. Most of the engine parameters such as the torque and the NOx levels are measured at low speed. The low speed measurements are measured at 10Hz (10 measurements per second), which is more than sufficient enough since these measurements are meant to be used to understand the trends during an average engine test. Other measurements such as the cylinder pressure are done at high speed. These are measurements required to understand the trends during each engine stroke, which happens very fast, and therefore these measurements are done at 500Hz (500 measurements per second). All the high and low speed sensors and their units are shown in Table 6 and 7, except for the PM measurements, which are registered by a separate computer.

Table 6: Low speed measurements done in the engine

Channel:	Unit:	Channel:	Unit:
Time	Date		
Exhaust fan	%	Fuel pressure valve	%
Supply air fan	%	Boost valve	%
EGT after turbine	°C	**Begin of main injection**	°
EGT cylinder 1	°C	Injection volume	mm3/inj
EGT cylinder 2	°C	Fuel consumption ECU	l/h
EGT cylinder 3	°C	Airmass flow ECU	kg/h
EGT cylinder 4	°C	Airmass flow stroke	g/str
EGT cylinder 5	°C	**Duration of main injection**	uS
EGT cylinder 6	°C	Engine control mode	int
Spill water	°C	Lambda estimated	-
Fuel temperature	°C	Pressure position - PT 1	°TDC
Oil temperature	°C	Max pressure - PT 1	MPaG
Temperature after cooler-TT2	°C	Turbine speed - SS 2	rpm
Temperature before cooler-TT3	°C	Fuel consumption - FT 1	l/h
Temperature before charger-TT4	°C	Fuel consumption total - FT 1	l
Water pressure - PT 6	hPaG	**Engine torque - Nm**	Nm
Oil pressure - PT 7	hPaG	Engine power - kW	kW
Boost pressure - PT 4	hPaA	Engine power - HP	HP
Process - M0	%	Pressure	hPaA
Exhau st pressure - PT 9	hPaG	Temperature	°C
Intake pressure - PT 10	hPaG	Humidity	%
ECU volt	Volt	**NOx**	ppm
Fuel pressure ECU	MPaG	**CO**	ppm
Boost pressure ECU	hPaA	**CO2**	vol%
Engine speed	Rpm	O2	vol%
Fuel quantity	mg/str	SO2	ppm

Table 7: High speed measurements done in the engine

Channel:	Unit:
Time	Date
Cylinder pressure - PT 1	MPaG
Exhaust pressure - PT 3	hPaA
Fuel pressure - PT 8	MPaG
Engine torque - TQ 1	Nm
Crank	Bool
TDC	Bool

The sensors marked in bold are the sensors that have been used for analysis in this project. When doing experiments, the measurements from the sensors were saved in a result-file. The results-files included results from all the sensors, at high speed and low speed measurements.

3.1.5 Gas analyzer

The measurements done of the exhaust gas emissions where measured by a gas analyzer. The gas analyzer used was a Horiba Portable gas analyzer PG-250. Figure 18 shows the gas analyzer.

Figure 18: Horiba PG-250 gas analyzer.

The Horiba PG-250 measures the exhaust gas emissions using different types of sensors for the different gases [46]. The methods used by the gas analyzer were [46].

- NDIR sensor for CO and CO_2
- Chemiluminescence sensor for NO_x

3.1.6 Particle sampler

The particle sampler used in the experiments was a difference mobility spectrometer (DMS) of the type Cambustion DMS500. The DMS500 has a resolution in particle size from 5nm to 2.5µm. The particle sampler included a heated sample line and a high ratio air diluter. The heated line and the diluter are used to vaporize any liquid droplets, and to reduce the amounts of particles which enters the sampler, to prevent it from clogging [47]. The DMS500 is seen in figure 19.

Figure 19: DMS500 particle sampler [47]

Figure 19 shows the DMS500 with the heated line coming up from the bottom of the figure, and at the end of the heated line is the high ratio diluter. The DMS500 is connected to the exhaust of the engine right after the turbocharger, and it takes a sample of the exhaust to analyze. The DMS500 also include a vacuum pump which is used to drag the sample out of the exhaust [47]. The DMS500 is connected to a computer and the particle readings can be saved and further analyzed.

3.1.7 Fuel

The fuels used in the engine test were a conventional B7 diesel, a FAME first generation biodiesel and a second generation biodiesel. B7 diesel means that the diesel contains 7% biodiesel. All diesel sold in Norway is B7, and this fuel is still thought to represents the behavior of a petroleum based fuel. The properties of the three fuels are summarized in Table 8:

Table 8: Properties of fuels used in experiments

	Conventional Diesel B7 [48]	1st generation biodiesel [49]	2nd generation biodiesel [50]
lower Heating Value [MJ/kg]	42.9	37.1 [51]	43.9 [48]
Cetane Number	53.4	53.1	79.4
Density [kg/m^3]	838.8	883.9	779.9
Viscosity [mm^2/s]	2.643	4.426	3.033
Flash Point [^{o}C]	68.0	159.0	80.0

Table 8 shows that the first generation biodiesel has a reduced lower heating value compared to the conventional diesel and the second generation biodiesel has an increased cetane number. There is also a large difference in viscosity and flashpoint between the three fuels. The first generation biodiesel generally has higher density and viscosity than the other two fuels. The conventional diesel is within the requirements for EN590, and the first generation biodiesel is within the EN14214 regulation.

The two biodiesel used was supplied by the company ECO1 Bioenergi. The first generation biodiesel was called "ECO1-Arctic 100%, FAME biodiesel", and was stored in fuel drum number 4. The second generation biodiesel was called "ECO1-Polar 2G 100%, Neste Green-100 diesel", and was stored in fuel drum number 2. The origin of these fuels are unknown.

All the three fuel are stored and kept in the lab, when changing fuel a clean new fuel tank was used, so that there were no contaminants from the old fuel in the tank.

Figure 20: Fuel tanks, the left picture show the tanks connected to the engine

Figure 20 shows the Fuel tank system. The two pictures in the left and in the middle show the barrels which the fuel is stored, and the right picture shows the fuel tanks connected to the engine.

3.1.8 Engine control computers

The engine is controlled through the virtual engineering workbench LabVIEW. LabVIEW is installed on the computer in the lab, which is situated in the room next to the engine. From the computer it is possible to start the engine and control all the important engine parameters and to log the measurements. The computer screens with LabVIEW opened are shown in Figure 21.
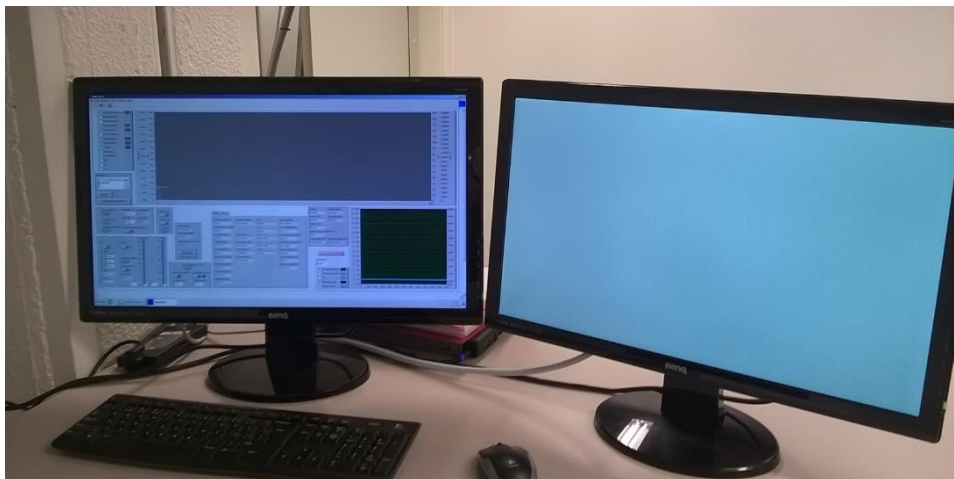
Figure 21: Engine control computers used to do experiments in the lab.

3.2 Experiment Test Procedure

3.2.1 Engine test modes

The object of this thesis is to test the behavior of biodiesel in terms of engine performance and engine emissions. To test this and to have a large number of measurements to compare, there were done several experiments at different loads and RPM. Each one of these different combination of RPM and load are defined as test modes. A test mode is a selected engine condition where the experiments are chosen to be conducted.

All the test modes were done at a locked load, either 10, 20, 30 or 40 % of the maximum load of pump 1, which supplies the water-brake. This means that it is the output torque that is locked and not the valve opening or the fuel amount. By locking the load it is easier to compare the

different fuels in a realistic way. It is the ability to produce torque which is the purpose of an engine in the first place. An on-road engine will have a minimum torque requirement to be able to push the car sufficiently. Therefore, the three different fuels are best compared at locked load. Since all the engine tests are at a locked load, there will be changes in the injected amount of fuel between the different fuels. The engine will increase the amount of fuel injected, if the fuel has a too low energy content to obtain the set load and RPM. The first generation biodiesel has a lower energy content than the conventional diesel and the second generation biodiesel (see table 8). Hence the first generation biodiesel is expected to have a higher amount of fuel injected than the two other fuels.

All the different engine modes that were tested are shown in table 9:

Table 9: Engine modes at which measurements were done

	10% load	20% load	30% load	40% load
1800 RPM	X	X	X	
2000 RPM	X	X	X	
2400 RPM	X	X	X	X
2600 RPM	X	X	X	X
2800 RPM	X	X	X	X

There were no tests done at 40% load and low RPM because the water brake started to surge at such a high loads, which was not noticeable at high RPM. Turbine surge is a phenomenon that happens when the turbine reaches its maximum designed load. Then the turbine starts to make noise, and the RPM increases rather than the load. The reason for no testing at low RPM test modes is because the engine is unstable between 1400 RPM and 1800 RPM, meaning the engine is shaking more than normal. This is thought to be caused by resonance between the engine driveshaft and the water-brake. The RPM's below 1400 RPM are having the same problems as at 1800 RPM and high load, the turbine starts to surge.

3.2.2 Setting engine parameters

There are several engine parameters that change the engine performance and emissions, this project focuses on the effect of different fuels, and other engine parameters would preferable be set to a constant value. Therefore the engine parameters that were possible to change, were set at a constant value. This was done at all engine modes, and it made sure that there were as few variables as possible, between the different engine modes. The parameters which were changed, were the injection timing and the turbocharger pressure.

The injection timing was set to -10 CAD at all the different engine modes. This was done using the engine control system on the engine control computer. The idea behind having an injection timing of -10 CAD was so that the SOC would become just too early at low RPM (just before TDC) and slightly too late at the high RPM (causing the cylinder pressure to decrease before SOC). This was necessary to achieve the same injection timing at all engine modes.

The turbo pressure was set to a constant value of 1.2 bar at all engine modes. This was chosen as it was a stable value and without any turbocharger turbine surge throughout all the engine modes. It was also above atmospheric pressure. This was important so that the engine operated with a higher inlet pressure than the cylinder pressure during the air intake, as all turbocharged engines are intended to do. By locking the turbocharged pressure, a constant inlet air pressure between the different engine modes was achieved.

3.2.3 Running engine tests

To avoid uncertainties, all the measurements were done in an arbitrary order and several test were done for each engine mode. Within the given time in the lab three complete series (measurements at each engine mode shown in table 9) of tests were done using conventional diesel and second generation biodiesel, and 2 complete series of tests using the first generation biodiesel.

All the measurements were done with a warm engine, and to make sure that the engine was properly warmed, the engine was run for 30 minutes to 1 hour before doing any measurements. There are two main reasons why this was beneficial. Firstly, it is well known that combustion engines yield the best performance result when properly warmed, and secondly the engine calibration was done at a warm engine. This means that the engine is performing far better in terms of combustion efficiency when it is warm compared to when it is cold. Doing the measurements when the engine was performing well and as intended to from the manufacturer, was thought to be the best arena to compare fuel performance.

The measurements were gathered using the engine control setup in LabVIEW, and logs where made measuring high speed and low speed. When changing the engine mode to do a new measurement, the engine was left to run at this engine mode for 15 minutes, to ensure that the engine was stable at this new engine mode.

3.2.4 Emissions measurements

The emission measurements were done using the Horiba gas analyzer and the Cambustion particle sampler. However, because of trouble with the particle sampler only one complete experiment measuring PM emissions was done. This complete experiment was done with the first generation biodiesel. The Cambustion particle sampler broke down because of electrical issues, and it was not possible to fix it within the timeframe of this project. The only comparable result that was collected was at three different engine modes between conventional diesel and first generation biodiesel.

The NOx, CO and CO_2 measurements were logged with LabVIEW workbench using the engine control computer, and the NOx, CO and CO_2 measurement data was included in the results file from the engine sensors. The particle sampler had to be run through a separate computer and was not included in the results file shown in section 3.1.3. The particle sampler results was saved in a separate results file. The user interface on the particle sampler computer is shown in figure 22.
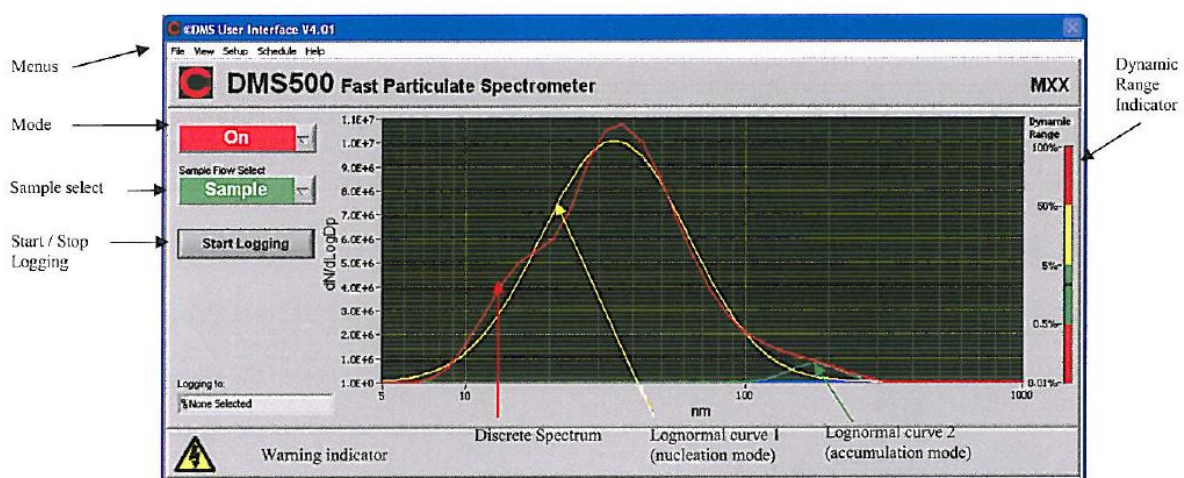
Figure 22: User interface on the particle sampler DMS500 [47]

39

Figure 22 shows how the particle measurement size distribution was visible at all time during the experiments. This made it possible to see that the size distribution was realistic before doing the test. It was then visible if any in-regularities entered the particle sampler during the measurements. If so, the test could be repeated. The particle sampler was used with a dilution factor of 100 and a heated line temperature of 150 ˚C. At this point all the size dirstubutions shown on the user interface was considered to be realistic.

3.3   Processing the data

3.3.1 Complexity with the gathered data
The gathered data from the experiments came in such a form that was not perfect for further analysis. The main difficulties with the results were:

- The engine pressure was linked to the computer clock and not to the engine CAD
- None of the results were averaged
- There were no heat release rate measurements done
- There was a considerable pressure drift in the pressure sensor
- There were no SOC measurement

These problems were solved by writing a Matlab script. How this Matlab script works and how the difficulties were solved, will be explained. The Matlab script is provided in appendix A. The script in appendix A, is a script which reads three result files and plots the results together in one plot. The three different result files are intended to be one for each fuel, so that the three fuels could be compared with ease.

3.3.2 Making a CAD axis
The pressure measurement were done at high speed and for several engine cycles each time. However, the crank angle at each pressure measurement was not known. The only known information on where the piston was during the measurements was the TDC signal. The TDC signal was a measurement done at high speed at the same time as the pressure measurements were done. The TDC signal is measured by a sensor which registers when a piston is at TDC. This means that the signal shows 6 TDC signals for each complete engine cycle (because the engine has 6 cylinders). One of these TDC signals represents the actual TDC in the cylinder where there is a pressure sensor mounted. The TDC signal was saved as a vector which changed value from 1 to 0 when the piston was at TDC, and changed from 0 to 1 when the piston was at BDC. A plot illustrating the relation between the TDC signal and the cylinder pressure can be seen in figure 23.
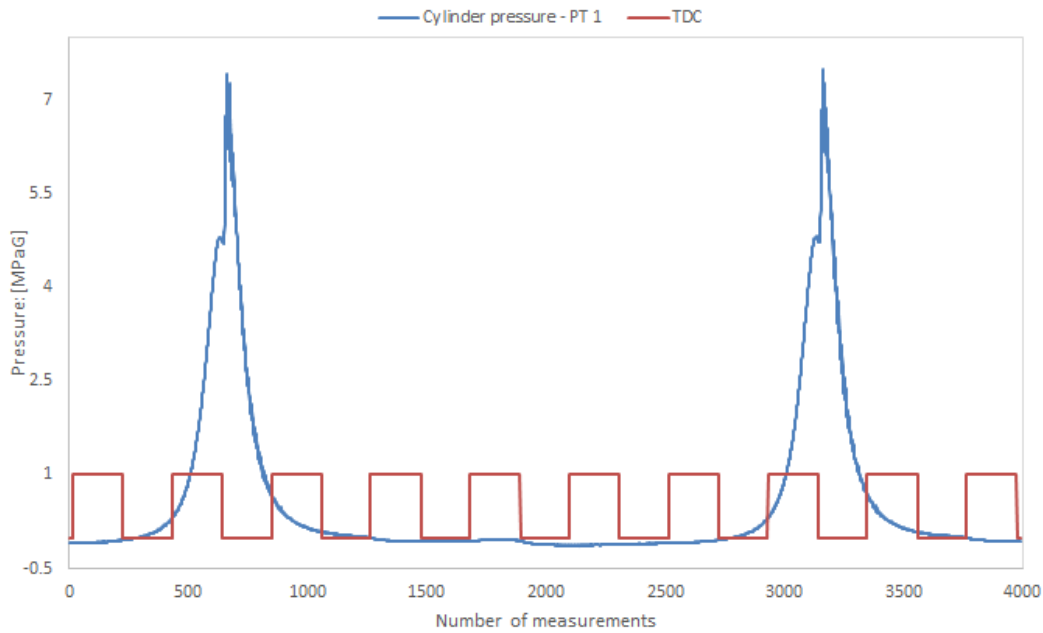
Figure 23: Cylinder pressure and the TDC signal

Figure 23 shows two cylinder pressure curves in blue and the corresponding TDC signals in red. It is visible that there are 6 changes from 0 to 1 between the two pressure peaks. The true TDC for the cylinder with the pressure sensor, is the TDC signal which corresponds to a high cylinder pressure. Figure 23 also shows that there is no CAD axis, only a list counting the number of measurements. There is one TDC signal which corresponds to the compression peak of the cylinder pressure, this is the true TDC for the cylinder with a pressure sensor.

To create the CAD axis, the Matlab script in appendix A is used. The Matlab script constructs a CAD axis by finding the true TDC and the number of measurement points in one complete engine cycle (number of points between each true TDC). The true TDC is defined as the TDC signal were the pressure is higher than 3 MPa. This can be seen in appendix A, between line 57 and 90. One complete cycle is considered to be 7 TDC signals long, as it has to contain two TDC signals for the cylinder with a pressure sensor. The number of measurements in a complete cycle can then easily be found, this can be seen between line 221 and 223 in appendix A. It is now possible to calculate the crank angle axis since it is known that a complete cycle is 720 CAD long. The Matlab script then divides 720 degrees by the number of measurements points in a complete cycle, and then it is known how many CAD it is between each measurement point. By doing this, it is assumed that the distance between each measurement point is the same between all the points in a complete cycle. It should be a safe assumption since the engine speed is locked. Then a complete crank angle axis is generated by defining TDC as 0 CAD. This can be seen between line 283 and 328 in appendix A.

The generated crank angle axis is saved as a vector, and together with a pressure vector which is read from the result files, a proper cylinder pressure curve is made. The cylinder pressure data is read from -360 CAD to 360 CAD, which corresponds to a full engine cycle with the true TDC in the middle of the vector.

3.3.3 Averaging cylinder pressure data

To get a representative cylinder pressure curve that is corrected for the individual variations between each engine cycle, it is necessary to average the data between several engine cycles. This is normally a very simple procedure in Matlab, and can be solved by simply using the function called "mean". However, averaging vectors implies that the vectors have the same

41

length, and this is not the case with the engine cycles from the experiments. Each cycle length may vary with several measurement points, and this had to be solved before the cycles could be averaged.

The cause of the different amounts of measurement points, is a small variation in engine speed during the experiments. The variation in engine speed can be in the scale of 10 RPM between each cycle. This RPM change causes a few extra or a few less measurement points in each cycle. The variation is less than one percent of the total amount of measurement points, which is higher 2000 points per engine cycle, dependent on the engine speed. However the variation still causes trouble when trying to average the cycles.

The way the problem with the different vector lengths was solved by adding zeros at the end of all the pressure vectors, except those that had the longest length. This meant that there were cylinder pressure values added at the end of the shorter engine cycles. As seen in figure 23, the engine pressure at end of the cylinder pressure vector is not far from zero, and therefore adding zero pressure does not change the pressure curve drastically. In addition, the cylinder pressures that are of interest are the cylinder pressures during combustion, and the end of the vector is far away from the end of combustion. The averaging of the cylinder pressure can be seen between line 90 and 156 in appendix A.

The amount of cycles that were averaged out was chosen to be 16. This was because the shortest result file from the engine experiments contained 16 engine cycles, and by choosing 16 cycles there was no need to change the Matlab script when analyzing the different engine modes. 16 averaged cycles were also considered to be enough to correct for variation between the different engine cycles.

3.3.4 Correcting for pressure drift
The pressure drift, or the thermal drift, of the pressure sensor was described in section 2.5.3. The pressure signal from the experiments was corrected by finding the minimum measured pressure in each cycle, and then setting it be 0 MPa. This means that each pressure measurement is subtracted by the minimum measured pressure, and for all the different cycles, the minimum pressure is 0. The correction for pressure drift can be seen in line 157 to 190 in appendix A.

It is important to remember that the pressure measurements are in gauge pressure, so the minimum measured pressure should actually be 0. Therefore this method is a simple and adequate method to remove the pressure drift.

3.3.5 Calculating heat release rate
The HRR is not measured in the experiments, and it therefore has to be calculated from the cylinder pressure. This is done using equation (11), (2) and (3) which were introduced in chapter 2. Equation (11) is dependent on the pressure rate and the volume rate. The pressure rate and volume rate were calculated by dividing the volume and pressure difference in each measurement point by the change in CAD. The calculation of HRR can be seen from line 219 to 400 in appendix A.

The specific heat capacity γ was chosen to be 1.32. This unit value is chosen simply because it lies between 1.3 and 1.35, which according to Heywood [11] is considered to be the appropriate range.

3.3.6 Ignition delay and 50 percent heat release
The ignition delay had to be calculated from the cylinder pressure or the HRR since the SOC was not measured. How SOC can be defined was discussed in section 2.1.7. In this project the SOC was chosen to be calculated from the HRR. The SOC is then defined as when the HRR goes from negative to positive just after SOI. The SOC can then easily be found using the

Matlab function called "sign", which makes it possible to find the measurement point and CAD where the HRR curve changes from negative to positive. In appendix A, from line 402 to line 473, the ignition delay is calculated.

The time until 50% heat release was found calculating the total HRR, and then finding out at which CAD half the total value was reached. This is done from line 487 to 553 in appendix A.

3.4   Simulation

3.4.1   Program and simulation method
The program LOGEsoft was used to simulate the conditions inside the engine numerically. The program is a sophisticated chemical mechanism simulation package with 0D and 1D reactor models. It has the ability to simulate engines using a PDF based SRM model [52].

The PDF based SRM model was described in section 2.6.4. LOGEsoft uses the PDF function combined with the Navier-Stokes equation to solve the physical behavior of the mixture and the Woschni heat transfer model to solve the heat transfer to the walls [52]. The resulting equation is:

$$\frac{\partial}{\partial t}F_\phi(\psi,t) + \frac{\partial}{\partial \psi_i}\Big(G_i(\psi)F_\phi(\psi,t)\Big) + \frac{\partial}{\partial \psi_{s+1}}\Big(U\big(\psi_{s+1}F_\phi(\psi,t)\big)\Big) = mixingterm \quad (25)$$

where $F_\phi(\psi,t)$ is the vector containing the state variables ψ, decided from the PDF statistical analysis and the corresponding bell shaped PDF curves shown in figure 13. The state variables are the chemical composition and temperature. The terms U and $G_i(\psi)$ describes the changes to the state variables due to chemical reactions, heat transfer and volume work. These are decided from separate equations which are considered to be out of the scope for this project.

All the parameters needed to solve equation (25) are given in the simulation settings. The chemical properties such as molecular weight, density, reaction rate and the heat capacity are given in the chemical mechanisms files that are supplied to software. Parameters such as wall surface area, volume and wall temperature are given in the simulation settings. The mixingterm is a term which is specific to the mixing model chosen to be used. This will add another term on the right hand side of equation (25) [52]. Equation 29 is solved numerically using a finite difference scheme which is described in equation 26:

$$\frac{1}{h}(U(\psi_{s+1})F(\psi,t) - U(\psi_{s+1}+h)F(\psi_1,\dots,\psi_s,\psi_{s+1}-h,t)) \quad (26)$$

where h is the fluctuation in temperature and t is the time. LOGEsoft uses a so called time-stepping method where the differential equation (25) is decomposed into 4 different parts; piston movement, mixing, chemical reaction and heat transfer. Each part of equation (25) are solved separately after each other. This makes the process faster, however, the equations are much longer. Each one of these equation are solved iteratively, and the convergence limits for iteration are given in the simulation settings [52].

3.4.2 Simulation procedure

The simulation procedure used consisted of four steps:

1. The chemical mechanism files were uploaded to LOGEsoft
2. The type of reactor and the simulation settings were chosen
3. The case was set to simulate through all the chosen CADs
4. The results were compared with experimental results

The user interface in LOGEsoft is shown in figure 24.
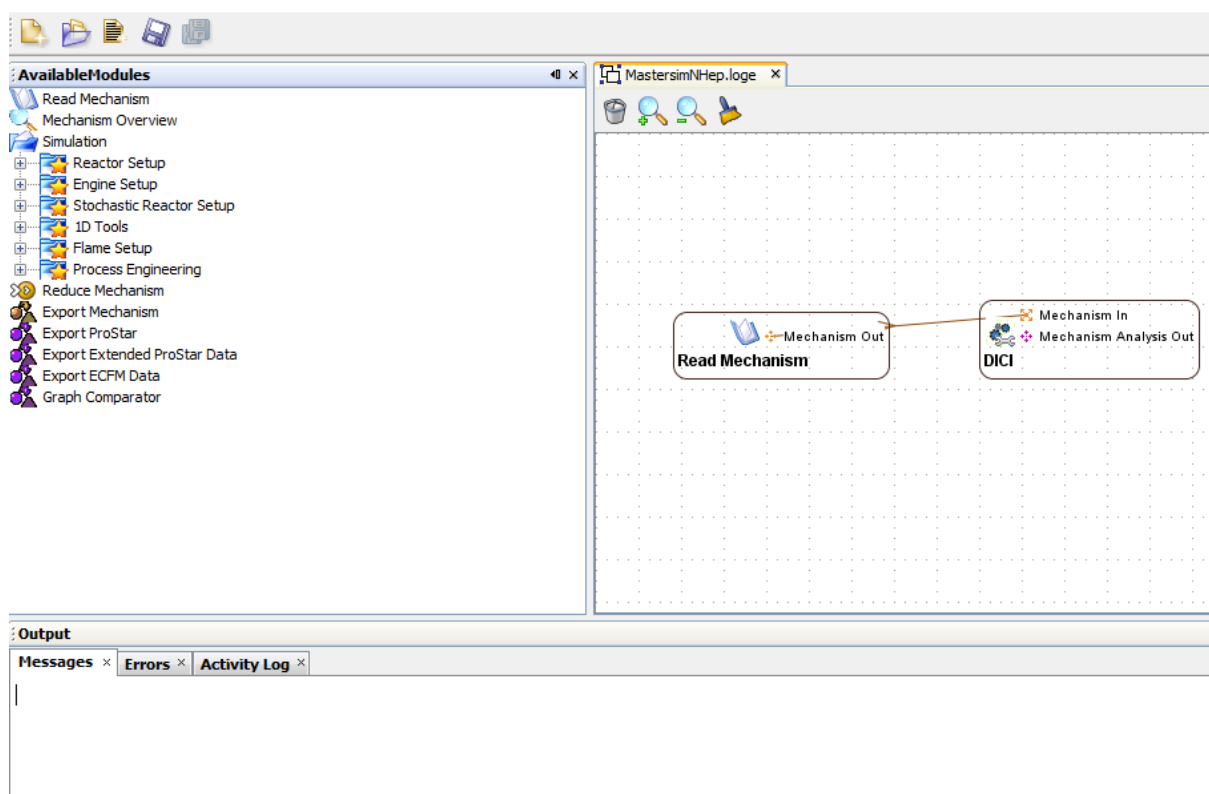
Figure 24: LOGEsoft user interface

Figure 24 shows the output panel in the bottom, where the simulation messages are displayed. The available modules on the left, where the type of simulation was chosen. The read mechanism node in the middle, where mechanisms are selected. And the DICI node on the right were the simulation settings are chosen.

The simulations were done with two different mechanism files. An n-heptane surrogate mechanism, and a mechanism, containing n-decane and 1-methylnapthalene species as a surrogate for diesel, and Methyldecanoate (MD) as a surrogate for biodiesel. The mechanism containing n-decane, 1-methylnapthalene and MD species was supplied by LOGEsoft, as they recommended it for diesel and biodiesel simulations. The properties of the fuel surrogates is shown in table 10.

Table 10: Properties of fuel surrogates [55] [56] [57]

	Heating value [MJ/kg]	Cetane number
N-heptane	44.6	56
Diesel surrogate	42.3	56
Methyldecanoate	34.1	47

The term diesel surrogate is used for the n-decane and 1-methylnapthalene mixture which is used. The mixture consist of 30% 1-methylnapthalene and 70% n-decane. It is noticeable that the two surrogates have very similar properties and are therefore expected to simulate equally good. By comparing table 10 with the fuel properties in table 8, it is clear that the two surrogates for diesel have properties close to conventional diesel. In contrast, the MD has a cetane number which is lower than the two biodiesels used in experiment.

3.4.3 Simulation settings

To give LOGEsoft the necessary information about the engine, the fuel and the simulation limits, the simulations settings were essential to get reliable results. Many of the simulation settings were specific to the engine used in the experiments while others, such as the Woschni constants, the inlet pressure and temperature were parameter which was not known. However some of them were essential to the simulation. To find the correct simulation settings, simple trial and error was used. This was done by comparing the simulated cylinder pressure curve with the experimental cylinder pressure curve.

When comparing the simulated cylinder pressure with the experimental cylinder pressure, the motored-pressure was used. The motored-pressure is the cylinder pressure curve in the engine if no fuel injection happens. The experimental motored-pressure and the simulated motored-pressure should match. If this is the case, it is an indicator that the simulation settings are correct. The most crucial simulation settings, with the largest effect on the motored-pressure, was found to be the inlet pressure and temperature. The simulation settings used in the final simulations are shown in figure 25 – 28.

Figure 25: Solver settings used in LOGEsoft simulations

Figure 25 shows the solver settings. The time step is set to 0.5 CAD, which means that for each 0.5 CAD, LOGEsoft will calculate all the state variables. The default solver settings include a low tolerance limit and a small time step. These are considered the most crucial values and having such low values are considered to be adequate. As mentioned in section 2.6, the shortest chemical timescale of short lived radicals are in the range of 10^{-10} and hence the minimum time step size is in the correct scale.

Figure 26: Engine data used in LOGEsoft simulations

Figure 26 shows the engine data. The engine data has to be the same as shown in table 5. In addition to the basic engine geometry, the Woschni factors, the swirl ratio, the engine RPM and the initial and end crank angle are chosen. The Woschni factors are the parameters which describe the heat transfer between the walls and the gas inside the combustion chamber [52].

The initial crank angle is chosen to be -100 CAD, because then it is safe to assumption that the inlet valves have closed. Therefore the inlet pressure and temperature can be matched against the experimental results. The final crank angle is chosen to be 100 CAD because then it should be safe to assume that the combustion is finished.

The Woschni factors are all chosen to be the default values. It was carried out simulations with varying Woschni parameters, but the result did only show small changes. Therefore it was concluded that the Woschni factors were best left at the default values. The effect of the wall temperature was also studied, it caused an increased motored pressure, however, the default value was considered to be the most realistic.

Figure 27: Stochastic data used in LOGEsoft simulations

The stochastic data defines the PDF based SRM model settings, the number of particles is defined, as well as the mixing model. The stochastic data were all chosen to be the default value, except for the mixing time. Through several simulations, reducing the mixing time showed much better results for the combustion phase of the cylinder pressure. Therefore the mixing time was set to 0.5E-3.

Figure 28: Gas Composition used in LOGEsoft simulations

The gas composition settings were some of the most important parameters that were adjusted. The inlet pressure and temperature proved to have a huge impact on the cylinder pressure curve. Trial and error revealed that:

- Lowering the inlet temperature increased the motored-pressure peak
- Lowering the inlet pressure lowered the motored-pressure peak.

The inlet air temperature was measured to be around 23˚C. However, choosing such a low inlet temperature resulted in no combustion. A fine-tuning between a low enough temperature to avoid a too high motored-pressure, and a high enough temperature to get a proper combustion peak had to be done.

When testing different inlet temperatures and pressures it was found that the higher the inlet temperature, the easier it was to find a simulated cylinder pressure which matched the experimental cylinder pressure. The 383K inlet temperature was selected as it was considered to be the highest realistic inlet temperature. The combination of an inlet pressure of 1.65bar and an inlet temperature of 383K was achieved through the trial and error process.

3.4.4 Fuel simulation settings

The diesel engine simulation model which is used in the simulations, require two input files which describe the fuel injection profile and the vaporization data. These two files are essential to the simulation, since this is where all the information about the fuel is given.

The fuel injection file consist of two columns; the first column contains the CAD and the second column contains the corresponding injection amount. An example injection file is shown appendix B. The file given in appendix B is the file made for the simulation done at 2400 RPM and 20 % load. From this file the first eight lines are shown in table 11. Table 11 shows how the fuel injection file also contains the information about the fuel temperature and which fuel species from the mechanism file that should be injected.

Table 11: First 8 lines of the fuel injection file at 2400 RPM and 20% load

Temperature = 3.1100e+02	
SpeciesLiquidDataFileName = "fuel_species_data.txt"	
molefraction	
BEGIN	
N-C7H16 = 1.00000e+00	
END	
totalfuelmass = 1.14E-05	
nbrofinjectiondata = 181	

For each engine mode it was necessary to make a new injection file, since the end of injection and total fuel mass is different for each engine mode. The injection profile shape had to be assumed, since there was no measurements of the injector needle lift. The only information known about the fuel injection was the start and finish. The shape chosen was a trapezoidal shape, because it is a realistic injection profile for many fuel injectors, and it was easy to generate. The shape of the injection profile at 2400 RPM and 20% load is seen in figure 29.
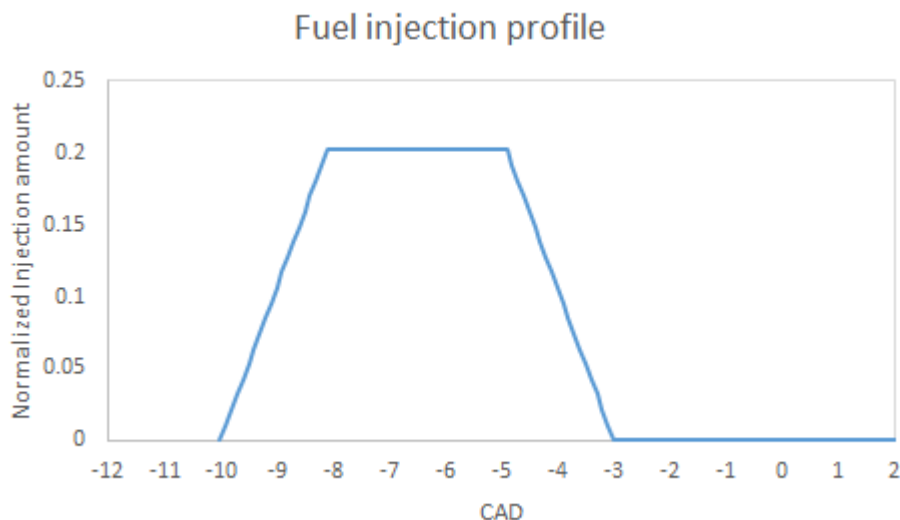
Figure 29: Fuel injection profile at 2400 RPM and 20% load

Figure 29 shows that the fuel injections starts at -10 CAD and ends at -3 CAD. The end of injection is found from the measured duration of the main injection, as was a result from the engine experiments. The injection profile is normalized having an area of 1, LOGEsoft

48

multiplies the profile by the total fuel mass to find the amount fuel that has to be injected at each CAD. The exact shape of the injection profile is found using the area formula for a trapezoidal:

$$A = \frac{1}{2}h(b_1 + b_2) \tag{27}$$

By setting the area equal to one, and assuming the values for b_1 and b_2 (b_1 and b_2 represents the two parallel sides of the trapezoidal with different length), it is possible to find the height h necessary to create a trapezoidal with an area of 1.

To make sure that the simulated combustion produces the same amount of energy as in the experiments, the injected fuel amount has to be corrected for the difference in the heating value of the diesel and the heating value of the surrogate used. This was done using equation (28):

$$sim.\,fuel = \frac{Q_{HV,surrogate}}{Q_{HV,Diessel}} \times measured\,fuel \tag{28}$$

where *sim.fuel* is the corrected fuel amount, which is specified in the injection file, and the measured fuel is the fuel measured from experiment.

The fuel species file is much simpler to construct than the injection file. The fuel species data contains the temperatures and pressures for which the fuel will vaporize. It also contains the NASA polynomials of the fuel. The NASA polynomials are used to find the thermodynamic properties such as the specific heat capacity as the temperature change. Because there was no data available for the n-decane, 1-methylnapthalene and the MD species, the data for the n-heptane was used for all these species.

3.4.5 HCCI simulations
Because of problems with the diesel engine simulations, it was necessary to simulate a Homogenously Charged Compression Ignition (HCCI) engine instead. In an HCCI engine, all the fuel is injected into the combustion chamber before the compression stroke, and the fuel air mixture is assumed to be homogenously mixed at combustion.

When simulating an HCCI engine the fuel amount is entirely decided by the equivalence ratio. A high equivalence ratio represents a lot of fuel, while a low equivalence ratio represents a low amount of fuel. Except from the fuel settings, the HCCI simulation is the same as the diesel engine simulations. The same simulation settings as in the diesel engine simulations were therefore selected for the HCCI simulations.

To find realistic equivalence ratios, which would represent the engine conditions in diesel engines, an approximate equivalence ratio of the lab engine was calculated. The engine control system measures the air amount and the injected fuel amount, and by comparing the air to fuel ratio with the stoichiometric air to fuel ratio from N-heptane, an approximate equivalence ratio is found using equation (5) from section 2.1.5. The Stoichiometric n-heptane reaction is given by:

$$C_7H_{16} + 11(O_2 + 3.76N_2) \rightarrow 7CO_2 + 8H_2O + 41.36\ N_2 \qquad (29)$$

Therefore the stoichiometric air to fuel ratio could be calculated by:

$$\left(\frac{A}{F}\right)_{stoichiometric} = \frac{11(M_{O_2} + 3.76M_{N_2})}{M_{C_7H_{16}}} \qquad (30)$$

The actual air to fuel ratio was found using the measured air amounts and the measured fuel amounts, shown in table 12.

Table 12: Measured amounts of fuel and air and resulting equivalence ratio

		Injected fuel [mg]	**Injected air [mg]**	**Equivalence ratio**
1800 load	**RPM-10%**	8.5	557	0.23
2400 load	**RPM-20%**	11.8	539	0.33
2800 load	**RPM-40%**	20.5	542	0.6

As seen in in table 12, the injected air was approximately the same between the three engine modes. This resulted in varying equivalence ratios. The equivalence ratio at 1800 RPM and 10% load was found to be too low to be able to simulate any combustion using the MD biodiesel surrogate. The same thing was a problem at 2400 RPM and 20% load, but by increasing the equivalence ratio to 0.4, this problem was avoided. The result was therefore two engine modes which was used for HCCI simulations, 2400 RPM and an equivalence ration of 0.4 and 2800 RPM and an equivalence ratio of 0.6.

3.4.6 Comparing with experimental data

To compare the simulated data and the experimental data, there was a separate Matlab script produced for each engine mode. This Matlab script is very similar to the Matlab script in appendix A, and is therefore not shown in this report. This Matlab script had to adjust the difference in pressure scale and do minor adjustments, so that the two data sets was comparable. The most important changes were:

- The pressure in the simulations where saved in Pa, while the experimental pressure data was given in MPa gauge pressure. This was fixed by multiplying the simulated pressure by 10^{-6} and removing one atmosphere pressure.
- To remove any inaccuracy in the measurements or in the simulations, and to make the two pressure curves comparable, both pressure curves were modified to have a pressure of 1.65 bars at -100 CAD.

4 Results and Discussion

4.1 Engine Experiment

In this section the results from the engine experiments will be presented. First the efficiency and specific fuel consumption will be showed, then the exhaust emissions, and after that the cylinder pressure and heat release rates. Lastly, the ignition delays and time until 50% heat release will be presented.

4.1.1 Efficiency and specific fuel consumption

The specific fuel consumption and fuel conversion efficiency give an idea of how the different fuels perform in the engine. In this section the results for both of these parameters are shown, for the different type of fuels, in order to give a good comparison between them.

Specific fuel consumption

Figure 30 shows the specific fuel consumption (sfc) of the engine, plotted against the brake mean effective pressure (bmep) at 1800 RPM, 2400 RPM and 2800 RPM.
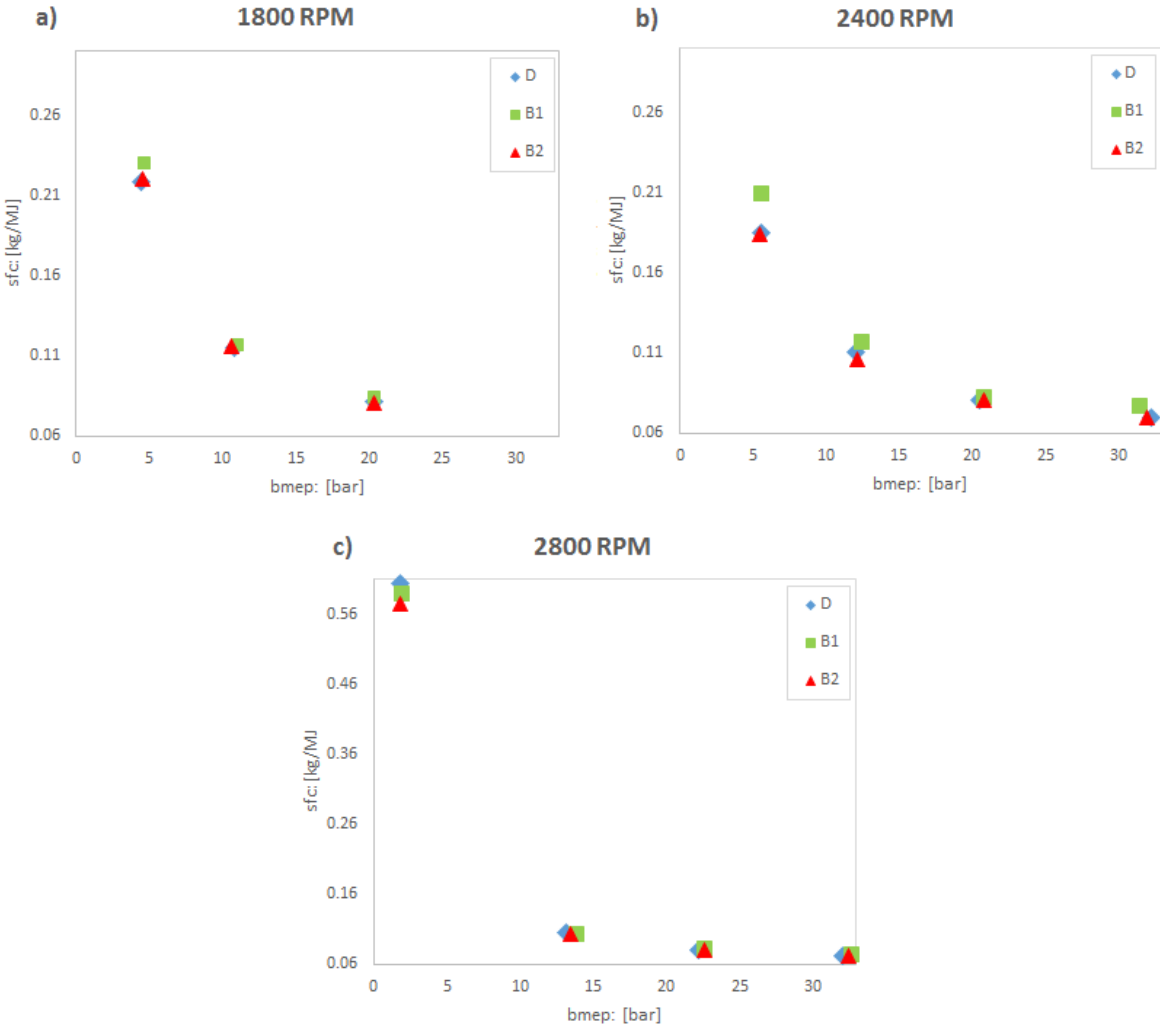
Figure 30: Specific fuel consumption for conventional diesel (D), first generation biodiesel (B1) and second generation biodiesel (B2)

The legends D, B1 and B2 in figure 30 represent the conventional diesel, the first generation biodiesel and the second generation biodiesel respectively. Figure 30 shows that there is almost no change in sfc between the three different fuels, but in figure 30b it can be seen that the first generation biodiesel has a somewhat higher fuel consumption than the other fuels. At all three RPMs sfc is highest at low load and lowest at high load. The sfc at low load and high RPM (figure 30c) is much higher than at any other engine operating point. At 2800 RPM and low load, the engine has a sfc of about 0.1 while at 2400 RPM and low load the engine has a sfc of about 0.03.

The sfc is a measure of the amount of fuel used per power out of the engine. The experiments were done using fixed loads, and the change in engine power between the different fuels is small. A high sfc would therefore mean that the engine is injecting more fuel than with a low sfc. Since the first generation biodiesel has a lower energy content than the two other fuels, it was expected that the first generation biodiesel would have a significantly higher sfc than the other fuels. However this is not confirmed by the results shown in figure 30, apart from a small increase that is seen at 2400 RPM and at low load for 1800RPM. This would suggest that the engine is running more efficiently on the first generation biodiesel. The second generation biodiesel and the conventional diesel perform very similarly for all engine modes.

The decreasing sfc with increasing load implies that the engine is not running efficiently at low loads. This could be considered as a consequence of too little fuel compared to the amount of air in the combustion chamber. In other words, the combustion has too high air to fuel ratio and becomes overly lean.

Since the fuel usage is not directly measured, but determined from ECU data and calibration, the true value of fuel consumption is not known. However, the data supplied by the ECU is adequate to determine the trend in fuel consumption, and the fact that there was little change between the different fuels is still thought to be a precise result.

Fuel conversion efficiency
The sfc did not show any big differences between the three fuels. To understand this better, the efficiency of the engine was calculated for the three fuels. The fuel conversion efficiency against bmep is shown in figure 31.
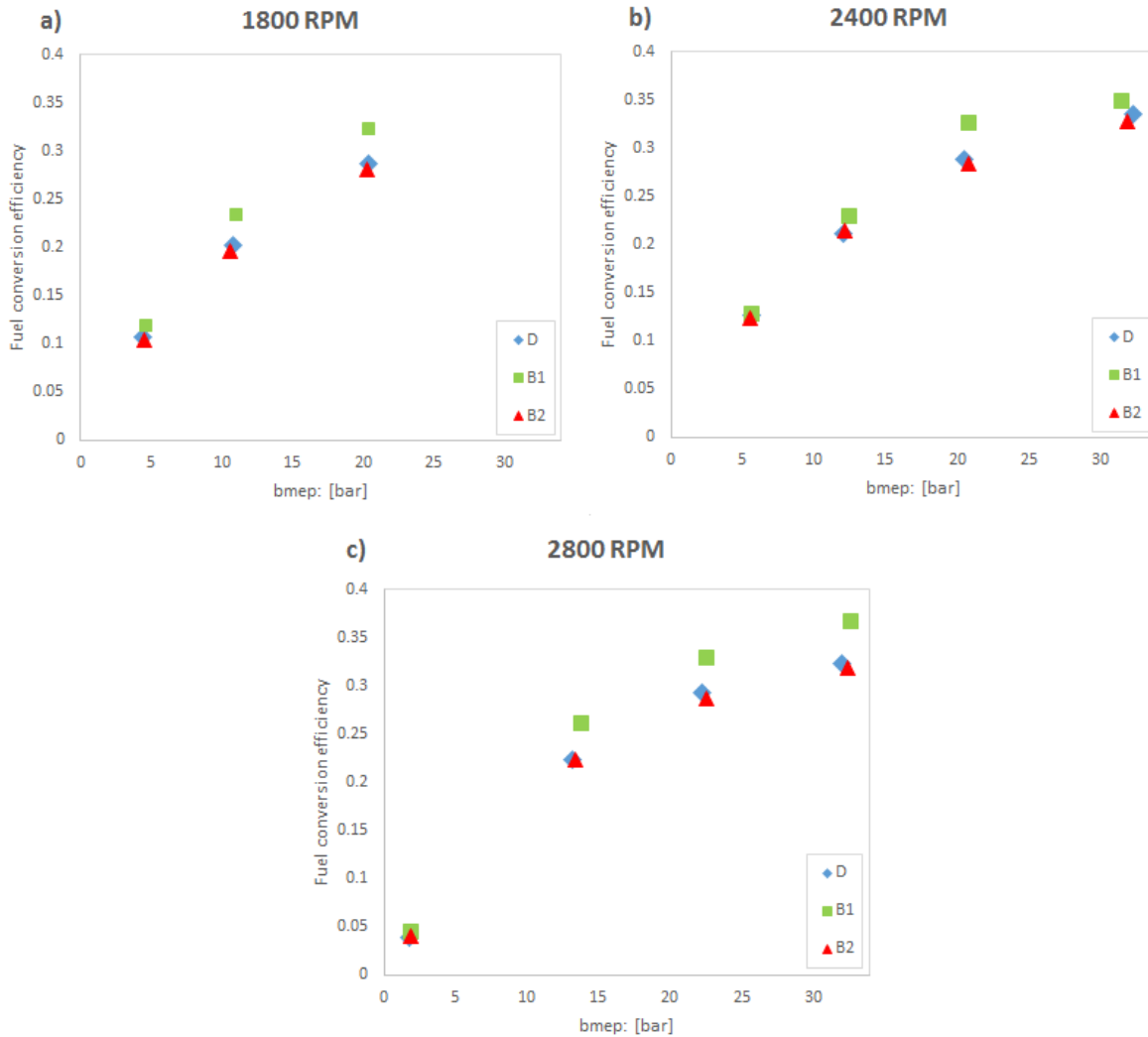
*Figure 31: Fuel conversion efficiency at the different engine conditions for conventional diesel (D),
first generation biodiesel (B1) and second generation biodiesel (B2)*

Figure 31 shows that the first generation biodiesel has a higher efficiency than the other fuels. This is visible at all the measured conditions, except at the lowest load. Figure 31 also shows that the fuel conversion efficiency is increasing as the load is increasing. The highest efficiency is measured at high RPM and high load, while the lowest efficiency is measured at high RPM and low load.

It was expected that the engine would have to inject more fuel when running on the first generation biodiesel, because of the lower energy content. Instead the results show that the engine is running more efficiently on the first generation biodiesel, and therefore the engine is still injecting about the same amount of fuel as when running on the other fuels. Just like the results for sfc, the second generation biodiesel behaves very similar to the conventional diesel.

When comparing the behavior at different engine conditions, the fuel conversion efficiency behaves just as the sfc, see equation (9). The low load has a high sfc and therefore a low fuel conversion efficiency, while at the high load the engine has a low sfc and therefore a high efficiency.

4.1.2 Emission results

Different fuels will change the emission characteristics of the engine, due to their different properties. In this section, the changes in NOx, CO and PM emissions will be studied.

NOx and CO emissions

Figure 32 shows the amount of NOx and CO emissions in parts per million (ppm) against the engine torque:
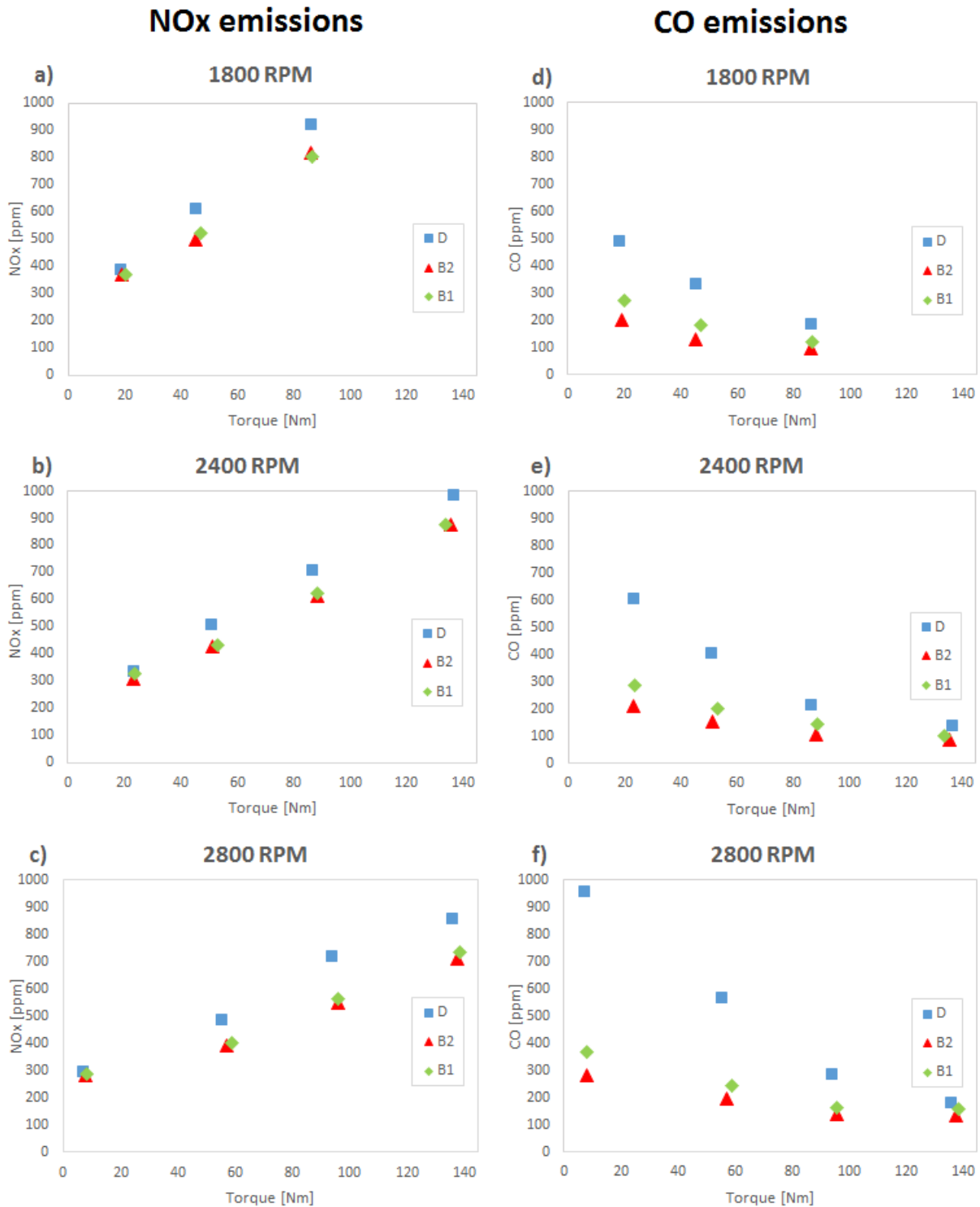
Figure 32: NOx and CO emissions at different engine torque and RPM for conventional diesel (D), first generation biodiesel (B1) and second generation biodiesel (B2)

54

Figure 32 shows that the NOx for conventional diesel are generally higher than the first generation and second generation biodiesel. Both biodiesels show a similar reduction in NOx emissions compared to conventional diesel, with the second generation biodiesel generally producing somewhat less NOx. The conventional diesel generally has higher CO emissions than the biodiesels, whilst the second generation biodiesel has lower CO emissions than the first generation biodiesel.

Figure 32 also shows that the CO emissions decrease with increasing load, while the NOx emissions increase with increasing load. There are not much difference in NOx emissions between the fuels at the lowest loads. As the load increases, the NOx emissions for the conventional diesel becomes higher than for the biodiesels. After a certain point this difference becomes somewhat constant, meaning that the NOx emissions increase at the same rate for all three fuels. On the other hand, the difference in CO emissions between the biodiesels and the conventional diesel is largest at the lowest loads and the difference between them decreases as the load increases. These differences between are best be explained by the HRR curves, which will be presented in section 4.1.3.

Low NOx and CO emissions were expected for the second generation biodiesel, because of the high cetane number. The results confirmed this, as seen in figure 32. But the difference in emissions between the fuels can not be explained by the difference in cetane number alone. The first generation biodiesel has lower amounts of NOx and CO than the conventional diesel, even though it has similar cetane number as the conventional diesel.

PM emissions
The results from the PM emission measurements are shown in figure 33.
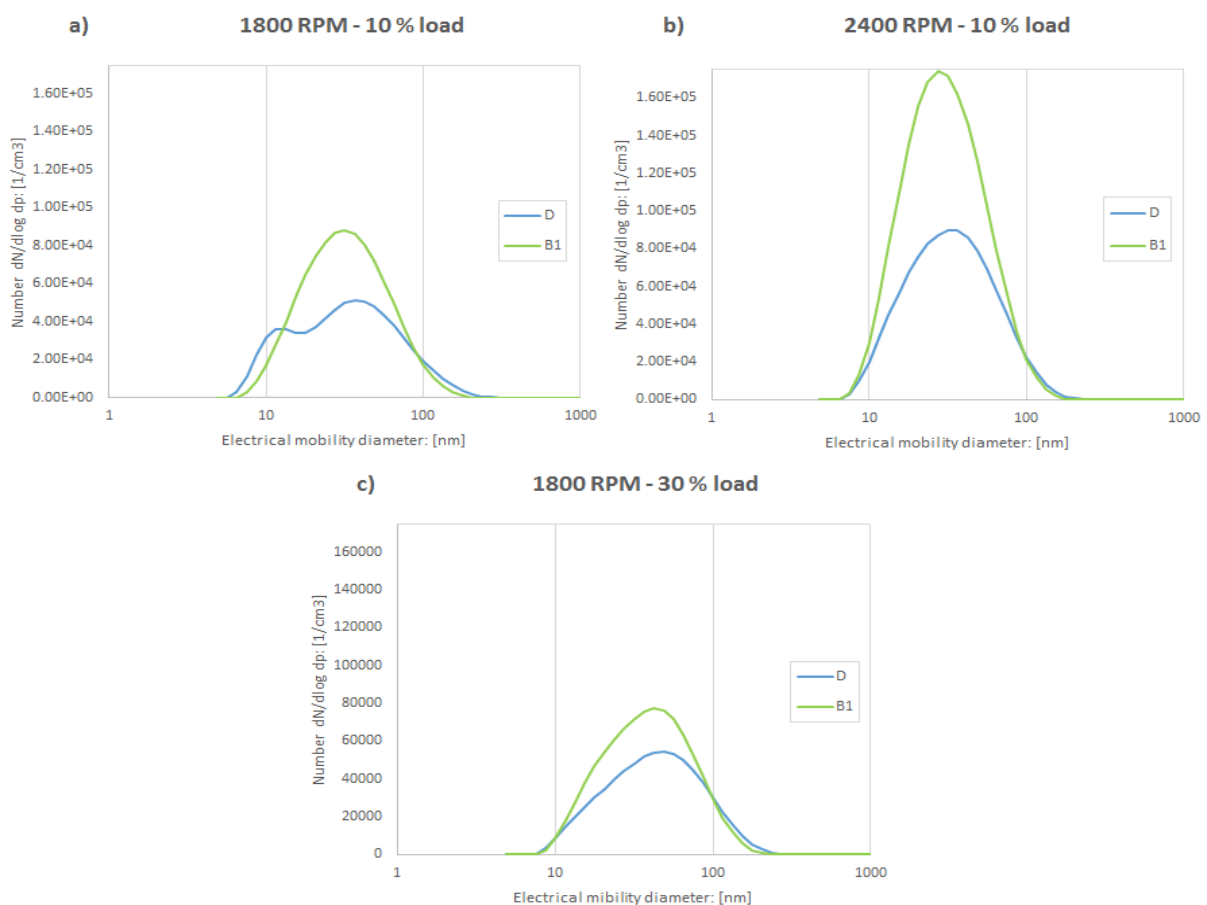
Figure 33: Size distribution of PM emissions for conventional diesel (D) and first generation biodiesel (B1)

The results shown in figure 33, are the results from the limited data that was collected before the particle sampler broke down, as explained in section 3.2.4.

Figure 33 shows that PM emissions are generally higher for the first generation biodiesel than for the conventional diesel. The results show a consistent accumulation mode peak for both fuels. Only at 1800 RPM − 10% load a small nucleation peak is seen when running on conventional diesel. The results also show that there are considerably higher amounts of particles at high RPM, and there are more large particles at 30% load then 10% load at 1800 RPM. Note that the scale of the x-axis in figure 33 is logarithmic, which means that the change in particle size is quite large.

The first generation biodiesel was expected to have increased amounts of small particles compared to the conventional diesel, but the results showed that the use of biodiesel gave an increase in all particle sizes. This must be seen in relation with higher aromatic content and higher fuel oxygen content in the biodiesel. Higher aromatic content is known to increase PM emissions, while higher oxygen content promotes the oxidation of soot [10]. The combined effect of these two changes will vary for different biodiesels, and in this first generation biodiesel it results in higher PM emissions of all sizes. Because of the limited amount of measurements further studies on this matter is necessary. The increased PM emissions at high load is logical, since there is more fuel to accumulate and to form soot.

4.1.3 Cylinder pressure and heat release rate

To further understand the difference in emissions between the three fuels, cylinder pressure and heat release rate are useful parameters. In this section the cylinder pressure and heat release rate at three different engine modes will be shown. Figure 34-36 shows the cylinder pressure curves, the heat release curves and the percentage change in emissions at 1800 RPM − 10% load, 2400 RPM − 20 % load and 2800 RPM − 40 % load. They represent three entirely different engine conditions.

a) Cylinder Pressure

b) Heat Release Rate

c) Percentage change in emissions
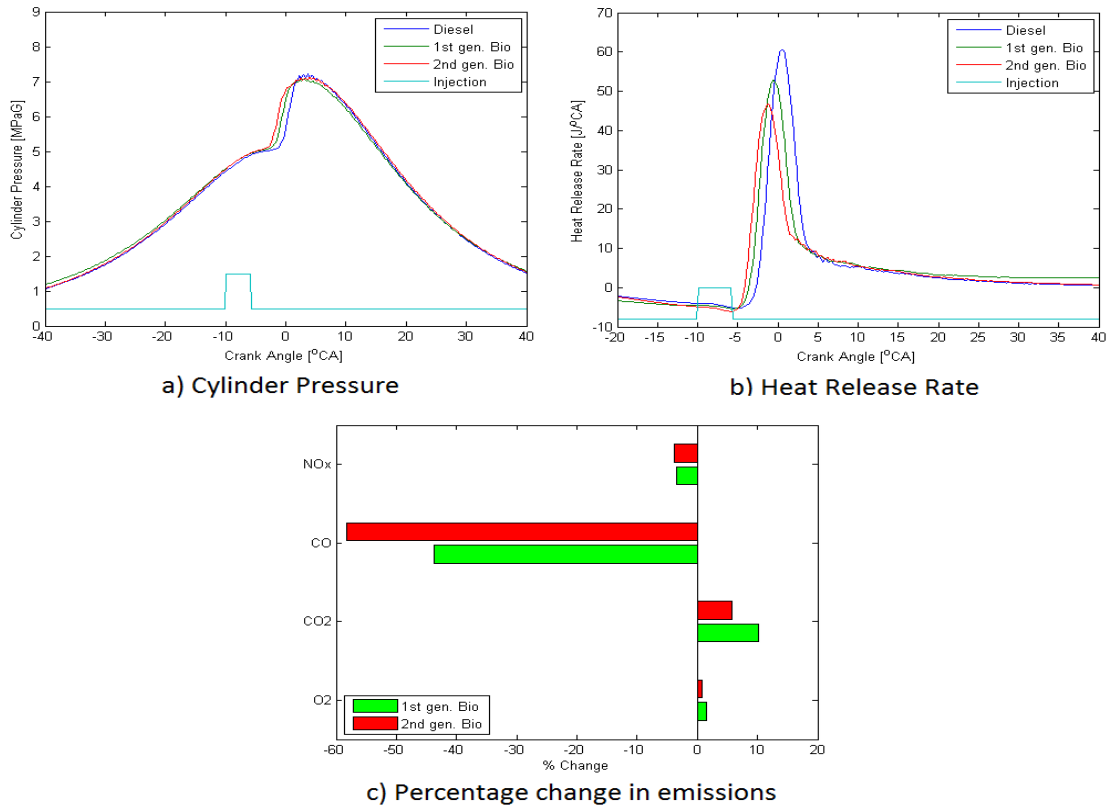
Figure 34: Cylinder pressure, heat release rate, and percentage change in emissions at 1800 RPM and 10 % load

a) Cylinder Pressure

b) Heat Release Rate

c) Percentage change in emissions
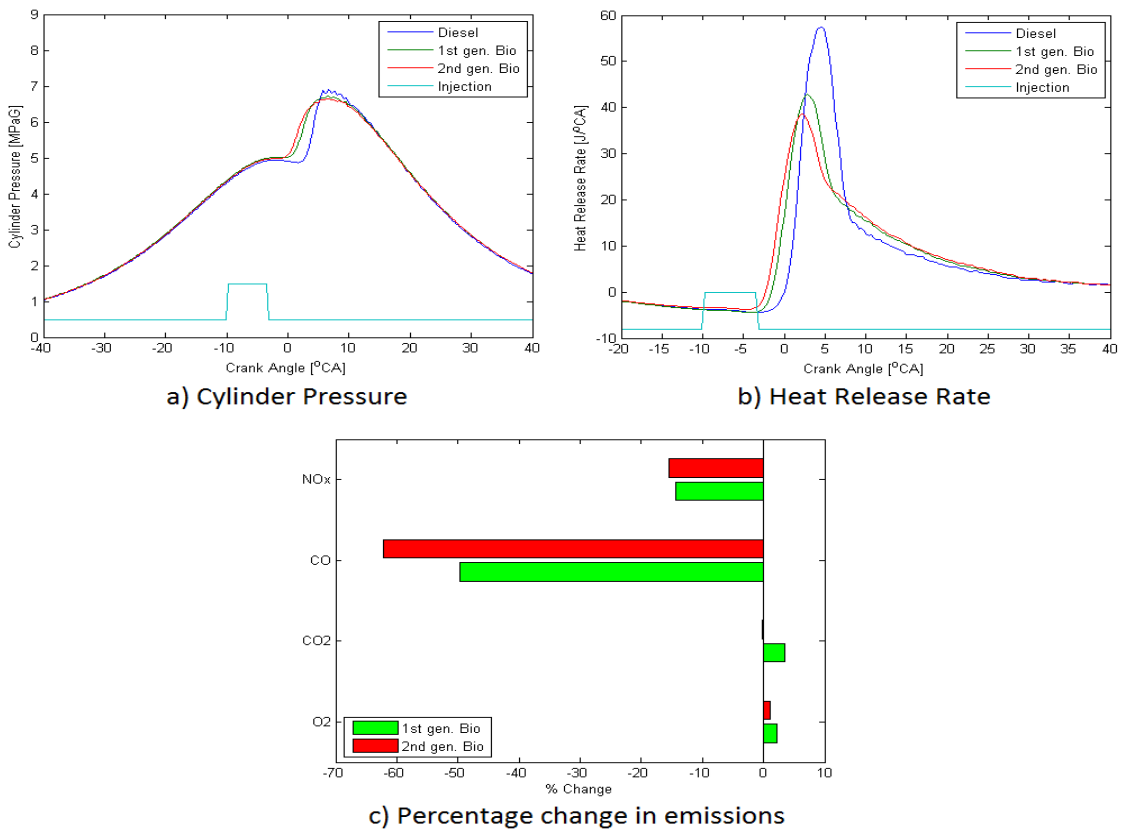
Figure 35: Cylinder pressure, heat release rate, and percentage change in emissions at 2400 RPM and 20 % load

a) Cylinder Pressure

b) Heat Release Rate

c) Percentage change in emissions
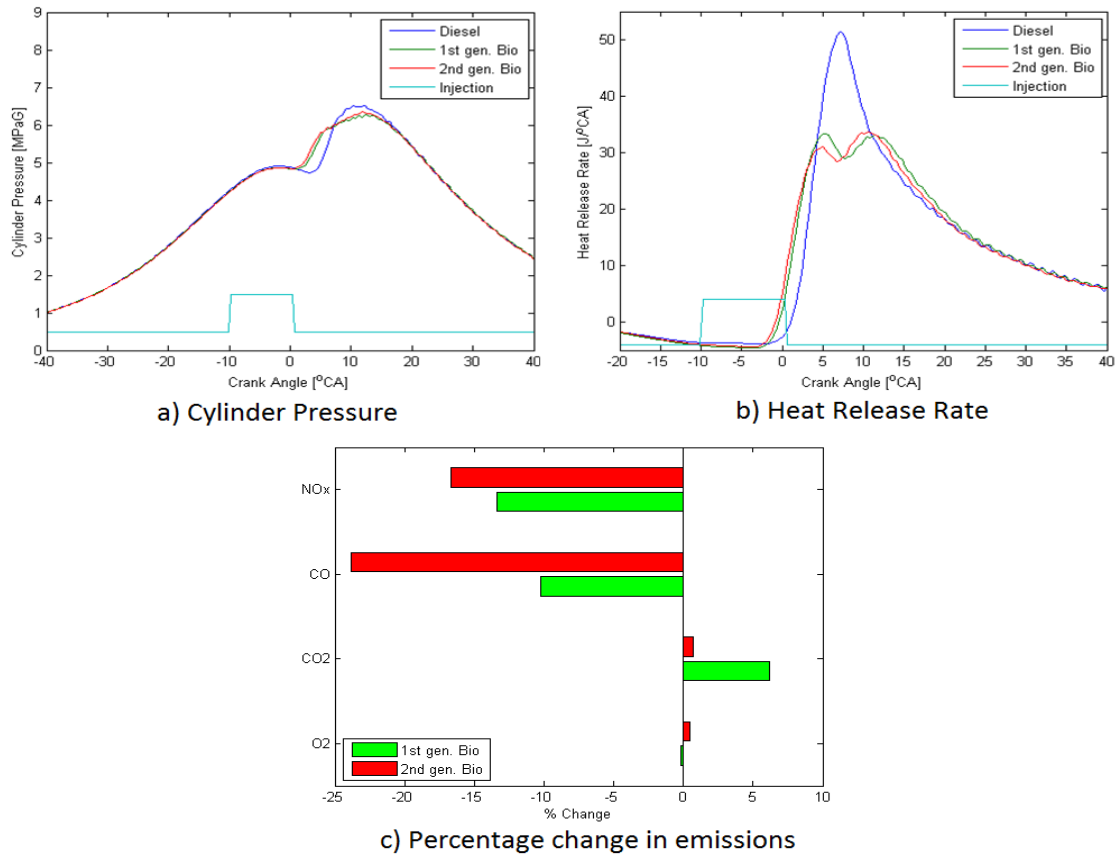
Figure 36: Cylinder pressure, heat release rate, and percentage change in emissions at 2800 RPM and 40 % load

The light blue line in figure 34-36a and b represents the injection duration, while the blue, green and red lines represent the cylinder pressures and the HRR for the three fuels. The injection starts at 10 CAD and ends at just before TDC, or just after TDC in figure 36. The injection duration curve is made as a reference for the start of injection and end of injection. Note that the values on the y-axis for this line has no reference to the amount of fuel injected. Figure 34-36c show the percentage change in emissions compared to conventional diesel, at each engine mode. It shows that the NOx and CO emissions are reduced for all the engine modes and a general increase in CO_2 emissions occur, especially for the first generation biodiesel.

The different reflections from the HRR curves and cylinder pressure curves will be discussed subsequently, beginning with the ignition delay and the time until 50% heat release. Then the different pollutants will be considered, and finally the changes and effects for all engine modes are highlighted

Ignition delay
Figure 34-36a show that after TDC, the cylinder pressure for the first and second generation biodiesel start to rise earlier than for the conventional diesel. This increase in cylinder pressure curves represents the start of combustion, and an early combustion represents a short ignition delay. In other words, the ignition delay for both biodiesels are shorter. Furthermore, the ignition delay is slightly longer for the first generation biodiesel than for the second generation biodiesel. The ignition delay can also be seen on the HRR curves. The start of combustion is defined as where the HRR curve crosses over to a positive value. Figure 34-36b shows that the HRR for the two biofuels begin to rise earlier than the conventional diesel. The ignition delay can be calculated from the HRR, as shown in section 3.3.5 and the results are shown in figure 37.

58
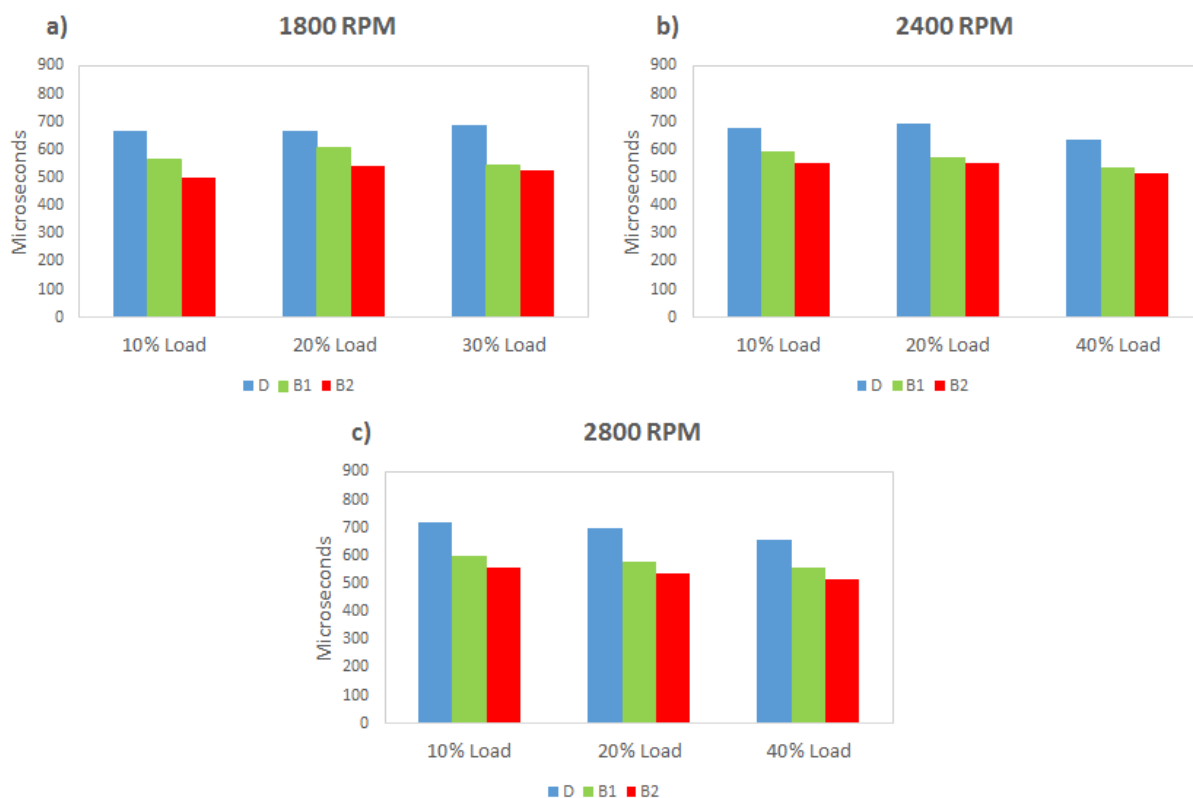
Figure 37: Ignition delay in microseconds at 1800, 2400 and 2800 RPM for conventional diesel (D), first generation biodiesel (B1) and second generation biodiesel (B2)

Figure 37 confirms what was seen in figure 34-36. The ignition delay is clearly lower for the first and second generation biodiesel compared to the conventional diesel, with the second generation biodiesel having the lowest ignition delay. It also shows that the effect on ignition delay is consistent between the different engine modes. This was not the expected behavior for the first generation biodiesel, as it has a similar cetane number as the conventional diesel. The second generation biodiesel show a reduction in ignition delay, as was expected from the higher cetane number compared to conventional diesel.

The changed ignition delay of the first generation biodiesel could be linked to the other changed fuel properties. The first generation biodiesel has an increased viscosity, density and fuel oxygen content compared to the conventional diesel. However, an increased fuel viscosity and density is normally associated with an increased ignition delay rather than a reduced ignition delay. But the higher density and viscosity of biodiesel has shown to affect the volatility of the fuel, and therefore reducing the ignitability of the fuel [10].

Fuel oxygen content could perhaps improve the ignitability of the fuel, fuel oxygen content supports complete combustion [10], and perhaps an earlier fuel oxidation. However, this needs to be investigated further, and more detailed chemical characterizations has to be done. The exact reason for the difference in ignition delay between the conventional diesel and the first generation biodiesel is therefore not known.

Time until 50% heat release
The time until 50% heat release is a measure of how much of the fuel that combusts as a premixed combustion and how much that combust as a diffusion flame combustion. The premixed combustion and diffusion flame combustion can be seen from the HRR curves. Figure 34-36b shows that there is significant difference in the premixed HRR peaks between the three fuels. At all engine modes the conventional diesel has the highest premixed combustion peak,

59

the first generation has the second highest peak, and the second generation biodiesel has the lowest peak.

After the premixed combustion phase, a distinct diffusion flame combustion phase can be seen for the two biodiesels. This is best seen in figure 36b where there is a clear double peak in the HRR curve for both biodiesels. It can also be seen in figure 34-35b after 10 CAD from the HRR curves for the two biodiesels, since they are higher than the conventional diesel HRR curve.

To demonstrate the amount of premixed combustion and diffusion flame combustion at all engine modes, the time until 50% heat release was calculated from the heat release rate curves (see section 3.3.5) and this is shown in figure 38:
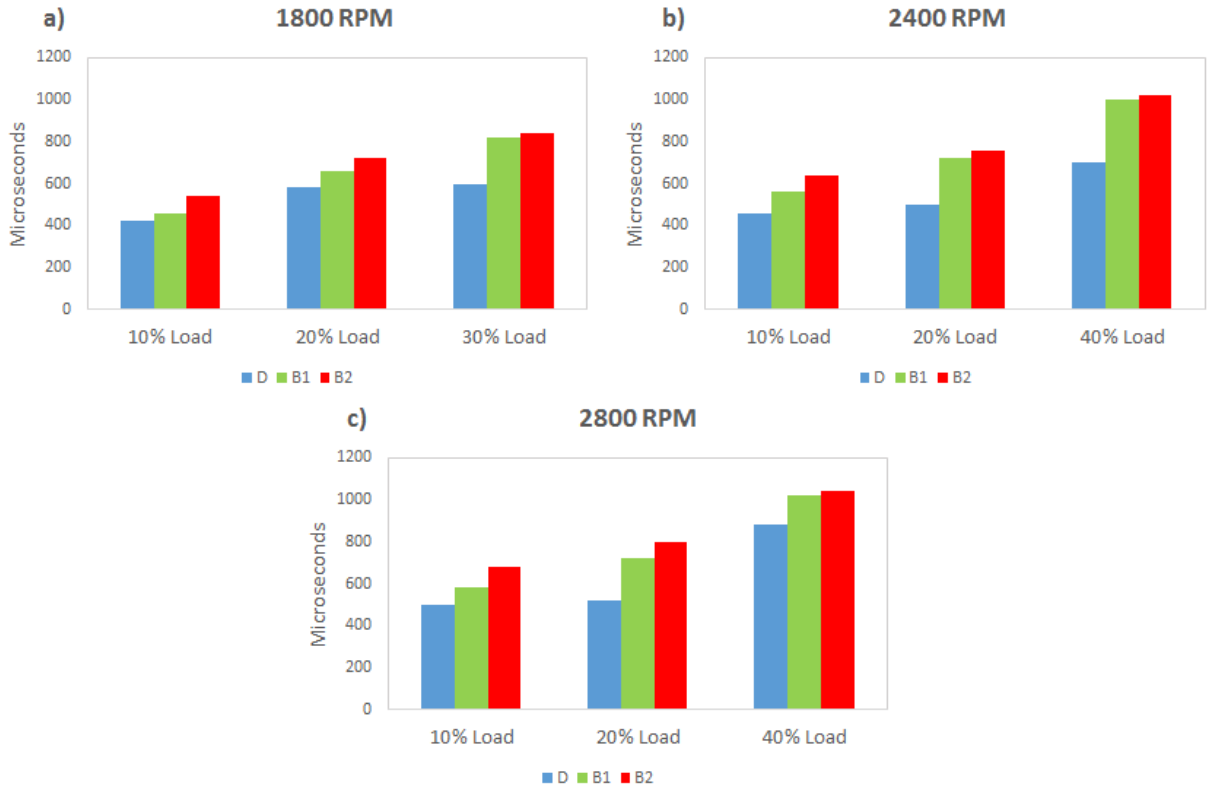
Figure 38: Time until 50% heat release for conventional diesel (D), first generation biodiesel (B1) and second generation biodiesel (B2)

In figure 38 it is seen that the time until 50% heat release is clearly longest for the second generation biodiesel and shortest for the conventional diesel. Figure 38 also shows that the conventional diesel has the largest amount of premixed combustion, while the second generation biodiesel has the lowest amount. Low time until 50% heat release corresponds to a high amount of premixed combustion. There is also a clear link between the time until 50% heat release and the ignition delay, which was shown in figure 37. The shorter the ignition delay, the longer the time until 50% heat release, and more fuel combust as a diffusion flame.

Before running experiments the second generation biodiesel was expected to show a less intense premixed combustion than the conventional diesel. The results shown in figure 38 are consistent with this. It is also visible that the first generation gives the same result. The ignition delay for the first generation biodiesel is shorter than the conventional diesel, even though the cetane number is the same. This means that the first generation biodiesel has a shorter premixed

combustion and a larger diffusion flame combustion. This difference from conventional diesel can be explained by the reduced mixing time that the two biodiesels have, since they ignite earlier. Since all the fuel is injected at the same time, and the biodiesels ignite earlier than the conventional diesel, it leads to a shorter mixing time and hence a lower premixed combustion peak.

NOx emissions
The amount of premixed combustion and diffusion flame combustion is a major contributor to the lower NOx emissions that are seen in the biodiesels. The reduction in the premixed HRR peaks is a very good indicator for the changes in NOx emissions. This is because a reduction in premixed combustion is consistent with a reduction in NOx emissions. The difference in NOx emissions make sense since a higher HRR is associated with more premixed combustion, which corresponds to a higher temperature inside the combustion chamber and NOx emissions are very dependent on the temperature [16].

Figure 32 showed that NOx emissions increased at the same rate for all three fuels. This can be explained by the small difference in the premixed combustion peaks between the different engine modes. Figure 34-36b show that for both 2400 RPM $-$ 20 % load and 2800 RPM $-$ 40% load the premixed combustion peak is at around 40J per CAD for the biodiesels and 60J per CAD for the conventional diesel. The explanation is that if both engine modes have the same mixing time, there is a maximum possible premixed combustion, because the amount of fuel which could be combusted as a premixed flame depends primarily on the amount of mixing and not the amount of fuel. A constant mixing time will then yield a constant amount of premixed combustion as the load increases, and hence give approximately the same temperature. Small change in temperature means no large change in NOx between the fuels as the load increases.

CO emissions
The CO emissions for biodiesel are lower than for the conventional diesel, which is consistent with the larger amount of diffusion flame combustion shown in the time until 50% heat release in figure 38. A diffusion flame generally produces lower amounts of CO than a premixed flame [10], however lower CO emissions from biodiesel combustion is most commonly explained by a higher fuel oxygen content. The higher oxygen content in biodiesel promotes complete combustion and therefore leads to the reduction in CO emissions [10]. Which of these two explanations that is the predominant reason for the lower CO emissions need further investigation.

Figure 32 showed that CO emissions reduced as the load was increased. This can be explained by the difference in diffusion flame combustion as the load increases. At low loads premixed combustion dominates and as the load increases, more and more fuel combusts as diffusion flame combustion and CO emissions reduce.

CO_2 emissions
A CO_2 increase can be best explained by the difference in CO emission. However there is little increase in CO_2 emission in the second generation biodiesel, which has the largest reduction in CO emissions. The CO_2 emission increase in the first generation biodiesel can be thought of as a consequence of a higher carbon number instead of the CO decrease. The first generation biodiesel has the highest density and viscosity of the three fuels, and this is often related to a high carbon number. A high carbon number is again linked to higher CO_2 emissions [60] [61].

Changes in HRR between different engine modes
A comparison between figure 36b and figure 34b are interesting since they represent two very different engine conditions. In figure 34b there is almost only premixed combustion for all the

fuels, while in figure 36b the biofuels show that there is both a clear premixed combustion period and a diffusion flame period, as there is a double peak in the HRR curve.

Remember that there is only combustion during the CAD where the HRR curve is above zero. This could be used to find the end of combustion. Figure 34b shows that the HRR curve is approximately zero already at 20 degrees CA after TDC, while in figure 36b the fuel has still not finished combustion at 40 CAD after TDC. The diffusion flame stretches out the HRR, curve so that it is not finished burning out all the fuel before closer to BDC, and causes a considerable late combustion phase. The premixed combustion peak is also much lower in 36b, even for the conventional diesel. Figure 36a shows that the cylinder pressure at high load has a lower peak around TDC when running on biodiesel than when running on conventional diesel. This pressure reduction coincides with the low premixed HRR peak of the two biodiesels. Since the HRR is not as big during this part of the cycle, there is a reduction in cylinder pressure simply because there is less heat from combustion to increase the pressure.

Effect of speed and load on Ignition delay
The ignition delay was shown in figure 37, in microseconds. This corresponds to the actual time the fuel was given before ignition. This is a logical way to present ignition delay, since the ignition delay then can be compared at the different RPMs. An alternative method is to present the ignition delay in CAD. Since the injection always happens at the same point in the cycle (10 CAD), the ignition delay in CAD shows the ignition delay relative to where in the cycle SOC occurs, rather than in absolute time. Figure 39 shows such a plot of ignition delay in CAD against percent load.
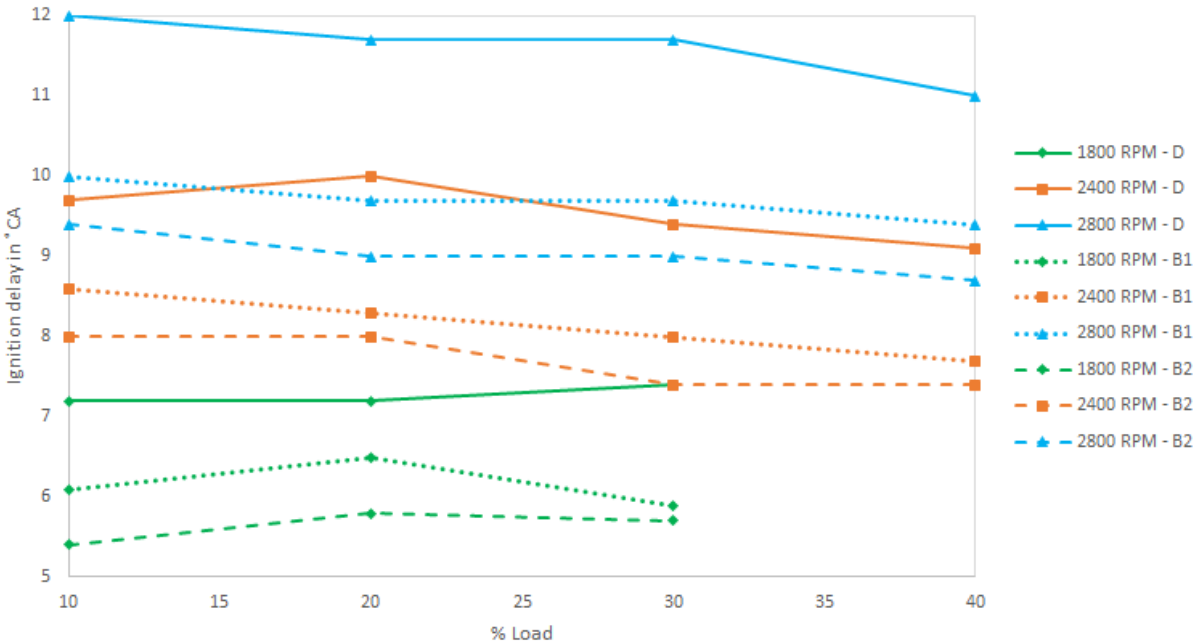
Figure 39: Ignition delay against the percentage load on the engine between all fuel and RPM for conventional diesel (D), first generation biodiesel (B1) and second generation biodiesel (B2)

Figure 39 shows the ignition delays at 2800 RPM, 2400 RPM and 1800 RPM in blue, orange and green respectively. Solid lines represents diesel, dotted lines represents first generation biodiesel and dashed lines represents second generation biodiesel. Generally the ignition delay is decreasing when the load is increasing, although this is not consistent between all the points. Note the difference in ignition delay between the different fuels, which is, as pointed out earlier, that the conventional diesel generally has a much larger ignition delay than the biodiesels.

It is logical that the ignition delay reduces when the load increases because at high load conditions the temperatures and pressures are generally higher, even at the same crank angle before combustion. To explain this it is useful to see the difference in motored-pressure between the different loads. In figure 40 the motored-pressure at 2800 RPM and 10, 20 and 40 % load is plotted.
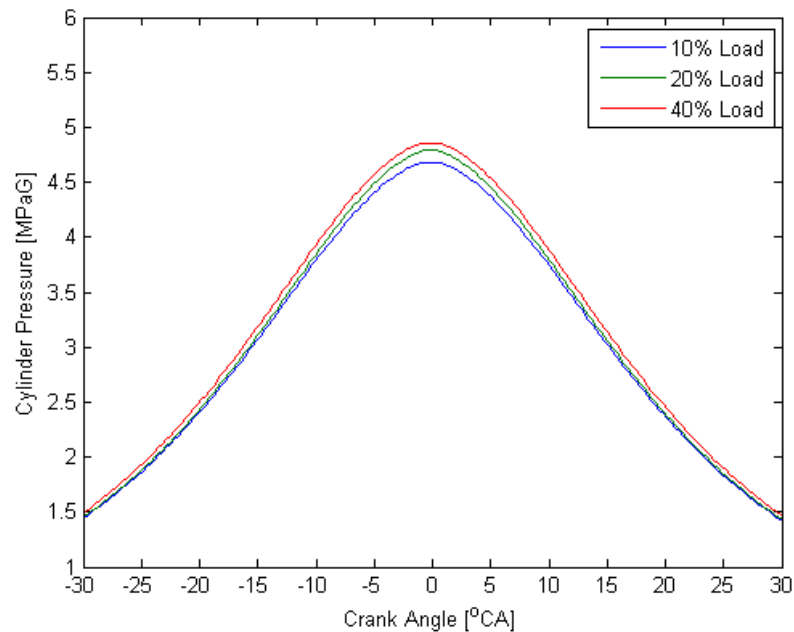
Figure 40: Motored pressure at 2800 RPM and 10, 20 and 40 % load

In figure 40 the pressure at TDC gets higher as the load increases. For a constant inlet of 1.2 bar at IVC. This can be explained by generally higher temperatures at high engine loads. This is a result of the wall being at a higher temperature at high loads than at low loads [62]. There is always a small amount of residual gas during the engine cycle as well and this residual gas will have a higher temperature at a high loads than at a low loads. These factors lead to higher temperatures at TDC, when the engine is running at high load compared to low load, causing slightly higher pressure at TDC. If the temperature and pressure close to TDC is higher, this will cause the fuel to ignite earlier, hence reducing ignition delay. This is consistent with what was show in figure 40 and 39.

4.2 Engine Simulations

In this section the results from the simulations in LOGEsoft will be shown. The emphasis is on the cylinder pressure, HRR, ignition delay and NOx emissions. The simulations done at 1800 RPM − 10% load, 2400 RPM − 20% load and 2800 RPM − 40% load will be presented. The conventional diesel simulations are shown in section 4.2.1 and the biodiesel simulations are shown in section 4.2.2.

4.2.1 Diesel simulations

The conventional diesel simulations were done using two different mechanisms and two different diesel surrogates. Two mechanisms were used as surrogates for diesel, the first was a mechanism containing n-heptane, and the second was a mechanism containing n-decane and 1-methylnapthalene species. The two different surrogates will be compared with the experimental diesel results, to show how these mechanisms perform. The n-decane and 1-methylnapthalene surrogate is hereby referred to as the diesel surrogate. The results from the simulations compared to the results from experiments can be seen in figure 41-43.

a) Cylinder Pressure

b) Heat Release Rate

c) Percentage change relative to expermient
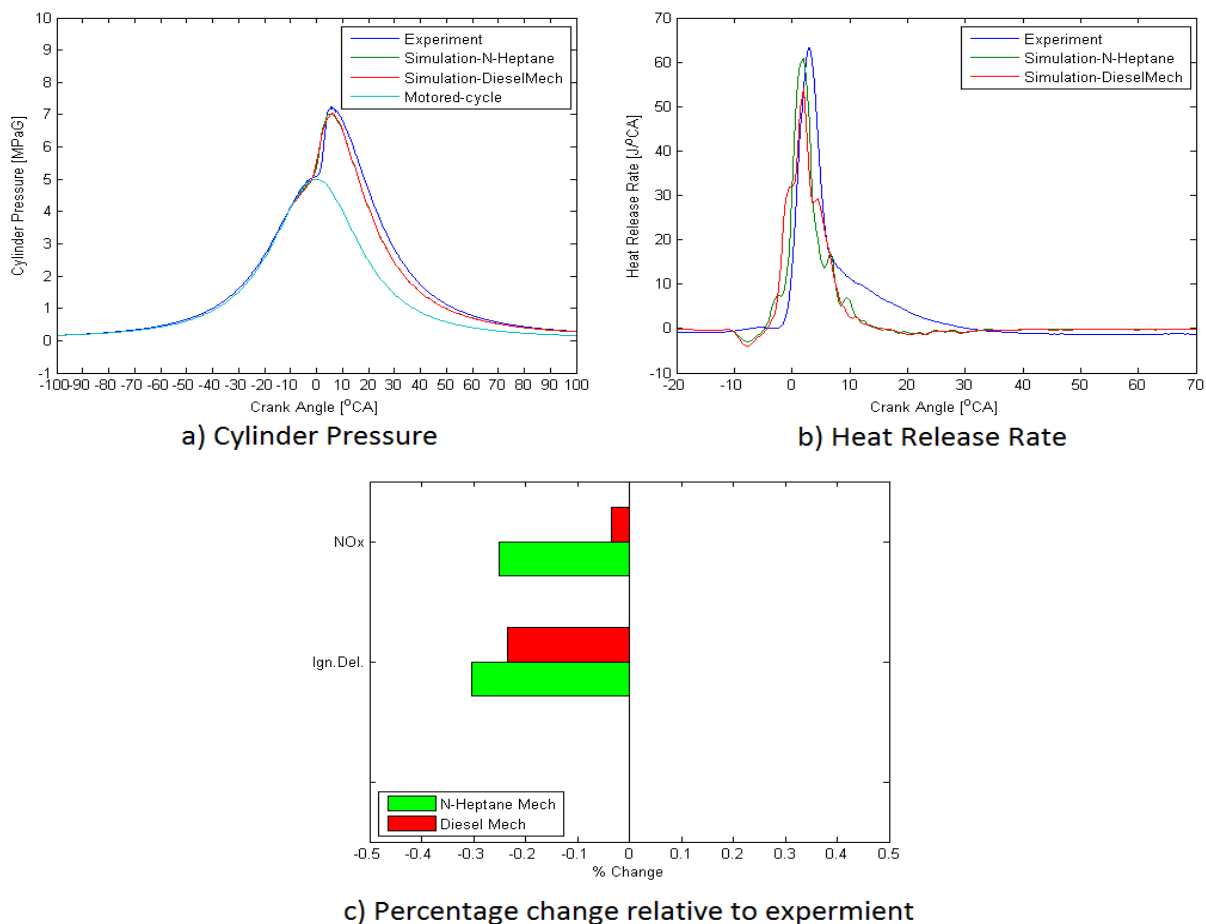
Figure 41: Cylinder pressure, HRR and percentage change in NOx and ignition delay at 1800 RPM and 10 % load

a) Cylinder Pressure

b) Heat Release Rate

c) Percentage change relative to expermient
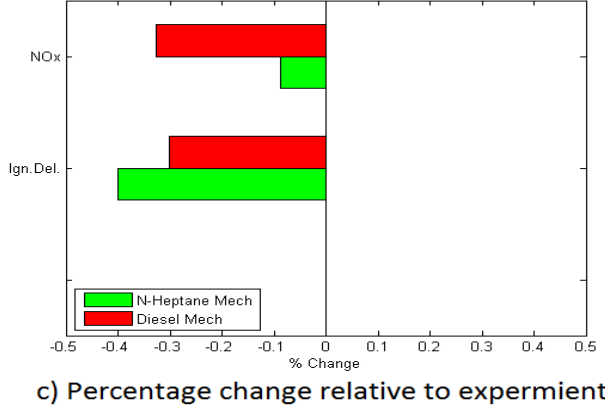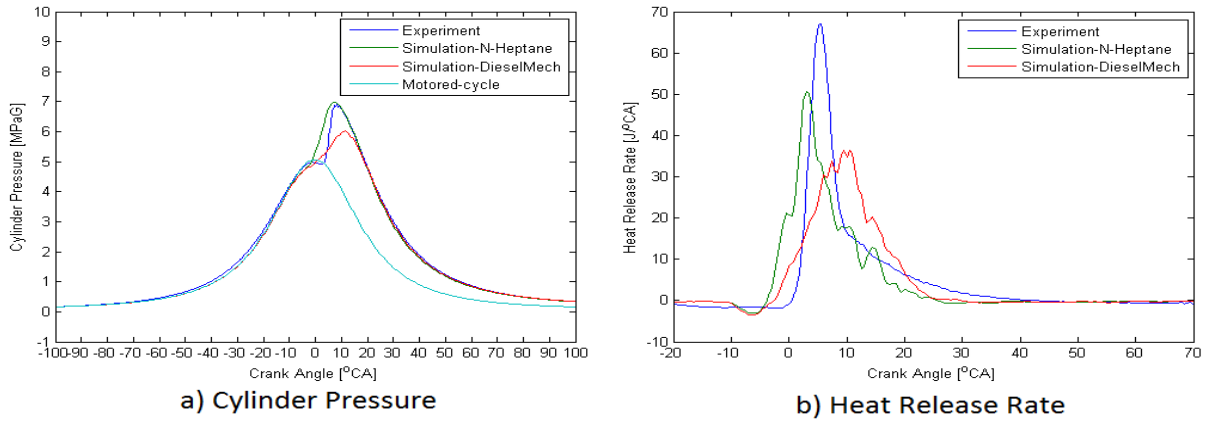
Figure 42: Cylinder pressure, HRR and percentage change in NOx and ignition delay at 2400 RPM and 20 % load

a) Cylinder Pressure

b) Heat Release Rate

c) Percentage change relative to expermient
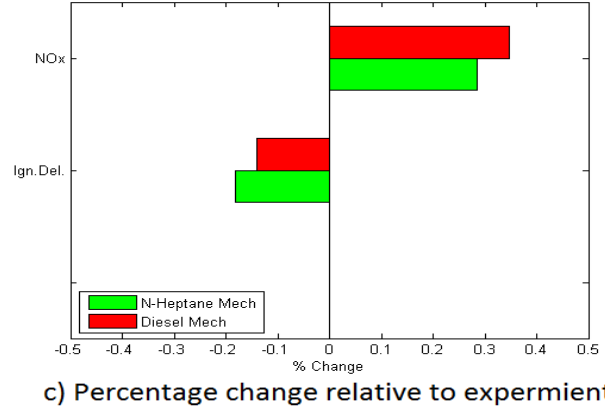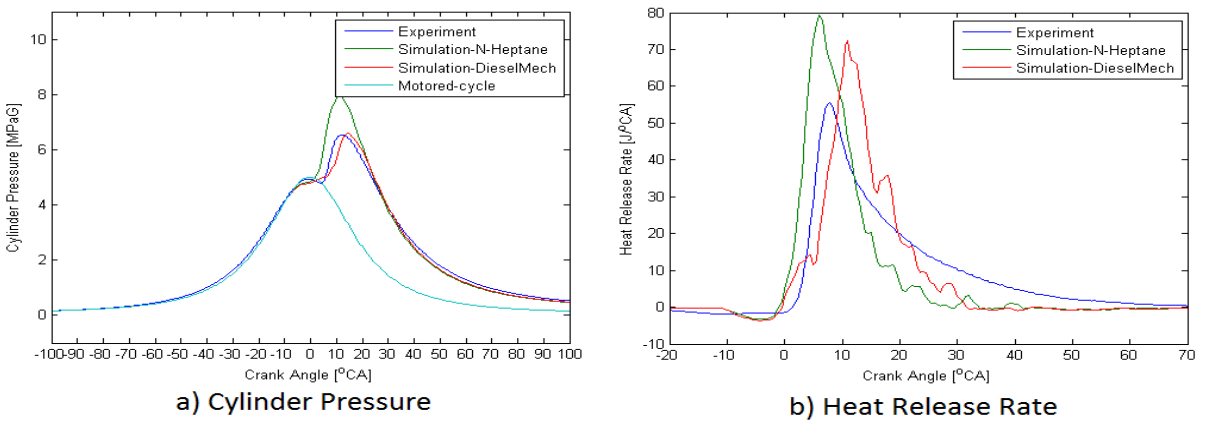
Figure 43: Cylinder pressure, HRR and percentage change in NOx and ignition delay at 2800 RPM and 40 % load

65

In figure 41-43 the dark blue line represents the cylinder pressure and HRR from the experimental data, the green line represents the simulated pressure and HRR using the n-heptane surrogate, and the red line represents the simulated pressure and HRR using the diesel surrogate. The light blue line represents the cylinder pressure created without any fuel injection (motored-pressure). The motored pressure is created from the simulations and is used as a confirmation for the simulation's initial conditions. Figure 41-43c show the percentage change in NOx and ignition delay for the two different mechanisms relative to the experimental values.

The reflections on the simulated results will be discussed subsequently, starting with the ignition delay and cylinder pressure, and ending with the reflection about the NOx emissions.

Ignition delay
Figure 41-43c shows that the diesel surrogate generally simulates the ignition delay closer to the experiments than the n-heptane surrogate. This can also be seen in figure 42-43a and b where it is clearly visible that the red diesel surrogate has a SOC later than the SOC of the n-heptane surrogate and closer to the experimental SOC. Figure 42-43 also show that the simulated ignition delay is shorter than the experimental ignition delay, for both mechanisms and all engine modes.

The diesel surrogate consist of n-decane and 1-methylnapthalene species which are hydrocarbons with higher carbon numbers than n-heptane. A higher carbon number fuel is typically less ignitable than a low carbon number fuel, but as shown in table 10, the two surrogates have the same cetane number. The difference in ignition delay between the two surrogates is therefore most likely caused by a difference in fuel vaporization.

Both surrogates showed a large reduction in igniting delay compared to the experimental ignition delay. This can either be linked to the mixing model used in the simulations, or the fuel properties. The mixing model chosen in the simulation is the default mixing model, which could be mixing the fuel too fast compared to the engine the experiments. The other possibility is that the two surrogates are more ignitable than the experimental diesel. As seen in table 10, the two surrogates have a slightly higher cetane number than the experiment diesel and the two surrogates should therefore ignite easier. There is also a possibility that the vaporization of the two surrogates are simulated wrong and the fuel vaporization is very important to the ignitability of a fuel. The details of the mechanism files used in the simulations are a subject for further studies.

Changes in cylinder pressure
The accuracy of the two surrogates vary between the engine modes. Figure 41 represents an engine mode where the combustion more or less only consists of a premixed flame, and both fuel surrogates seem to handle this and predicts the cylinder pressure well.

Figure 45 shows that the n-heptane surrogate simulates the pressure profile with good accuracy, while the diesel surrogate simulates a too low combustion peak. Figure 42 also represents a combustion which is mostly premixed, however there are more fuel injected. The diesel surrogate simulates the ignition delay slightly better than the n-heptane surrogate, but the combustion peak is too low. The diesel surrogate seems to simulate a too large diffusion flame combustion compared the experimental case.

Figure 46 shows that the diesel surrogate simulates the cylinder pressure best, while the n-heptane surrogate simulates a combustion pressure peak which is much higher than the experimental combustion peak. The n-heptane surrogate seems to simulate a too large premixed flame period. Generally the diesel surrogate is simulating more diffusion flame than the n-heptane surrogate. Depending on the engine mode, it is noticeable that the two diesel surrogates

66

are either simulating too much premixed combustion or too much diffusion flame combustion relative to the experiments. This is can be linked with the change in ignition delay, but the difference in in premixed combustion and diffusion flame combustion seem to be larger than the ignition delay difference. This is seen in figure 43, where the ignition delay prediction is quite accurate, but there is a large difference in all combustion phases compared to the experimental results.

NOx emissions
Figure 41-43 show that the n-heptane surrogate generally simulates NOx emissions closer to the experiments than the diesel surrogate, except for at low load − low speed, where the diesel surrogate gives the best result. Figure 41-42c also show that the NOx emissions are decreased in the simulations compared to the experiments, while figure 43c show an increase in NOx emissions in the simulations. There is a link between the premixed combustion peak and the NOx emissions. This link is seen where there is a reduction or increase in premixed peaks compared to the experiments. This leads to less NOx emissions or more NOx emissions respectively. Except for these effects, there are no other clear links between the NOx emissions and the changes in premixed combustion peaks.

The NOx emission results from simulation need further discussion. Firstly it is seen in figure 41 and 43, that the surrogate with the highest premixed peak does not necessarily have the highest NOx emissions. Secondly in figure 41 and 43 the surrogate which simulates the premixed peak closest to the experimental premixed peak, does not simulate the resulting NOx emissions closest to the experimental NOx emissions. Figure 43b and figure 41b shows that the n-heptane surrogate has the largest premixed peak, but it has lower NOx emissions than the diesel surrogate. Figure 43b and figure 41b show that the diesel surrogate premixed peak is closer to the experimental premixed peak than the n-heptane premixed peak. However, the n-heptane surrogate does a better job simulating the NOx emissions.

The NOx emissions are mostly dependent on the temperatures inside the combustion chamber, and therefore it was expected that the NOx emission trends would clearly follow the trends in HRR. The reason why the two different surrogates do not behave exactly like expected, is not known. It can be a results of differences in the two chemical mechanisms, or it can be an inaccuracy in the physical model. By looking through the mechanism files, it is clear that both mechanisms contain the same amount of NOx species and NOx reactions, so it is difficult to make any conclusion based on this. The chance that there are mistakes in the mechanism files are considerable, as they are both heavily reduced mechanism and chemical mechanisms are always a work in progress. However, further work on this matter is necessary. If the inaccuracy is in the physical model, the mixing model would be a likely source of the inaccuracy,

4.2.2 Biodiesel simulations
Because the evaporation data and the NASA polynomials for the biodiesel surrogate methyldecanoate (MD) was not available, no successful biodiesel simulations with the SRM diesel engine model was achieved. The MD surrogate used the evaporation data and the NASA polynomials from n-decane instead, and this resulted in no combustion in all the MD simulations. However, biodiesel simulations in an HCCI engine worked, which indicated that the problem with using MD was in the injection simulation. To get some results, the MD was then simulated using an HCCI engine model. The HCCI engine results will show how the three different surrogates (n-decane and 1-methylnapthalene, n-heptane and MD) compare in terms of ignition delay and NOx emissions. This will show if the MD surrogate has the same trends when compared to diesel surrogates, like the biodiesel showed when compared to the conventional diesel in experiments. There are however no experimental data for HCCI engines to compare with.

Like a diesel engine an HCCI engine is a compression ignition engine. The difference is that the fuel is injected before the compression stroke and is assumed to be completely mixed with the air (homogenously mixed). This means that all the combustion in an HCCI engine is premixed. The HRR plot is therefore not considered that important since the amount of premixed combustion is already known. The results from the HCCI simulations are shown in figure 44.

a) Cylinder pressure -2400 RPM

b) Cylinder pressure - 2800 RPM

c) Reduction in NOx using MD
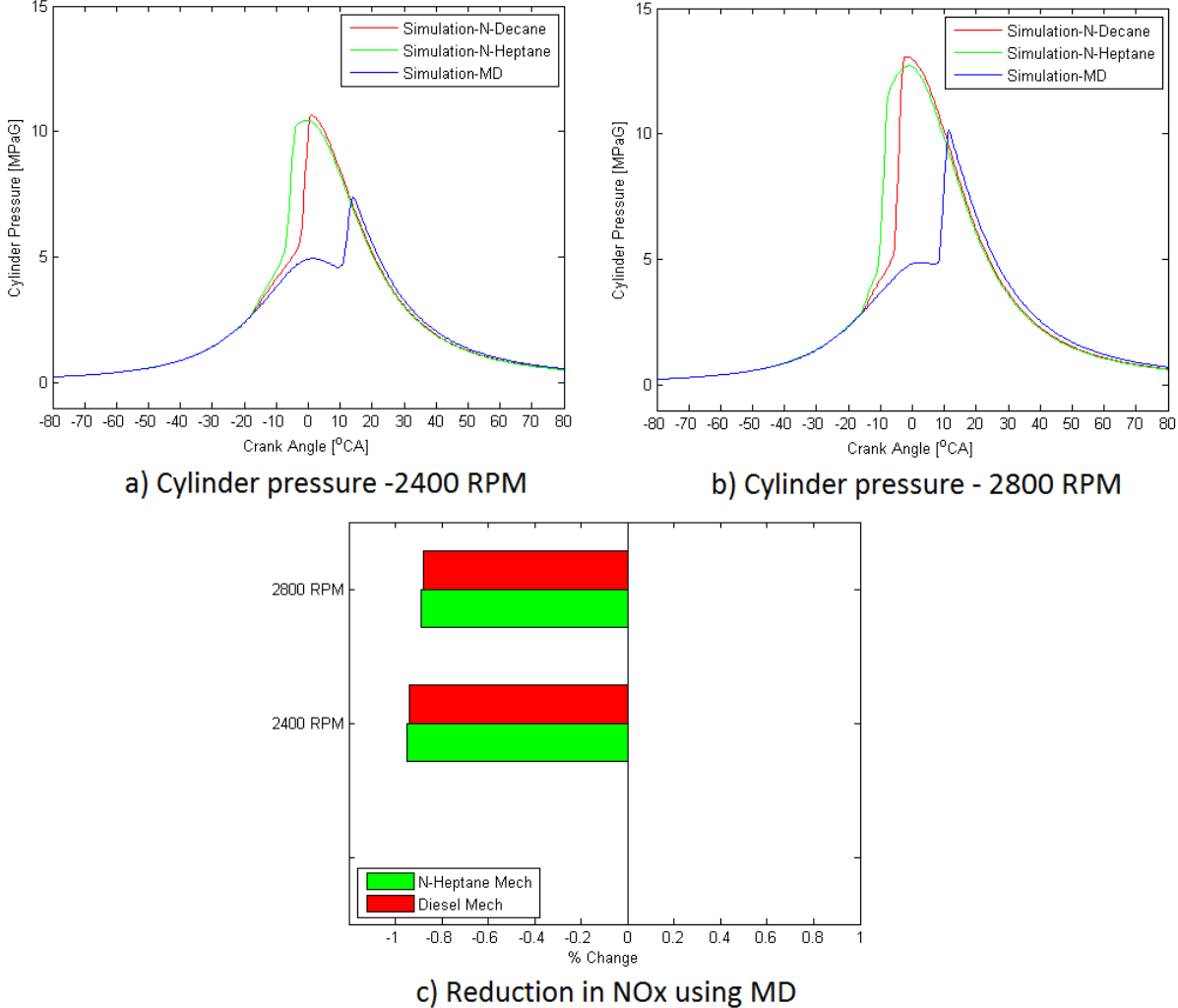
Figure 44: HCCI simulations for biodiesel and conventional diesel

In figure 44 there are two cases, the 2400 RPM case represents simulation done at 2400 RPM with an equivalence ratio of 0.4, and the 2800 RPM case represents simulation done at 2800 RPM with an equivalence ratio of 0.6. These two cases represent about the same engine conditions as the 2400 RPM − 20% load and the 2800 RPM − 40% load which was used in the previous section. In the HCCI engine simulations the equivalence ratio is the only factor that can be used to decide the fuel amount. The equivalence ratios chosen are found like shown in section 3.4.5. During the simulations trial and error showed that a lower equivalence ratio resulted in no combustion for the MD surrogate. Figure 44c shows the percentage change in NOx emissions when simulating with MD, compared with the diesel surrogate and the n-heptane surrogate, at both engine conditions.

The reflections on the simulated results will be discussed subsequently, starting with the changes in cylinder pressure, and ending with the reflection about the NOx emissions.

Changes in cylinder pressure
Figure 44a and b show that the MD surrogate ignites much later than the two diesel surrogates. This is clear from the rise in cylinder pressure, which happens much later for the MD than for the diesel surrogates. At 2400 RPM the MD surrogate show a very late ignition and the engine is at a point where it is barely igniting. The difference between the two engine modes is larger combustion pressure peaks for all the surrogates at 2800 RPM and an earlier ignition for the MD at 2800 RPM.

All the combustion in an HCCI engine is premixed, and if the fuel amount increases there will be more premixed combustion. This explains the difference in cylinder pressure between the two different simulation cases. Figure 44b has a higher equivalence ratio and hence more fuel.

Figure 44 shows that at 2400 RPM with equivalence ratio of 0.4 the MD surrogate is not able to combust until 10 CAD. At 2800 RPM with an equivalence ratio of 0.6 the MD surrogate is igniting before 10 CAD. The main difference between the two engine modes is the equivalence ratio. Since a low equivalence ratio mixture is harder to ignite than a low equivalence ratio mixture, this difference shows that the MD surrogate is far more vulnerable to overly lean mixtures than the diesel surrogates.

The difference between the three surrogates are seen as a difference in ignition delay and combustion pressure peaks. The MD surrogate shows a longer ignition delay as well as a lower combustion pressure peak, compared to the other surrogates. These differences are linked, and the reduced pressure peaks are a result of the long ignition delay. If the combustion happens after TDC this will reduce the pressure peaks, since the combustion starts as the piston moves downwards.

NOx emissions
Figure 44c shows that the NOx emissions are reduced when using MD compared to the diesel surrogate and the n-heptane surrogate. The reduction is as large as 90%. This is a much larger reduction than what was visible in the experiments with conventional diesel and biodiesel. There is a consistent difference in NOx emissions compared with both the n-heptane and the diesel surrogates, as well as between the two different engine modes.

The reduction in NOx emissions is thought to be directly linked to the reduction in combustion peaks as the MD delivers a lower temperature because of the reduced cylinder pressure. This reduction in simulated NOx emissions can not be used to confirm the reduction in NOx emissions that was shown in the experiments. The reason being that the reduction is caused by a longer ignition delay in the simulations, and by a shorter ignition delay in the experiments. Therefore, this should be a topic for further research.

5   Conclusion

This project aimed to analyze the behavior of different types of biodiesels used in a diesel engine, and compare them with the behavior of conventional diesel. Biodiesel changes the emission characteristics of diesel engines in different ways, depending on the type of biodiesel. The difference is often seen as increased NOx and decreased PM, but it has been shown that this is not always the case. The two different types of biodiesel used in this project were a first generation biodiesel and a second generation biodiesel. The first generation biodiesel had a cetane number which was similar to the conventional diesel, but had a lower energy content, higher density and higher viscosity. In addition, first generation biodiesels normally have higher oxygen content and aromatic hydrocarbon content than conventional diesels. The second generation biodiesel had a similar energy content to the conventional diesel, but a higher cetane number and a lower viscosity. To analyze the behavior of these biodiesels the focus was on engine experiments, using a modern turbocharged diesel engine. Simulation were also done in order to study the experimental results in more detail.

During the experiments CO, PM and NOx measurements were done, and cylinder pressure, fuel consumption and engine torque were measured. PM measurements were limited, and were only obtained for first generation biodiesel and the conventional diesel. The simulations were performed with a SRM model in the simulation software LOGEsoft. In the simulations two different surrogates for conventional diesel and one surrogate for biodiesel were used. The surrogates for conventional diesel were n-heptane and a mixture of n-decane and 1–methylnaphthalene, while methyldecanoate was used as a biodiesel surrogate.

Before running the experiments and simulations, it was expected that the second generation biodiesel would have lower CO and NOx emissions compared to conventional diesel because of the higher cetane number. It was also expected that the first generation biodiesel had a higher specific fuel consumption than conventional diesel because of the lower energy content in the fuel.

The main findings from the experiments and the simulations were:

- The engine experiments yielded lower NOx, and CO emissions for both types of biodiesels, compared to the conventional diesel. This was explained by a shorter ignition delay for both biodiesels, which results in a lower amount of premixed combustion compared to diffusion flame combustion. This was clearly seen on the HRR curves and from the calculated time until 50% heat release.
- Changed ignition delay for the first generation biodiesel was a somewhat unforeseen result. This ignition delay could not be explained by a change in cetane number alone, as it was for the second generation biodiesel. The first generation biodiesel therefore has an unexplained ability to easily mix with air and form an ignitable mixture before the conventional diesel does.
- The engine was generally operating more efficient when running on the first generation biodiesel. It was not injecting more fuel because of the lower energy content in first generation biodiesel, as was originally expected.
- First generation biodiesel had higher amounts of PM in all sizes. The change in ignition delay and the larger aromatic content of the first generation biodiesel was thought to be the main cause for this difference.
- The simulations showed that the two conventional diesel surrogates simulated diesel with varying accuracy. At low load and low RPM, both surrogates were close to the experimental results. At higher loads the n-decane and 1–methylnaphthalene mixture

showed a promising results in cylinder pressure and HRR, but this was not reflected in the emission simulations.

- Proper biodiesel simulations were not obtained using the SRM diesel engine model, so the biodiesel was simulated in a HCCI engine instead. These simulations showed that the MD was much harder to ignite than the diesel surrogates and because of the increased ignition delay it had a large decrease in NOx emissions compared to the diesel surrogates.

6   Further Work

There is still a lot of research potential left within this field. Some topics were out of the scope of this project, and some suggested improvements have already been emphasized. Suggested further work and topics of relevance are as follows:

1. Experiments with more biodiesel types and different blends

There are several types of biodiesel, and there are different types of first generation and second generation biodiesel as well, depending on the source and the production. There are also other types of biodiesel such as third generation biodiesel. All types of biodiesel are relevant for experimental testing and simulations. This project showed reduce NOx emissions for the two biodiesels that were studied, but this is not necessary correct for all types of biodiesel.

2. Experiments with biodiesel additives

Biodiesel additives are important for the aging properties of biodiesel. Biodiesel age during storage, when the biodiesel oxidizes due to the oxygen content in the fuel. Fuel additives can stop this oxidization and are therefore added to biodiesel in a larger extent than conventional diesel. The effect of these additives on the fuel combustion is mostly unknown [63].

3. More experiments with the particle sampler

The particle sampler used in this project broke down, and could not be fixed within the given time frame of this project. Finishing the particle measurements would be of great interest. Especially seeing the effect of the second generation biodiesel on the PM emissions, as second generation biodiesels have lower aromatic content than first generation biodiesels. Perhaps the second generation biodiesel would show lower PM emissions than both the first generation biodiesel and the conventional diesel.

4. Experiments with a new fuel flow meter and improved engine computer, linking cylinder pressure to CAD

The flow meter used in the experiment gave an uncertainty related to the fuel efficiency and specific fuel consumption measurements. A new flow meter could provide more accurate results. Linking the pressure profile to the CAD instead of the computer's internal clock, removes one uncertainty and the long Matlab scrip is not needed to plot the cylinder pressure against the CAD.

5. Experiments with different engine parameter

The use of EGR (Exhaust Gas Recirculation) and different injection strategies, such as multiple fuel injections and pilot injections, is standard in many modern diesel engines today [19]. EGR, multiple injections and pilot injection were by purpose not included in the experiments done in this project to limit the uncertainties. Seeing the effect of these parameters could still be interesting, and if they would affect the engine differently depending on fuel type.

6. Simulations of biodiesel in diesel engines

The biodiesel simulations were not completed. Simulating biodiesel in a diesel engine was intended, but it was done using an HCCI engine due to problems with the injection files and the unknown NASA polynomials for MD. Completing the biodiesel simulations and comparing them to the experimental biodiesel results would be a natural way to continue this project.

7. Trying different types of species as surrogates for diesel

N-heptane and the mixture of n-decane and 1-methylnapthalene is not the only surrogates available for conventional diesel. The use of n-heptane in combination with other species as a surrogate for diesel, has shown good results [54] [64]. Trying different types of diesel surrogates can yield better emission and engine performance calculations, and using different chemical mechanisms can verify the general chemical simulations.

8. Making a mixing model for the simulations

The mixing model for the engine simulation is a very important factor when simulating the combustion processes. LOGEsoft has the ability to include a so called mixing profile, where the fuel mixing time can be specified differently between the different crank angles. This enables calibration of the fuel mixing so that the simulated combustion matches with the experiments. This would probably improve the emission results greatly.

9. Trying to use a MD and N-heptane mixture as a surrogate for biodiesel

The simulation showed that the MD had a lower ignitability than the other surrogate fuels. This could be solved using a combination of n-heptane and MD, as a biodiesel surrogate. The n-heptane has shown to have a high ignitability, and the combination of n-heptane and MD as a biodiesel surrogate has shown good results [65].

10. CFD simulations of diesel engines

In this project, the SRM model was used. However, it is known that a full CFD analysis yields better results for the physical simulations. Taking a step further within this field would naturally involve a full CFD simulation of the engine. Using two different types of physical simulation methods, this would verify the physical simulation done in LOGEsoft, just like using different chemical mechanisms verify the chemical simulations.

References

[1] Intergovernmental Panel on Climate Change (IPCC), 2014, Carbon Dioxide: Projected emissions and concentrations [Online] Available at: http://www.ipcc-data.org/observ/ddc_co2.html. [Accessed 29 May 15].

[2] Intergovernmental Panel on Climate Change (IPCC). 2014. IPCC press release. [Online] Available at: http://ipcc.ch/pdf/ar5/pr_wg3/20140413_pr_pc_wg3_en. [Accessed 29 May 15].

[3] Intergovernmental Panel on Climate Change (IPCC). 2007. Summary for Policymakers. [Online] Available at: http://www.ipcc.ch/pdf/assessment-report/ar4/wg3/ar4-wg3-spm.pdf. [Accessed 29 May 15].

[4] M. Cames, E. Helmers, 2013. Critical evaluation of the European diesel car boom - global comparison, environmental effects and various national strategies. Environmental Sciences Europe, 25, 15.

[5] FAO Forestry Department Wood Energy Programme, 2004. Unified Bioenergy Terminology, Rome, Italy: Food and Agriculture Organization of the United Nations.

[6] Jason Hill, Erik Nelson, David Tilman, Stephen Polasky, Douglas Tiffany, 2006. Environmental, economic, and energetic costs and benefits of biodiesel and ethanol biofuels. PNAS, 103, 1206–11210

[7] Aftenposten/Jørgen Svarstad. 2015. Oslo sier ja til forbud mot dieselbiler. [Online] Available at: http://www.aftenposten.no/nyheter/iriks/Oslo-sier-ja-til-forbud-mot-dieselbiler-6849835.html. [Accessed 29 May 15].

[8] N. Guillén-Hurtado, V. Rico-Perz, A. Garcia-Garcia, D. Loxano-Castelló, A. Bueno-Lopez,. Three-Way Catalysts: Past, Present and Future. DYNA, ISSN 0012-7353, 114-121.

[9] Jan Kašpar, Paolo Fornasiero, Neal Hickey, 2003. Automotive catalytic converters: current status and some perspectives. Catalysis Today, 77, 419–449.

[10] Jinlin Xue, Tony E. Grift, Alan C. Hansen, 2011. Effect of biodiesel on engine performances and emissions. Renewable and Sustainable Energy Reviews, 15, 1098–1116

[11] John B. Heywood, 1988. Internal Combustion Engine Fundamentals. 1st ed. New York: McGraw-Hill.

[12] J. Warnatz, Ulrich Maas, Robert W. Dibble, 2006. Combustion. 4th ed. Berlin: Springer.

[13] Günter P. Merker, Christian Schwarz, Gunnar Stiesch, Frank Otto, 2006. Simulating Combustion. 1st ed. Berlin: Springer.

[14] Google Patents, Adya S. Tripathi, Chester J. Silvestri. 2012. Internal combustion engine control for improved fuel efficiency . [Online] Available at: http://www.google.com/patents/US8336521. [Accessed 30 May 15].

[15] Jack Erjavec, 2009. Automotive Technology: A Systems Approach, 5th Edition. Cengage Learning

[16] Mikael Lindström, 2011. Methods for Characterization of the Diesel Combustion and Emission Formation Processes. Ph.D. Stockholm: KTH- Royal institute of Technology.

[17] National Center for Environmental Assessment, 2002. Health assessment document for diesel engine exhaust. Washington, DC. U.S. Environmental Protection Agency (EPA). Report number: EPA/600/8-90/057F.

[18] National Fire Protection Association (NFPA), 2003. Flammable and Combustible Liquids Code. [Online]. Available from: https://law.resource.org/pub/us/cfr/ibr/004/nfpa.30.2003.pdf. [Accessed 22 May 15].

[19] Richard Stone, 2012. Introduction to Internal Combustion Engines, 4th ed. Warrendale, US: SAE International.

[20] Sara McAllister, Jyh-Yuan Chen, A. Carlos Fernandez-Pello, 2011. Fundamentals of Combustion Processes, 1st ed. London: Springer.

[21] United States Environmental Protection Agency, 2006. The PM Centers Program 2005-2010 Overviews and Abstracts. [Online]. Available from: http://www.epa.gov/ncer/publications/workshop/11-30-2005/pmcentersabstract.pdf. [Accessed 31 May 15].

[22] Barouch Giechaskiel, Matti Maricq, Leonidas Ntziachristos, Christos Dardiotis, Xiaoliang Wang, Harald Axmann, Alexander Bergmann, Wolfgang Schindler, 2014. Review of motor vehicle particulate emissions sampling and measurement: From smoke and filter mass to particle number. Journal of Aerosol Science, 67, 48–86.

[23] Mohr, M., Lehmann, U., and Margaria, G., 2003. ACEA Programme on the Emissions of Fine Particulates from Passenger Cars(2) Part 2: Effect of Sampling Conditions and Fuel Sulphur Content on the Particle Emission. SAE Technical Paper, 2003-01-1890.

[24] Mari Pietikäinena, Ari Väliheikkia, Kati Oravisjärvia, Tanja Kollia, Mika Huuhtanena, Seppo Niemib, Sampo Virtanenc, Toomas Karhuc, Riitta L. Keiskia, 2015. Particle and NOx emissions of a non-road diesel engine with an SCR unit: The effect of fuel. Renewable Energy, 77, 377-385.

[25] Nicos Ladommatos, Mohammad Parsi and Angela Knowles, 1995. The effect of fuel cetane improver on diesel pollutant emissions. Fuel, 75, 8-14.

[26] S. Kent Hoekman, Curtis Robbins, 2012. Review of the effects of biodiesel on NOx emissions. Fuel Processing Technology, 96, 237–249.

[27] Lundberg, Nils H, 2009. Dieselolje. Store norske leksikon. [Online]. Available from: https://snl.no/dieselolje. [Accessed 22 May 15]

[28] International Agency for Research on Cancer (IARC), 1989. Diesel Fuels: IARC Monographs Volume 45. Lyon, World Health Organization

[29] Jon H. Van Gerpen, Brian He, 2010. Biodiesel Production and Properties: Thermochemical Conversion of Biomass to Liquid Fuels and Chemicals, edited by: Mark Crocker, The Royal Society of Chemistry, Cambridge UK.

[30] Wikipedia. 2014. EN 590. [Online] Available at: http://en.wikipedia.org/wiki/EN_590 [Accessed 30 May 15].

[31] Fangrui Maa, Milford A. Hanna, 1999. Biodiesel production: a review. Bioresource Technology 70, 1-15.

[32] Wikipedia. 2015. EN 14214. [Online] Available at: http://en.wikipedia.org/wiki/EN_14214. [Accessed 30 May 15].

[33] Masayuki Adachi, 2000. Emission measurement techniques for advanced powertrains. Measurement Science and Technology, 11, 113–129.

[34] Steven Gluck, Chuck Glenn, Tim Logan, Bac Vu, Mike Walsh & Pat Williams, 2003. Evaluation of NOx Flue Gas Analyzers for Accuracy and Their Applicability for Low-Concentration Measurements. Journal of the Air & Waste Management Association, 53, 749–758.

[35] Peter R. Griffiths. Fourier Transform Infrared Spectrometry, 2007. 1st ed. Hoboken-US, Wiley & Sons Inc.

[36] Jason Seitz & Chenan Tong, 2013. Application Report: LMP91051 NDIR CO2 Gas Detection System. Texas Instruments SNAA207.

[37] Frank Drewnick, Silke S. Hings, Peter DeCarlo, John T. Jayne, Marc Gonin, Katrin Fuhrer, Silke Weimer, Jose L. Jimene, Kenneth L. Demerjian, Stephan Borrmann & Douglas R. Worsnop, 2005. A New Time-of-Flight Aerosol Mass Spectrometer (TOF-AMS)—Instrument Description and First Field Deployment. Aerosol Science and Technology, 39, 637–658.

[38] W. C. Wiley And I. H. McLaren, 1955.Time-of-Flight Mass Spectrometer with Improved Resolution. The Review of Scientific Instruments, 26, 1150-1157

[39] Ivan Fanelli, Sergio M. Camporeale and Bernardo Fortunato, 2012. Efficient On-Board Pegging Calculation from Piezo-Electric Sensor Signal for Real Time In-Cylinder Pressure Offset Compensation. SAE International, 5, 672-682.

[40] CD-adapco. 2014. DARS overview, IISc Bangalore. [Online] Available at: http://www.cd-adapco.com/sites/default/files/Presentation/DARS%20introductory.pdf. [Accessed 31 May 15].

[41] Martin Tunér, 2008. Stochastic Reactor Models for Engine Simulations. Ph.D. Sweden: Lund University.

[42] Haiyun Su, 2010. Stochastic Reactor Models for Simulating Direct Injection Homogeneous Charge Compression Ignition Engines. Ph.D. Cambridge: University of Cambridge.

[43] Carfolio.com. 2011. 1999 Mercedes-Benz E 320 CDI technical specifications. [ONLINE] Available at: http://www.carfolio.com/specifications/models/car/?car=249887. [Accessed 31 May 15].

[44] Mike Caruso, Steve Fox, Dave Hagen, Yolanda Carranza, Scott Groves, 2006. Connecting Rod Manual April 2006. 1st ed. Buffalo Grove - US: AERA - Engine Builders Association.

[45] T. E. Passenbrunner, M. Sassano, H. Trogmann, L. del Re, M. Paulweber, M. Schmidt and H. Kokal, (2011). Inverse Torque Control of Hydrodynamic Dynamometers for Combustion Engine Test Benches. In 2011 American Control Conference. San Francisco, June 29 2011-July 1 2011. San Francisco: IEEE. 4598 - 4603.

[46] Horiba. Portable Gas Analyzer PG-250. [Online] Available at: http://www.horiba.com/fileadmin/uploads/Process-Environmental/Documents/HRE2849G_-_PG250.pdf. [Accessed 31 May 15].

[47] Cambustion, 2010. DMS500 Fast Spectrometer with Heated Sample Line High Ratio Diluter, User Manual. Cambustion Ltd. Cambridge, UK

[48] Azhar Malik & Terese Løvås. Report on fuel characteristics: systematic identifications of characteristic properties of bio-fuels. NTNU

[49] Intertek, Geir H. Ingeborgrud, 2013. Report of Analysis, Sample ID: 2013-ATRP-003033-A-008. Sample Designated as: FAME. Antwerp, Belgium .

[50] Intertek, M. Weber, 2014. Report of Analysis, Sample ID: 14/P153623. Sample Designated as: NEX BTL. Hamburg, Germany.

[51] European Biofuels. 2011. Fatty Acid Methyl Esters (FAME). [Online] Available at: http://www.biofuelstp.eu/factsheets/fame-fact-sheet.pdf. [Accessed 31 May 15].

[52] LOGEsoft, 2014. Scientific Software for Modelling of Chemical Kinetic Systems, MANUAL - BOOK 3, Engine Models. LOGE AB. Sweden

[53] C. Thomas Avedisian , 2014. Novel Combustion Concepts for Sustainable Energy Development – Developing Surrogates for liquid Transportation Fuels: The Role of Spherically Symmetric Droplet Combustion. 2014 Edition. Springer.

[54] William J. Pitz, Charles J. Mueller, 2011. Recent progress in the development of diesel surrogate fuels. Progress in Energy and Combustion Science, 37, 330-350.

[55] M. Meijer. 2010. Characterization of n-heptane as a single component Diesel surrogate fuel. [Online] Available at: http://w3.wtb.tue.nl/fileadmin/wtb/ct-pdfs/Master_Theses/FinalThesisMaarten.pdf. [Accessed 07 June 15].

[56] Yiguang Ju. 2011. Studies of kinetics and flame chemistry of methyl-esters and C0 -C2 foundation fuels. [Online] Available at: http://www.princeton.edu/cefrc/Files/2011%20Annual%20Conf/research-of-ju-group.pdf. [Accessed 07 June 15].

[57] Olivier Herbinet, William J. Pitz, Charlie K. Westbrook, 2008. Detailed chemical kinetic oxidation mechanism for a biodiesel surrogate. Combustion and Flame, Elsevier, 154 (3), pp.507- 528. 10.1016/j.combustflame.2008.03.003. hal-00724801

[58] Charles J. Mueller, André L. Boehman, and Glen C. Martin, 2009. An Experimental Investigation of the Origin of Increased NOx Emissions When Fuelling a Heavy-Duty Compression-Ignition Engine with Soy Biofuels. SAE International, 2009-01-1792.

[59] A S Cheng, A Upatnieks, C J Mueller, 2005. Investigation of the impact of biodiesel fuelling on NOx emissions using an optical direct injection diesel engine. International Journal of Engine Research, 7.

[60] NGVA Europe. 2009. Position Paper: Natural Gas and C02 Natural gas is a champion in road transport and also saving CO2 emissions. [Online] Available at: https://www.ngvaeurope.eu/members/position-papers/NGVA-Europe-Position-Paper-CNG-CO2.pdf. [Accessed 09 June 15].

[61] Klaus H. Altgelt, 1993. Composition and Analysis of Heavy Petroleum Fractions: 54 (Chemical Industries). 1st Edition. CRC Press. Page 171.

[62] R.K. Rajput, 2013. Thermal Engineering (SI Units). 9th Edition. Laxmi Publications. Page 1139.

[63] Georgios Karavalakis, Despina Hilari, Lida Givalou, Dimitrios Karonis, Stamos Stournas, 2011. Storage stability and ageing effect of biodiesel blends treated with different antioxidants. Energy, 36, 369-374.

[64] Jing Luo, Mingfa Yao, Haifeng Liu, Binbin Yang, 2012. Experimental and numerical study on suitable diesel fuel surrogates in low temperature combustion conditions. Fuel, 37, 621–629.

[65] Olivier Herbinet, William J. Pitz, Charles K. Westbrook, 2010. Detailed chemical kinetic mechanism for the oxidation of biodiesel fuels blend surrogate. Combustion and Flame, 157, 893–908.

Appendix A. Matlab Code – Experimental data averaging, correction and plotting

```matlab
clc
close all
clear

prompt='Enter file name Diesel: ';
file1=input(prompt,'s');

prompt='Enter file name 1st Gen. Bio: ';
file2=input(prompt,'s');

prompt='Enter file name 2nd Gen. Bio: ';
file3=input(prompt,'s');

%Reading files
X1=xlsread(file1,'High speed', 'B2:B200000');
Y1=xlsread(file1,'High speed','H2:H200000');
T1=xlsread(file1,'Low speed','CB2:CB8');
I1=xlsread(file1,'Low speed','CG2:CG8');
N1=xlsread(file1,'Low speed','BX2:BX8');
NOx1=xlsread(file1,'Low speed','DA2:DA8');
CO1=xlsread(file1,'Low speed','DB2:DB8');
CO21=xlsread(file1,'Low speed','DC2:DC8');
Nm1=xlsread(file1,'Low speed','CU2:CU8');
kW1=xlsread(file1,'Low speed','CV2:CV8');
ExT1=xlsread(file1,'Low speed','U2:U8');
O21=xlsread(file1,'Low speed','DD2:DD8');
F1=xlsread(file1,'Low speed','BY2:BY8');

X2=xlsread(file2,'High speed', 'B2:B200000');
Y2=xlsread(file2,'High speed','H2:H200000');
T2=xlsread(file2,'Low speed','CB2:CB8');
I2=xlsread(file2,'Low speed','CG2:CG8');
N2=xlsread(file2,'Low speed','BX2:BX8');
NOx2=xlsread(file2,'Low speed','DA2:DA8');
CO2=xlsread(file2,'Low speed','DB2:DB8');
CO22=xlsread(file2,'Low speed','DC2:DC8');
Nm2=xlsread(file2,'Low speed','CU2:CU8');
kW2=xlsread(file2,'Low speed','CV2:CV8');
ExT2=xlsread(file2,'Low speed','U2:U8');
O22=xlsread(file2,'Low speed','DD2:DD8');
F2=xlsread(file2,'Low speed','BY2:BY8');

X3=xlsread(file3,'High speed', 'B2:B200000');
Y3=xlsread(file3,'High speed','H2:H200000');
T3=xlsread(file3,'Low speed','CB2:CB8');
I3=xlsread(file3,'Low speed','CG2:CG8');
N3=xlsread(file3,'Low speed','BX2:BX8');
NOx3=xlsread(file3,'Low speed','DA2:DA8');
CO3=xlsread(file3,'Low speed','DB2:DB8');
CO23=xlsread(file3,'Low speed','DC2:DC8');
Nm3=xlsread(file3,'Low speed','CU2:CU8');
kW3=xlsread(file3,'Low speed','CV2:CV8');
ExT3=xlsread(file3,'Low speed','U2:U8');
```

```matlab
54    O23=xlsread(file3,'Low speed','DD2:DD8');
55    F3=xlsread(file3,'Low speed','BY2:BY8');
56
57    %Finding TDC signals
58    d1=(diff(Y1));
59    Z1=find(d1==-1);
60
61    d2=(diff(Y2));
62    Z2=find(d2==-1);
63
64    d3=(diff(Y3));
65    Z3=find(d3==-1);
66
67    %Finding true TDC
68    start1=0;
69    start2=0;
70    start3=0;
71    for j=4:9
72        if X1(Z1(j,1))>3
73            start1=j-3;
74            TDC1=Z1(j,1)-Z1(start1,1);
75            end
76    end
77    for j=4:9
78        if X2(Z2(j,1))>3
79            start2=j-3;
80            TDC2=Z2(j,1)-Z2(start2,1);
81        end
82    end
83    for j=4:9
84        if X3(Z3(j,1))>3
85            start3=j-3;
86            TDC3=Z3(j,1)-Z3(start3,1);
87        end
88    end
89
90    %Saving 16 cycles in a cell array, starting at 360 Deg before TDC and
91    %stopping at 360Deg after TDC
92    n=0;
93    m=0;
94    k=0;
95    x=0;
96    findMax=zeros(1,54);
97
98    for i=(start1):6:(start1+96)
99        n=n+1;
100       SampleStart=Z1(i,1);
101       SampleStop=Z1(i+6,1);
102       x=X1(SampleStart:SampleStop);
103       findMax(n)=length(x);
104       A1{n}=x;
105   end
106   for i=(start2):6:(start2+96)
107       m=m+1;
108       SampleStart=Z2(i,1);
109       SampleStop=Z2(i+6,1);
110       x=X2(SampleStart:SampleStop);
111       findMax(m+n)=length(x);
112       A2{m}=x;
113   end
```

```matlab
114    for i=(start3):6:(start3+96)
115        k=k+1;
116        SampleStart=Z3(i,1);
117        SampleStop=Z3(i+6,1);
118        x=X3(SampleStart:SampleStop);
119        findMax(k+m+n)=length(x);
120        A3{k}=x;
121    end
122
123    %Adding zeroes to the end of the shorter cycles so that all cycles have the
124    %same length, and then putting each cycle into a separate column in a
125    %matrix
126    a1=0;
127    a2=0;
128    a3=0;
129    Max=max(findMax);
130
131    All1=zeros(Max,16);
132    All2=zeros(Max,16);
133    All3=zeros(Max,16);
134    for n=1:16
135        x=A1{n};
136        xpad=Max-length(x);
137        a1=padarray(x,xpad,'post');
138        All1(:,n)=a1;
139    end
140
141    for n=1:16
142        x=A2{n};
143        xpad=Max-length(x);
144        a2=padarray(x,xpad,'post');
145        All2(:,n)=a2;
146    end
147    for n=1:16
148        x=A3{n};
149        xpad=Max-length(x);
150        a3=padarray(x,xpad,'post');
151        All3(:,n)=a3;
152    end
153
154    %correcting for pressure drift
155    M1=zeros(1,16);
156    M2=zeros(1,16);
157    M3=zeros(1,16);
158
159    Pressure1=zeros(Max,16);
160    Pressure2=zeros(Max,16);
161    Pressure3=zeros(Max,16);
162
163    for n=1:16
164        M1(n)=min(All1(:,n));
165        if M1<0
166            Pressure1(:,n)=All1(:,n)+abs(M1(n));
167        else
168            Pressure1(:,n)=All1(:,n)-abs(M1(n));
169        end
170    end
171    for n=1:16
172        M2(n)=min(All2(:,n));
173        if M2<0
```

```matlab
174              Pressure2(:,n)=All2(:,n)+abs(M2(n));
175         else
176              Pressure2(:,n)=All2(:,n)-abs(M2(n));
177         end
178     end
179     for n=1:16
180         M3(n)=min(All3(:,n));
181         if M3<0
182              Pressure3(:,n)=All3(:,n)+abs(M3(n));
183         else
184              Pressure3(:,n)=All3(:,n)-abs(M3(n));
185         end
186     end
187
188     %Averaging the 18 cycles and smoothing them
189     Ave1=mean(Pressure1,2);
190     Ave2=mean(Pressure2,2);
191     Ave3=mean(Pressure3,2);
192
193     smo1=smooth(Ave1);
194     smo2=smooth(Ave2);
195     smo3=smooth(Ave3);
196
197     Mtot1=min(smo1);
198     if Mtot1<0
199         smo1=smo1+abs(Mtot1);
200     else
201         smo1=smo1-abs(Mtot1);
202     end
203     Mtot2=min(smo2);
204     if Mtot2<0
205         smo2=smo2+abs(Mtot2);
206     else
207         smo2=smo2-abs(Mtot2);
208     end
209     Mtot3=min(smo3);
210     if Mtot3<0
211         smo3=smo3+abs(Mtot3);
212     else
213         smo3=smo3-abs(Mtot3);
214     end
215
216     %calculating pressure rate in Pa/degCA
217
218     deg1=720/(Z1(7,1)-Z1(1,1));
219     deg2=720/(Z2(7,1)-Z2(1,1));
220     deg3=720/(Z3(7,1)-Z3(1,1));
221
222     corP1=smo1*10^6+101325;
223     Prate1=zeros(1,Max);
224     for i=1:Max
225         if i==Max
226              Prate1(i)=(corP1(i-1)-corP1(i))/deg1;
227         else
228              Prate1(i)=(corP1(i+1)-corP1(i))/deg1;
229         end
230     end
231     smoPrate1=smooth(Prate1,15);
232
233     corP2=smo2*10^6+101325;
```

```
234    Prate2=zeros(1,Max);
235    for i=1:Max
236        if i==Max
237            Prate2(i)=(corP2(i-1)-corP2(i))/deg2;
238        else
239            Prate2(i)=(corP2(i+1)-corP2(i))/deg2;
240        end
241    end
242    smoPrate2=smooth(Prate2,15);
243
244    corP3=smo3*10^6+101325;
245    Prate3=zeros(1,Max);
246    for i=1:Max
247        if i==Max
248            Prate3(i)=(corP3(i-1)-corP3(i))/deg3;
249        else
250            Prate3(i)=(corP3(i+1)-corP3(i))/deg3;
251        end
252    end
253    smoPrate3=smooth(Prate3,15);
254
255
256    %finding adjusted TDC
257
258    Pratesignchange1=find(abs(diff(sign(smoPrate1)))==2);
259    realTDC1=TDC1;
260    for j=1:length(Pratesignchange1)
261        if Pratesignchange1(j)<TDC1 && Pratesignchange1(j)>TDC1-20
262            realTDC1=Pratesignchange1(j);
263        end
264    end
265    Pratesignchange2=find(abs(diff(sign(smoPrate2)))==2);
266    realTDC2=TDC2;
267    for j=1:length(Pratesignchange2)
268        if Pratesignchange2(j)<TDC2 && Pratesignchange2(j)>TDC2-20
269            realTDC2=Pratesignchange2(j);
270        end
271    end
272    Pratesignchange3=find(abs(diff(sign(smoPrate3)))==2);
273    realTDC3=TDC3;
274    for j=1:length(Pratesignchange3)
275        if Pratesignchange3(j)<TDC3 && Pratesignchange3(j)>TDC3-20
276            realTDC3=Pratesignchange3(j);
277        end
278    end
279
280    %Calculating the degrees for x-axis
281    D1=zeros(1,Max);
282    D2=zeros(1,Max);
283    D3=zeros(1,Max);
284    D1(1,realTDC1)=0;
285    D2(1,realTDC2)=0;
286    D3(1,realTDC3)=0;
287
288    Deg=0;
289    Deg2=0;
290    for m=realTDC1:1:(Max-1)
291        Deg=Deg+deg1;
292        D1(m+1)=Deg;
293    end
```

```matlab
294     for t=1:1:realTDC1-1
295         h=realTDC1-t;
296         Deg2=Deg2-deg1;
297         D1(h)=Deg2;
298     end
299
300     Deg=0;
301     Deg2=0;
302     for m=realTDC2:1:(Max-1)
303         Deg=Deg+deg1;
304         D2(m+1)=Deg;
305     end
306     for t=1:1:realTDC2-1
307         h=realTDC2-t;
308         Deg2=Deg2-deg2;
309         D2(h)=Deg2;
310     end
311
312     Deg=0;
313     Deg2=0;
314     for m=realTDC3:1:(Max-1)
315         Deg=Deg+deg3;
316         D3(m+1)=Deg;
317     end
318
319     for t=1:1:realTDC3-1
320         h=realTDC3-t;
321         Deg2=Deg2-deg3;
322         D3(h)=Deg2;
323     end
324
325
326     %calculating Heat Release Rate
327
328     B=88*10^-3; %Bore [m]
329     L=88.3*10^-3; %Stroke [m]
330     a0=L/2; %Crank radius [m]
331     l=145*10^-3; %Connecting rod length [m]
332     gamma=1.32; %Specific heat ratio
333     rc=18; %Compression ratio
334
335     Area=(pi/4)*B^2;
336     Vc=Area*L/(rc-1);
337     s1=zeros(1,Max);
338     s2=zeros(1,Max);
339     s3=zeros(1,Max);
340     V1=zeros(1,Max);
341     V2=zeros(1,Max);
342     V3=zeros(1,Max);
343     Vrate1=zeros(1,Max);
344     Vrate2=zeros(1,Max);
345     Vrate3=zeros(1,Max);
346
347     HRR1=zeros(1,Max);
348     HRR2=zeros(1,Max);
349     HRR3=zeros(1,Max);
350
351     for n=1:Max
352     s1(n)=a0*cosd(D1(n))+sqrt((l^2)-(a0^2)*(sind(D1(n)))^2);
353     V1(n)=Vc+Area*(l+a0-s1(n));
```

```matlab
354    end
355    for n=1:Max
356    s2(n)=a0*cosd(D2(n))+sqrt((l^2)-(a0^2)*(sind(D2(n)))^2);
357    V2(n)=Vc+Area*(l+a0-s2(n));
358    end
359    for n=1:Max
360    s3(n)=a0*cosd(D3(n))+sqrt((l^2)-(a0^2)*(sind(D3(n)))^2);
361    V3(n)=Vc+Area*(l+a0-s3(n));
362    end
363
364    for n=1:Max
365        if n==Max
366            Vrate1(n)=(V1(n-1)-V1(n))/deg1;
367        else
368            Vrate1(n)=(V1(n+1)-V1(n))/deg1;
369        end
370    end
371    for n=1:Max
372        if n==Max
373            Vrate2(n)=(V2(n-1)-V2(n))/deg2;
374        else
375            Vrate2(n)=(V2(n+1)-V2(n))/deg2;
376        end
377    end
378    for n=1:Max
379        if n==Max
380            Vrate3(n)=(V3(n-1)-V3(n))/deg3;
381        else
382            Vrate3(n)=(V3(n+1)-V3(n))/deg3;
383        end
384    end
385
386    for n=1:Max
387    HRR1(n)=(gamma/(gamma-1))*corP1(n)*Vrate1(n)+(1/(gamma-
388    1))*V1(n)*smoPrate1(n);
389    HRR2(n)=(gamma/(gamma-1))*corP2(n)*Vrate2(n)+(1/(gamma-
390    1))*V2(n)*smoPrate2(n);
391    HRR3(n)=(gamma/(gamma-1))*corP3(n)*Vrate3(n)+(1/(gamma-
392    1))*V3(n)*smoPrate3(n);
393    end
394
395    smoHRR1=smooth(HRR1);
396    smoHRR2=smooth(HRR2);
397    smoHRR3=smooth(HRR3);
398
399    %Finding Ignition delay,
400
401    HRRsignchange1=find(abs(diff(sign(HRR1)))==2);
402    HRRsignchange2=find(abs(diff(sign(HRR2)))==2);
403    HRRsignchange3=find(abs(diff(sign(HRR3)))==2);
404
405    C1=length(HRRsignchange1);
406    C2=length(HRRsignchange2);
407    C3=length(HRRsignchange3);
408
409    %Finding which degrees that the 0's correspond to
410    degHRRchange1=zeros(1,C1);
411    degHRRchange2=zeros(1,C2);
412    degHRRchange3=zeros(1,C3);
413    for n=1:C1
```

```matlab
414        degHRRchange1(n)=D1(HRRsignchange1(n));
415    end
416    for n=1:C2
417        degHRRchange2(n)=D2(HRRsignchange2(n));
418    end
419    for n=1:C3
420        degHRRchange3(n)=D3(HRRsignchange3(n));
421    end
422    %Saving the point where betweeen -15deg CA and 10deg CA
423    for n=1:C1
424        if degHRRchange1(n)>-15 && degHRRchange1(n)<10
425            combstart1=degHRRchange1(n);
426        end
427    end
428    for n=1:C2
429        if degHRRchange2(n)>-15 && degHRRchange2(n)<10
430            combstart2=degHRRchange2(n);
431        end
432    end
433    for n=1:C3
434        if degHRRchange3(n)>-15 && degHRRchange3(n)<10
435            combstart3=degHRRchange3(n);
436        end
437    end
438
439    %Saving the point where between 10deg CA and 180deg CA
440    for n=1:C1
441        if degHRRchange1(n)>10 && degHRRchange1(n)<180
442            combend1=degHRRchange1(n);
443        end
444    end
445    for n=1:C2
446        if degHRRchange2(n)>10 && degHRRchange2(n)<180
447            combend2=degHRRchange2(n);
448        end
449    end
450    for n=1:C3
451        if degHRRchange3(n)>10 && degHRRchange3(n)<180
452            combend3=degHRRchange3(n);
453        end
454    end
455    %finding the injection timing and ignition delay
456    injstart1=-mean(T1);
457    injstart2=-mean(T2);
458    injstart3=-mean(T3);
459    speed1=mean(N1);
460    speed2=mean(N2);
461    speed3=mean(N3);
462    igndelayDeg1=combstart1-injstart1;
463    igndelayDeg2=combstart2-injstart2;
464    igndelayDeg3=combstart3-injstart3;
465    DegSec1=(speed1/60)*360;
466    DegSec2=(speed2/60)*360;
467    DegSec3=(speed3/60)*360;
468    igndelayMikroSec1=(igndelayDeg1/DegSec1)*10^6;
469    igndelayMikroSec2=(igndelayDeg2/DegSec2)*10^6;
470    igndelayMikroSec3=(igndelayDeg3/DegSec3)*10^6;
471
472    %finding the injection duration
473
474    injDur1=mean(I1);
```

```matlab
475    injDur2=mean(I2);
476    injDur3=mean(I3);
477    injDurDeg1=DegSec1*injDur1*10^-6;
478    injDurDeg2=DegSec2*injDur2*10^-6;
479    injDurDeg3=DegSec3*injDur3*10^-6;
480    injend1=injstart1+injDurDeg1;
481    injend2=injstart2+injDurDeg2;
482    injend3=injstart3+injDurDeg3;
483
484    %Finding the time until 50 %HRR
485    Startcomb1=find(D1==combstart1);
486    Startcomb2=find(D2==combstart2);
487    Startcomb3=find(D3==combstart3);
488    Endcomb1=find(D1==combend1);
489    Endcomb2=find(D2==combend2);
490    Endcomb3=find(D3==combend3);
491    HRRtot1=0;
492    HRRtot2=0;
493    HRRtot3=0;
494    HRRtotVec1=zeros(1,(Endcomb1-Startcomb1));
495    HRRtotVec2=zeros(1,(Endcomb2-Startcomb2));
496    HRRtotVec3=zeros(1,(Endcomb3-Startcomb3));
497
498    for n=Startcomb1:1:Endcomb1
499        HRRtot1=HRRtot1+smoHRR1(n);
500        HRRtotVec1(n)=HRRtot1;
501    end
502    for n=Startcomb2:1:Endcomb2
503        HRRtot2=HRRtot2+smoHRR2(n);
504        HRRtotVec2(n)=HRRtot2;
505    end
506    for n=Startcomb3:1:Endcomb3
507        HRRtot3=HRRtot3+smoHRR3(n);
508        HRRtotVec3(n)=HRRtot3;
509    end
510
511    HalfHRR1=HRRtot1/2;
512    HalfHRR2=HRRtot2/2;
513    HalfHRR3=HRRtot3/2;
514    HalfHRRlist1=zeros(1,Endcomb1);
515    HalfHRRlist2=zeros(1,Endcomb2);
516    HalfHRRlist3=zeros(1,Endcomb3);
517    for n=Startcomb1:1:Endcomb1
518        if HRRtotVec1(n)>HalfHRR1
519            HalfHRRlist1(n)=HRRtotVec1(n);
520        end
521    end
522    for n=Startcomb2:1:Endcomb2
523        if HRRtotVec2(n)>HalfHRR2
524            HalfHRRlist2(n)=HRRtotVec2(n);
525        end
526    end
527    for n=Startcomb3:1:Endcomb3
528        if HRRtotVec3(n)>HalfHRR3
529            HalfHRRlist3(n)=HRRtotVec3(n);
530        end
531    end
532    HalfHRRlistmin1=HalfHRRlist1(HalfHRRlist1~=0);
533    HalfHRRlistmin2=HalfHRRlist2(HalfHRRlist2~=0);
534    HalfHRRlistmin3=HalfHRRlist3(HalfHRRlist3~=0);
535    fiftyPercent1=min(HalfHRRlistmin1);
```

```
536    fiftyPercent2=min(HalfHRRlistmin2);
537    fiftyPercent3=min(HalfHRRlistmin3);
538    fiftyPercentHRR1=find(HalfHRRlist1==fiftyPercent1);
539    fiftyPercentHRR2=find(HalfHRRlist2==fiftyPercent2);
540    fiftyPercentHRR3=find(HalfHRRlist3==fiftyPercent3);
541    fiftyPercentHRRDeg1=D1(fiftyPercentHRR1);
542    fiftyPercentHRRDeg2=D2(fiftyPercentHRR2);
543    fiftyPercentHRRDeg3=D3(fiftyPercentHRR3);
544    fiftyPercentDegChange1=fiftyPercentHRRDeg1-combstart1;
545    fiftyPercentDegChange2=fiftyPercentHRRDeg2-combstart2;
546    fiftyPercentDegChange3=fiftyPercentHRRDeg3-combstart3;
547
548    fiftyHRRmSec1=(fiftyPercentDegChange1/DegSec1)*10^6;
549    fiftyHRRmSec2=(fiftyPercentDegChange2/DegSec2)*10^6;
550    fiftyHRRmSec3=(fiftyPercentDegChange3/DegSec3)*10^6;
551
552
553    injstart=[injstart1,injstart2,injstart3]
554    injend=[injend1,injend2,injend3]
555    combstart=[combstart1,combstart2,combstart3]
556    ignitionDelay=[igndelayDeg1,igndelayDeg2,igndelayDeg3]
557    ignitionDelayMikroSec=[igndelayMikroSec1,igndelayMikroSec2,igndelayMikroSec
558    3]
559    combend=[combend1,combend2,combend3]
560    fiftyPercentHRRDeg=[fiftyPercentHRRDeg1,fiftyPercentHRRDeg2,fiftyPercentHRR
561    Deg3]
562    fiftyPercentDegChange=[fiftyPercentDegChange1,fiftyPercentDegChange2,fiftyP
563    ercentDegChange3]
564    fiftyHRRmSec=[fiftyHRRmSec1,fiftyHRRmSec2,fiftyHRRmSec3]
565
566    Injstart=round(injstart*10)/10;
567    Injend=round(injend*10)/10;
568    Combstart=round(combstart*10)/10;
569    IgnitionDelay=round(ignitionDelay*10)/10;
570    IgnitionDelayMikroSec=round(ignitionDelayMikroSec*10)/10;
571    Combend=round(combend*10)/10;
572    FiftyPercentHRRDeg=round(fiftyPercentHRRDeg*10)/10;
573    FiftyPercentDegChange=round(fiftyPercentDegChange*10)/10;
574    FiftyHRRmSec=round(fiftyHRRmSec*10)/10;
575
576    %Emissions, power and torque
577    NOxem1=mean(NOx1);
578    NOxem2=mean(NOx2);
579    NOxem3=mean(NOx3);
580    NOxChange1st=((NOxem2/NOxem1)-1)*100;
581    NOxChange2nd=((NOxem3/NOxem1)-1)*100;
582
583    COem1=mean(CO1);
584    COem2=mean(CO2);
585    COem3=mean(CO3);
586    COchange1st=((COem2/COem1)-1)*100;
587    COchange2nd=((COem3/COem1)-1)*100;
588
589    CO2em1=mean(CO21);
590    CO2em2=mean(CO22);
591    CO2em3=mean(CO23);
592    CO2change1st=((CO2em2/CO2em1)-1)*100;
593    CO2change2nd=((CO2em3/CO2em1)-1)*100;
594
595    O2em1=mean(O21);
```

```matlab
596    O2em2=mean(O22);
597    O2em3=mean(O23);
598    O2change1st=((O2em2/O2em1)-1)*100;
599    O2change2nd=((O2em3/O2em1)-1)*100;
600
601    Torque1=mean(Nm1);
602    Torque2=mean(Nm2);
603    Torque3=mean(Nm3);
604
605    Power1=mean(kW1);
606    Power2=mean(kW2);
607    Power3=mean(kW3);
608
609    Temp1=mean(ExT1);
610    Temp2=mean(ExT2);
611    Temp3=mean(ExT3);
612
613
614    NOx=[NOxem1,NOxem2,NOxem3]
615    ExhaustTemp=[Temp1,Temp2,Temp3]
616    CO=[COem1,COem2,COem3]
617    CO2=[CO2em1,CO2em2,CO2em3]
618    O2=[O2em1,O2em2,O2em3]
619    Torque=[Torque1,Torque2,Torque3]
620    Power=[Power1,Power2,Power3]
621
622    % Making Ignition profile
623    ign1=zeros(1,Max);
624    for n=1:Max
625        if D1(n)< injstart1
626            ign1(n)=0.5;
627        elseif D1(n)>injstart1 && D1(n)<injend1
628            ign1(n)=1.5;
629        elseif D1(n)>injend1
630            ign1(n)=0.5;
631        end
632    end
633    ign2=zeros(1,Max);
634    for n=1:Max
635        if D1(n)< injstart1
636            ign2(n)=-8;
637        elseif D1(n)>injstart1 && D1(n)<injend1
638            ign2(n)=0;
639        elseif D1(n)>injend1
640            ign2(n)=-8;
641        end
642    end
643
644    %finding the indicated energy output and the indicated fuel efficiency
645    n=0;
646    g=0;
647    h=0;
648    t=0;
649    for i=1:Max
650        if D1(i)>-180 && D1(i)<0
651            n=n+1;
652            VolLow1=zeros(n,1);
653            PressLow1=zeros(n,1);
654        elseif D1(i)>0 && D1(i)<180
655            g=g+1;
```

```matlab
656            VolHigh1=zeros(g,1);
657            PressHigh1=zeros(g,1);
658        elseif D1(i)>-360 && D1(i)<-180
659            h=h+1;
660            VolExLow1=zeros(h,1);
661            PressExLow1=zeros(h,1);
662        elseif D1(i)>180 && D1(i)<360
663            t=t+1;
664            VolExHigh1=zeros(t,1);
665            PressExHigh1=zeros(t,1);
666        end
667    end
668    n=0;
669    g=0;
670    h=0;
671    t=0;
672    for i=1:Max
673        if D1(i)>-180 && D1(i)<0
674            n=n+1;
675            VolLow1(n,1)=V1(i);
676            PressLow1(n,1)=corP1(i);
677        elseif D1(i)>0 && D1(i)<180
678            g=g+1;
679            VolHigh1(g,1)=V1(i);
680            PressHigh1(g,1)=corP1(i);
681        elseif D1(i)>-360 && D1(i)<-180
682            h=h+1;
683            VolExLow1(h,1)=V1(i);
684            PressExLow1(h,1)=corP1(i);
685        elseif D1(i)>180 && D1(i)<360
686            t=t+1;
687            VolExHigh1(t,1)=V1(i);
688            PressExHigh1(t,1)=corP1(i);
689        end
690    end
691    EnergLow1=trapz(VolLow1,PressLow1);
692    EnergHigh1=trapz(VolHigh1,PressHigh1);
693    PowerStr1=EnergHigh1+EnergLow1;
694    ExLow1=trapz(VolExLow1,PressExLow1);
695    ExHigh1=trapz(VolExHigh1,PressExHigh1);
696    Exhaust1=ExHigh1+ExLow1;
697    Energy1=PowerStr1-Exhaust1;
698
699    n=0;
700    g=0;
701    h=0;
702    t=0;
703    for i=1:Max
704        if D2(i)>-180 && D2(i)<0
705            n=n+1;
706            VolLow2=zeros(n,1);
707            PressLow2=zeros(n,1);
708        elseif D2(i)>0 && D2(i)<180
709            g=g+1;
710            VolHigh2=zeros(g,1);
711            PressHigh2=zeros(g,1);
712        elseif D2(i)>-360 && D2(i)<-180
713            h=h+1;
714            VolExLow2=zeros(h,1);
715            PressExLow2=zeros(h,1);
716        elseif D2(i)>180 && D2(i)<360
```

```matlab
            t=t+1;
            VolExHigh2=zeros(t,1);
            PressExHigh2=zeros(t,1);
        end
    end
    n=0;
    g=0;
    h=0;
    t=0;
    for i=1:Max
        if D2(i)>-180 && D2(i)<0
            n=n+1;
            VolLow2(n,1)=V2(i);
            PressLow2(n,1)=corP2(i);
        elseif D2(i)>0 && D2(i)<180
            g=g+1;
            VolHigh2(g,1)=V2(i);
            PressHigh2(g,1)=corP2(i);
        elseif D2(i)>-360 && D2(i)<-180
            h=h+1;
            VolExLow2(h,1)=V2(i);
            PressExLow2(h,1)=corP2(i);
        elseif D2(i)>180 && D2(i)<360
            t=t+1;
            VolExHigh2(t,1)=V2(i);
            PressExHigh2(t,1)=corP2(i);
        end
    end
    EnergLow2=trapz(VolLow2,PressLow2);
    EnergHigh2=trapz(VolHigh2,PressHigh2);
    PowerStr2=EnergHigh1+EnergLow1;
    ExLow2=trapz(VolExLow2,PressExLow2);
    ExHigh2=trapz(VolExHigh2,PressExHigh2);
    Exhaust2=ExHigh2+ExLow2;
    Energy2=PowerStr2-Exhaust2;

    n=0;
    g=0;
    h=0;
    t=0;
    for i=1:Max
        if D3(i)>-180 && D3(i)<0
            n=n+1;
            VolLow3=zeros(n,1);
            PressLow3=zeros(n,1);
        elseif D3(i)>0 && D3(i)<180
            g=g+1;
            VolHigh3=zeros(g,1);
            PressHigh3=zeros(g,1);
        elseif D3(i)>-360 && D3(i)<-180
            h=h+1;
            VolExLow3=zeros(h,1);
            PressExLow3=zeros(h,1);
        elseif D3(i)>180 && D3(i)<360
            t=t+1;
            VolExHigh3=zeros(t,1);
            PressExHigh3=zeros(t,1);
        end
    end
    n=0;
    g=0;
```

```
778   h=0;
779   t=0;
780   for i=1:Max
781       if D3(i)>-180 && D3(i)<0
782           n=n+1;
783           VolLow3(n,1)=V3(i);
784           PressLow3(n,1)=corP3(i);
785       elseif D3(i)>0 && D3(i)<180
786           g=g+1;
787           VolHigh3(g,1)=V3(i);
788           PressHigh3(g,1)=corP3(i);
789       elseif D3(i)>-360 && D3(i)<-180
790           h=h+1;
791           VolExLow3(h,1)=V3(i);
792           PressExLow3(h,1)=corP3(i);
793       elseif D3(i)>180 && D3(i)<360
794           t=t+1;
795           VolExHigh3(t,1)=V3(i);
796           PressExHigh3(t,1)=corP3(i);
797       end
798   end
799   EnergLow3=trapz(VolLow3,PressLow3);
800   EnergHigh3=trapz(VolHigh3,PressHigh3);
801   PowerStr3=EnergHigh3+EnergLow3;
802   ExLow3=trapz(VolExLow3,PressExLow3);
803   ExHigh3=trapz(VolExHigh3,PressExHigh3);
804   Exhaust3=ExHigh3+ExLow3;
805   Energy3=PowerStr3-Exhaust3;
806
807   Energy=[Energy1,Energy2,Energy3];
808
809   LHV1=42.9;
810   LHV2=37.7;
811   LHV3=43.9;
812   FuelAmount1=mean(F1);
813   FuelAmount2=mean(F2);
814   FuelAmount3=mean(F3);
815   FuelEnergy1=LHV1*FuelAmount1;
816   FuelEnergy2=LHV2*FuelAmount2;
817   FuelEnergy3=LHV3*FuelAmount3;
818
819   Efficiency1=Energy1/FuelEnergy1;
820   Efficiency2=Energy2/FuelEnergy2;
821   Efficiency3=Energy3/FuelEnergy3;
822
823   Efficiency=[Efficiency1,Efficiency2,Efficiency3]
824
825   %Finding IMEP
826   IMEP1=Energy1/(3.2/6);
827   IMEP2=Energy2/(3.2/6);
828   IMEP3=Energy3/(3.2/6);
829
830   IMEP=[IMEP1,IMEP2,IMEP3]
831
832   %Finding ISFC
833   ISFC1=FuelAmount1/Energy1;
834   ISFC2=FuelAmount2/Energy2;
835   ISFC3=FuelAmount3/Energy3;
836
837   ISFC=[ISFC1,ISFC2,ISFC3]
```

```matlab
838
839    %Plotting
840    figure(1);
841    plot(D1,smo1,D1,smo2,D1,smo3,D1,ign1);
842    xlim([-40,40]);
843    ylim([0,9]);
844    xlabel('Crank Angle [^{o}CA]');
845    ylabel('Cylinder Pressure [MPaG]');
846    legend('Diesel','1st gen. Bio','2nd gen. Bio','Injection');
847    set(gca,'XTick',(-40:10:40))
848
849    figure(2);
850    plot(D1,smoHRR1,D1,smoHRR2,D1,smoHRR3,D1,ign2);
851    xlim([-20,40])
852    ylim([-10,70])
853    xlabel('Crank Angle [^{o}CA]');
854    ylabel('Heat Release Rate [J/^{o}CA]');
855    legend('Diesel','1st gen. Bio','2nd gen. Bio','Injection');
856    set(gca,'XTick',(-20:5:40))
857
858    figure(3);
859    ax1 = gca;
860    plot(ax1,D1,smo1,D1,smo2,D1,smo3);
861    xlim([-30,60]);
862    ylim([-1,7.4]);
863    set(gca,'XTick',(-30:5:60))
864    ax2 = axes('Position',get(ax1,'Position'),...
865        'XAxisLocation','bottom',...
866        'YAxisLocation','right',...
867        'Color','none','XColor','k','YColor','k',...
868        'XLim',[-30 60],'YLim',[-12 78],'NextPlot','add');
869    plot(ax2,D1,smoHRR1,D1,smoHRR2,D1,smoHRR3);
870    ylabel(ax1,'Cylinder Pressure [MPaG]')
871    xlabel(ax1,'Crank Angle [^{o}CA]')
872    ylabel(ax2,'Heat Release Rate [J/^{o}CA]')
873    legend('Diesel','1st gen. Bio','2nd gen. Bio');
874    title('Cylinder Pressure and Heat Release Rate');
875
876    figure(4)
877    barvec=[O2change1st O2change2nd; CO2change1st CO2change2nd;...
878        COchange1st COchange2nd; NOxChange1st NOxChange2nd];
879    barh(barvec)
880    barname={'O2','CO2','CO','NOx'};
881    set(gca,'yticklabel',barname)
882    xlabel('% Change');
883    legend('1st gen. Bio','2nd gen. Bio','location','southwest');
884    ax = get(gca);
885    cat = ax.Children;
886
887    %set the first bar chart style
888    set(cat(1),'FaceColor','red');
889
890    %set the second bar chart style
891    set(cat(2),'FaceColor','green')
892
893    figure(5)
894    plot(V1,corP1)
895    xlabel(ax1,'Volume [m^{3}]')
896    ylabel(ax2,'Pressure [Pa]')
897
```

898

Appendix B. Injection File – For DICI simulation in LOGEsoft at 2400RPM and 20%load

Temperature =   3.1100e+02

SpeciesLiquidDataFileName = "fuel_species_data.txt"

molefraction

BEGIN

N-C7H16 =   1.00000e+00

END

totalfuelmass =   1.14E-05

nbrofinjectiondata =   101

-10	0.01063264
-9.9	0.02126528
-9.8	0.03189793
-9.7	0.04253057
-9.6	0.05316321
-9.5	0.06379585
-9.4	0.0744285
-9.3	0.08506114
-9.2	0.09569378
-9.1	0.10632642
-9	0.11695906
-8.9	0.12759171
-8.8	0.13822435
-8.7	0.14885699
-8.6	0.15948963
-8.5	0.17012228
-8.4	0.18075492
-8.3	0.19138756
-8.2	0.2020202
-8.1	0.2020202
-8	0.2020202

-7.9	0.2020202
-7.8	0.2020202
-7.7	0.2020202
-7.6	0.2020202
-7.5	0.2020202
-7.4	0.2020202
-7.3	0.2020202
-7.2	0.2020202
-7.1	0.2020202
-7	0.2020202
-6.9	0.2020202
-6.8	0.2020202
-6.7	0.2020202
-6.6	0.2020202
-6.5	0.2020202
-6.4	0.2020202
-6.3	0.2020202
-6.2	0.2020202
-6.1	0.2020202
-6	0.2020202
-5.9	0.2020202
-5.8	0.2020202
-5.7	0.2020202
-5.6	0.2020202
-5.5	0.2020202
-5.4	0.2020202
-5.3	0.2020202
-5.2	0.2020202
-5.1	0.2020202
-5	0.2020202
-4.9	0.19138756
-4.8	0.18075492

-4.7	0.17012228
-4.6	0.15948963
-4.5	0.14885699
-4.4	0.13822435
-4.3	0.12759171
-4.2	0.11695906
-4.1	0.10632642
-4	0.09569378
-3.9	0.08506114
-3.8	0.0744285
-3.7	0.06379585
-3.6	0.05316321
-3.5	0.04253057
-3.4	0.03189793
-3.3	0.02126528
-3.2	0.01063264
-3.1	0
-3	0
-2.9	0
-2.8	0
-2.7	0
-2.6	0
-2.5	0
-2.4	0
-2.3	0
-2.2	0
-2.1	0
-2	0
-1.9	0
-1.8	0
-1.7	0
-1.6	0

-1.5	0
-1.4	0
-1.3	0
-1.2	0
-1.1	0
-1	0
-0.9	0
-0.8	0
-0.7	0
-0.6	0
-0.5	0
-0.4	0
-0.3	0
-0.2	0
-0.1	0
0	0